MASTER IN BIOLOGY

Investigation of mechanisms responsible for increased expression of the small conductance calcium-activated potassium channel 3 (SK3) in hyaluronidase 1 deficient (Hyal1-/-) mice

Gillessen, Maud

Award date:
2022

Awarding institution:
University of Namur

UNIVERSITE DE NAMUR

Faculté des Sciences

Investigation of mechanisms responsible for increased expression of the small conductance calcium-activated potassium channel 3 (SK3) in hyaluronidase 1 deficient (Hyal1$^{-/-}$) mice

Mémoire présenté pour l'obtention

du grade académique de master 120 en biochimie et biologie moléculaire et cellulaire

Maud GILLESSEN

Janvier 2016

Université de Namur
FACULTE DES SCIENCES
Secrétariat du Département de Biologie
Rue de Bruxelles 61 - 5000 NAMUR
Téléphone: + 32(0)81.72.44.18 - Téléfax: + 32(0)81.72.44.20
E-mail: joelle.jonet@unamur.be - http://www.unamur.be

Investigation of mechanisms responsible for increased expression of the small conductance calcium-activated potassium channel 3 (SK3) in hyaluronidase 1 deficient (Hyal1$^{-/-}$) mice

GILLESSEN Maud

Summary

Endothelial cells play a major role in the development of micro- and macro-vascular complications of diabetes. Their involvement in the regulation of vascular tone is, amongst others, mediated by the small conductance calcium-activated potassium channel 3 (SK3) as part of the endothelium-derived hyperpolarization (EDH) mediated vasodilation. The endothelial glycocalyx, a carbohydrate-rich network on the surface of endothelial cells, is a mechanotransducer of shear stress and modulates the vasodilatory capacity of endothelial cells. One of its major components, hyaluronan (HA), is subject to a high turnover, with hyaluronidases such as HYAL1 as main enzymes for HA degradation. Previous studies discovered increased expression of SK3 in Hyal1 deficient (Hyal1-/-) mice as a possible explanation for their preserved EDH-mediated vasodilatation when exposed to streptozotocin-induced diabetes mellitus. These mice also display a thicker endothelial glycocalyx.

A first hypothesis to explain increased expression of SK3 in Hyal1-/- mice suggests that the deficiency of Hyal1 per se impacts SK3 expression. This was tested in vitro by using micro- (HMEC-1) and macro-vascular endothelial cells (EA.hy926), as well as a non-endothelial breast cancer cell line MFC7 as a reference. A dual luciferase assay, based on the idea that the estrogen receptor alpha (ER-α) acts as mediator between HYAL1 and SK3, exposure to high glucose to mimic hyperglycemia as observed in diabetes, and HYAL1 overexpression by simple transfection or by endocytosis of HYAL1 were all used to test the effect of HYAL1 on SK3. The results of these experiments could neither confirm nor reject the theory.

A second hypothesis suggesting an effect of the endothelial glycocalyx on SK3 expression was tested in vivo by the injection of heparinase III in Hyal1-/- mice in order to degrade the endothelial glycocalyx. However, contrary to expectations, heparinase did not reduce the thickness of the glycocalyx measured by transmission electron microscopy, so the second hypothesis could not be tested.

In summary our experiments could not determine the cause of the increase in SK3 in the absence of HYAL1 but they have set the stage for further experiments in this regard.

Mémoire de master 120 en biochimie et biologie moléculaire et cellulaire

Janvier 2016

Promoteur: B. Flamion

Université de Namur
FACULTE DES SCIENCES
Secrétariat du Département de Biologie
Rue de Bruxelles 61 - 5000 NAMUR
Téléphone: + 32(0)81.72.44.18 - Téléfax: + 32(0)81.72.44.20
E-mail: joelle.jonet@unamur.be - http://www.unamur.be

Investigation de mécanismes responsables de l'augmentation de l'expression du canal potassique à faible conductance 3 (SK3) dans des souris déficientes en hyaluronidase 1 (Hyal1$^{-/-}$)

GILLESSEN Maud

Résumé

Les cellules endothéliales jouent un rôle central dans la fonction de vasodilatation et le développement de nombreuses pathologies telles que les complications micro- et macro-vasculaires du diabète. Le signal de vasodilatation est transmis entre autres par une hyperpolarisation endothélium-dépendante (EDH) dont le canal potassique à faible conductance 3 activé par le calcium (SK3) est un acteur principal. Le glycocalyx, riche en hydrates de carbone, couvre la surface des cellules endothéliales et participe à la fonction endothéliale par sa capacité de transmettre des signaux générés par les forces de cisaillement. Un des éléments majeurs de cette voie est l'acide hyaluronique (HA) qui est dégradé par des hyaluronidases, dont HYAL1. Les souris déficientes en Hyal1 (Hyal1$^{-/-}$) présentent un glycocalyx endothélial plus épais que les souris sauvages et conservent un bon fonctionnement de la voie EDH en cas de diabète induit par la streptozotocine. Ce phénomène semble dû à une augmentation de l'expression de SK3.
Une hypothèse pour expliquer l'augmentation de l'expression de SK3 dans des souris Hyal1$^{-/-}$ est qu'Hyal1 influence directement l'expression de SK3.Nous avons testé cette hypothèse au moyen d'expériences *in vitro* sur des lignées cellulaires endothéliales micro- (HMEC-1) ou macro-vasculaires (EA.hy926), en prenant la lignée non-endothéliale tumorale mammaire MCF7 comme modèle de référence. Des expériences basées sur deux gènes rapporteurs de luciferase testant le rôle suggéré du récepteur à l'œstrogène (ER-α), l'exposition des cellules à des niveaux de glucose représentant l'hyperglycémie observée dans le diabète, ou des transfections et l'endocytose d'HYAL1 ont été effectuées mais n'ont pas permis d'accepter ou de rejeter l'hypothèse qu'HYAL1 diminue l'expression de SK3.
Une deuxième hypothèse suggérant que l'augmentation de l'épaisseur du glycocalyx augmente l'expression de SK3 a été testée *in vivo* par l'injection d'héparinase III dans les souris Hyal1$^{-/-}$. Cependant, contrairement aux attentes, l'héparinase III n'a pas permis de réduire la taille du glycocalyx mesurée en microscopie électronique à transmission.
En résumé, nos expériences n'ont pas permis de démontrer la cause de l'augmentation de SK3 en absence d'HYAL1 mais ont montré sur quelles bases techniques précises de futures expériences pourraient, elles, le faire.

Mémoire de master 120 en biochimie et biologie moléculaire et cellulaire

Janvier 2016

Promoteur: B. Flamion

Acknowledgments

This master thesis is the result of almost one year of intensive work consisting of practicing, reading, discussing, and writing. Altogether, it was a great experience that improved not only my scientific skills but also my personal skills. Without the help, support, and time of some special people, this master thesis would not have been possible. I want to thank all of them.

First of all, I want to thank my promoter Prof. Dr. Bruno Flamion for hosting me in his laboratory, correcting my scripts and giving me advices during the entire project as well as the basis of the scientific thinking needed for good research.

Special thanks go to my tutor Sophie Dogné for supervising my project and spending a lot of time to answer my questions.

Thirdly, I would like to thank all the URPhyM laboratory members for their help and advices in the everyday work, especially Martine for giving technical advises and the help to evolve in my experiments, as well as Charlotte for all the helpful talks. I enjoyed the time with all of you!

I would like to take this opportunity to thank the URBC laboratory for providing the HMEC-1 cell line used in this study, Guillaume for his helpful advices to realize several assays and providing several results as well as Corry and Caroline for the help with the transmission electron microscope.

Thanks to Florence Chainiaux-Debacq, Marielle Boonen, Catherine Lambert, and Jean-Michel Dogné for being part of the jury and reading this script.

Lastly, and most of all, I want to thank my family for supporting me. My parents, my brother, my grandparents, my boyfriend Marc, and all the other family members supported me during the 10 month of hard working. It is entirely thanks to them, and especially my parents, that I had the confidence and the moral that was necessary during the last five years. Without you, I would not be who I am now, personally and scientifically. Thank you! Danke!

Index table

Index table

List of abbreviations

List of Abbreviations

ACh	Acetylcholin
CD44	Cluster of differentiation antigen 44
Ch/ChS	Chondroitine/Chondroitine sulfate
CTL	Control
Da	Dalton
DMEM	Dulbecco's modified Eagle's Medium
DOX	Tetracycline derivative doxycycline
E2	17β-estradiol
ECM	Extracellular matrix
EDH	Endothelium-dependent hyperpolarization
EDRF	Endothelium derived relaxing factor
EG	Endothelial glycocalyx
EGF	Endothelial growth factor
ER-α	Estrogen receptor alpha
ERE	Estrogen response element
FBS	Foetal bovine serum
GAG	Glycosaminoglycan
GlcNAc	N-acetylglucosamine
GluUA	Glucuronic acid
GPI	Glycophosphatidylinositol
HA	Hyaluronan/Hyaluronic acid
HARE	HA receptor for endocytosis
Has/HAS	Hyaluronan synthase
Hyal/HYAL	Hyaluronidase
ICAM-1/-2	Intercellular Adhesion Molecule -1/ -2
IK1	Intermediate conductance calcium-activated potassium channel 1
KIAA1199 or HYBID	Hyaluronan binding protein involved in HA depolymerization
K_M	Michaelis constant
KO	Knockout
LYVE-1	Lymphatic vessel endothelial HA receptor 1
NO	Nitric oxide
PAD	Proton acceptance and donation
PECAM-1	Platelet/endothelial cell adhesion molecule 1
PGI_2	Prostacyclin
qPCR	Quantitative polymerase chain reaction
RHAMM	Receptor for HA-mediated motility
RNase	Ribonuclease
RT	Reverse transcription
SDS	Sodium dodecyl sulfate
SK3	Small conductance calcium-activated potassium channel 3
Sp1	Specificity protein 1
STZ	Streptozotocin
T1DM	Type 1 diabetes mellitus
TSG-6	Tumor necrosis factor-inducible gene-6 protein
U	Enzyme unit
UDP	Uridine diphosphate
VCAM-1	Vascular cell adhesion molecule 1

Introduction

1 Introduction

1.1 Vascular endothelium

1.1.1 Vascular endothelium: an overview

The cardiovascular system, as present in all mammalian organisms, is composed of a heart pumping the blood through arteries, which are called arterioles when their diameter decreases to finally become thin-walled vessels, the capillaries. Arterioles make up most of the 'resistance arteries', i.e. those small diameter arteries that contribute significantly to the creation of the resistance to flow and the regulation of blood pressure. The capillary network enables a high exchange between the blood and tissues by transporting oxygen and immune cells through the blood to the tissues and taking up carbon dioxide and other waste products. The blood continues its journey by passing through postcapillary venules and veins that close the cycle by arriving at the heart (Ross and Pawlina, 2006).

1.1.2 Endothelial cells: playing a pivotal role in the maintenance of vascular integrity

Independent of type and size, all vessels are composed of a simple squamous epithelium termed endothelium. Although endothelial cells are part of all vessels, they differ in their phenotype, expression profile and responses to external stimuli according to the vessel type or part of the vessel (Galley, 2004). Initially thought an inert barrier, it became clear that the endothelium takes an active part in the regulation of the structural and functional vascular integrity. Indeed, the endothelial cell layer, the interface between blood and tissues, interacts with the circulating cells as well as smooth muscle cells of the vascular wall, playing the role of a selective permeability barrier (Michiels, 2003). Furthermore, endothelial cells play crucial roles in the regulation of immune responses (Middleton et al., 2002), coagulation, and thrombosis (Pearson, 1999), as well as in the control of relaxation and contraction of smooth muscle cells, thus influencing local blood pressure and vascular tone as detailed below (Furchgott and Zawadzki, 1980). Thus, it is not surprising that the disturbance of endothelial function, described as an impaired vasodilating response to acetylcholine (ACh) or impaired flow-induced vasorelaxation, is associated with many cardiovascular diseases such as atherosclerosis (Gerrity, 1981), hypertension (Perticone et al., 2001), or micro- and macrovascular complications of diabetes (Wakabayashi et al., 1987).

1.1.2.1 A focus on the regulation of vascular tone

The importance of endothelial cells in the regulation of vascular tone became clear in 1980, when Furchgott and Zawadzki discovered that intact endothelial cells are indispensable to transmit the vasodilating response triggered by ACh to smooth muscle cells (Furchgott and Zawadzki, 1980). It turned out later that the so-called endothelium-derived relaxing factor (EDRF) is nitric oxide (NO) synthesized by a NO synthase (called eNOS in endothelial cells) from L-arginine and oxygen. NO is one of the major endothelium-derived vasodilators together with prostacyclin (PGI_2), a cyclooxygenase-dependent product derived from arachidonic acid (Dusting, Moncada and Vane, 1977; Palmer et al., 1987). As these two major actors, NO and PGI_2, failed to explain all endothelium-dependent transient hyperpolarization and relaxation evoked by ACh, an additional mechanism implicated in endothelium-derived relaxation, but independent of NO or PGI_2, was suggested (Félétou and Vanhoutte, 1988; Komori et al., 1988). Direct evidence for the existence of a distinct endothelium-derived hyperpolarization factor (EDHF) was provided by a study conducted by Chen et al. (1988). They showed that haemoglobin and methylene blue inhibited the ACh-induced relaxation, but

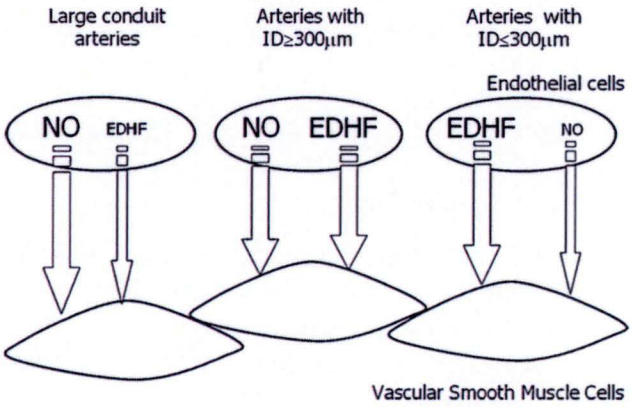

Figure 1.1. Schematic representation of the vessel-size dependent contributions of the three vasodilator pathways to vasodilation. The contribution of endothelium-derived hyperpolarization mediated vasodilation increases with decreased vessel size whereas nitric oxide increases with the internal diameter of vessels. *NO: nitric oxide, EDHF: endothelium-derived hyperpolarization factor* (Luksha et al., 2009).

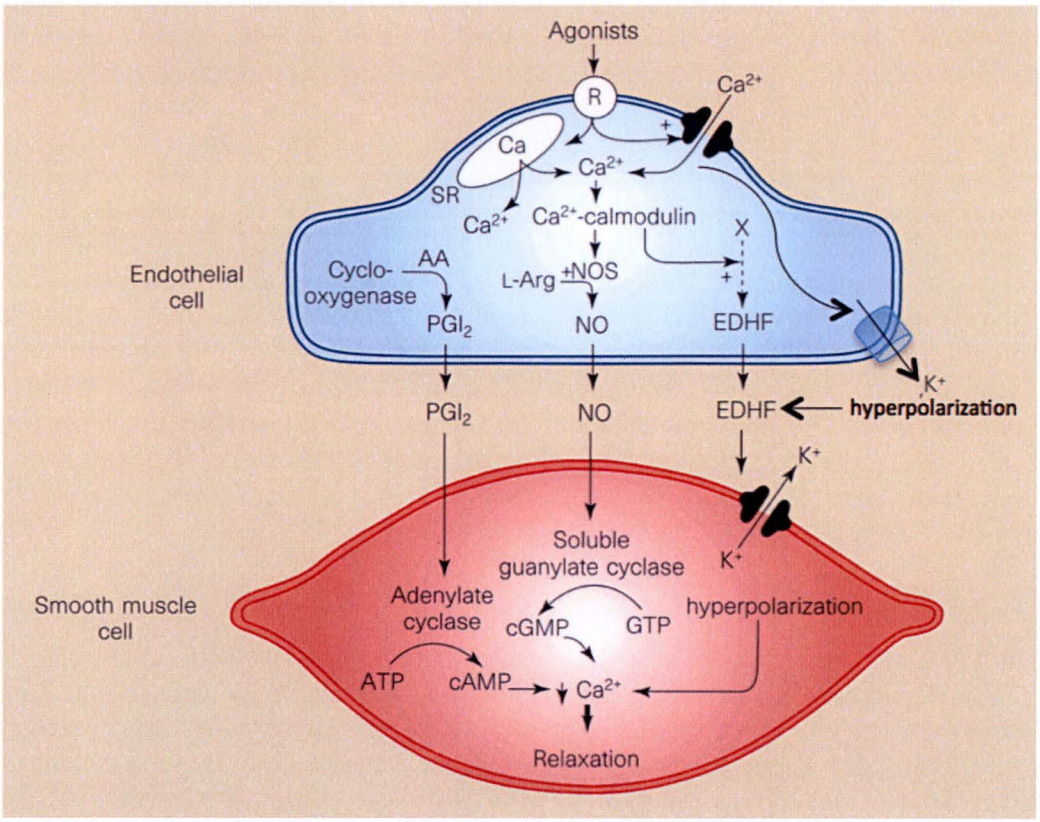

Figure 1.2. Cartoon of the relaxation of smooth muscle cells by the three pathways of vasodilation triggered by endothelial cells. Prostacyclin (PGI_2) induces adenylase activity leading to increased levels of cyclic AMP (cAMP), which has a negative effect on the myosin light chain kinase (MLCK) necessary for smooth muscle contraction. Nitric oxide (NO) activates soluble guanylate cyclase, leading to increased levels of cyclic GMP (cGMP), which in turn acts positively on the myosin light chain phosphatase implicated in relaxation. Endothelium derived hyperpolarization (EDH) is mediated by diffusible factors such as K^+ and arachidonic acid derivatives, or by cell-to-cell contacts and involves Ca^{2+}-dependent K^+ channels located on endothelial cells. *AA: arachidonic acid, NOS: nitric oxide synthase, SR: sarcoplasmic reticulum* (Luksha et al., 2009).

not the transient hyperpolarization, with the conclusion that an alternative pathway mediating vasodilation through hyperpolarization exists but that this unknown factor initially called EDHF may only play a minor role in relaxation (Chen et al. 1988). It was revealed later that the contribution of EDHF to the endothelium-dependent dilatation increases as the vessel size decreases (Fig. 1.1) (Urakami-Harasawa et al., 1997; Tomioka et al., 1999). The nature of endothelium-derived hyperpolarization-mediated vasodilation factors was long unclear but according to the findings in the last decade could be grouped into diffusible factors including nitric oxide, hydrogen peroxide, arachidonic acid derivatives, epoxyeicosatrienoic acids, and potassium ions, on one hand, and contact-mediated mechanisms between the endothelial and smooth muscle cells, leading to the use of 'endothelium-derived hyperpolarization (EDH)' as a more appropriate term, on the other hand (Luksha et al. 2009; Garland et al. 2011; Félétou and Vanhoutte, 2013).

As represented in Figure 1.2, EDH mediated relaxation begins in the endothelial cell, where, after external chemical or physical stimuli, an increase in intracellular Ca^{2+} activates Ca^{2+}-dependent K^+ channels to cause an efflux of K^+ ions into the extracellular space, resulting in hyperpolarization of the endothelial cell. This hyperpolarization can be transmitted between endothelial cells through interendothelial gap junctions or between endothelial and smooth muscle cells through myoendothelial gap junctions by means, or by synthesis, of diverse diffusible factors of the EDH pathway. This leads to the activation of K^+ channels located on the smooth muscle cells such as the Na^+/K^+-ATPase and the inwardly rectifying K^+ channels (K_{IR}), resulting in hyperpolarization and subsequent closure of voltage-sensitive Ca^{2+}-channels, transporting extracellular Ca^{2+} into the cell. The final result is the relaxation of the smooth muscle cell (Edwards et al., 1998; Luksha et al., 2009).

Through the use of various agents blocking different K^+ channels (small, intermediate or large conductance), it was shown that the voltage-independent small conductance Ca^{2+}-activated K^+ channel called SK3 (or KCNN3, $KCa_{3.1}$) and the intermediate conductance calcium-activated potassium channel IK1 ($KCa_{2.3}$) are both expressed by endothelial cells but not, or barely, by vascular smooth muscle cells. Both play a major role in the EDH mediated vasorelaxation (Corriu et al., 1996; Zygmunt et al., 1997; Köhler et al., 2000; Eichler et al., 2003; Brähler et al., 2009). Striking evidence of their importance in EDH mediated vasodilatation was given by *in vivo* studies where IK1 and SK3 deficiency in mice were both associated with impaired EDH pathway leading to chronic hypertension (Brähler et al., 2009). The individual contribution of IK1 and SK3 to the EDH pathway can vary and remains to be fully elucidated.

Before explaining the implication of potassium channels in the vasodilation function of the endothelium in more detail, it is important to note that endothelial cells have a mechanosensing function to shear stress, a frictional force on the surface of endothelial cells caused by blood flow (in the direction of the flow) as well as pressure stretch caused by blood pressure (perpendicularly to the endothelial surface). Both types of forces influence the endothelium dependent vasodilation (Malek and Izumo, 1996; Xiao et al., 1997; Michiels, 2003). By means of *in vitro* studies, it could be shown that NO synthase expression is upregulated in response to shear stress in cultured endothelial cells (Ranjan et al. 1995; Xiao et al., 1997). These observations could be confirmed by *in vivo* studies on iliac arteries, where induced shear stress leads to elevated production of NO which in turn stimulates vasodilation so that the endothelial cells are less exposed to shear stress (Kelly and Snow, 2007). Additionally to NO, the SK3 channel involved in EDH mediated vasodilation plays a role in

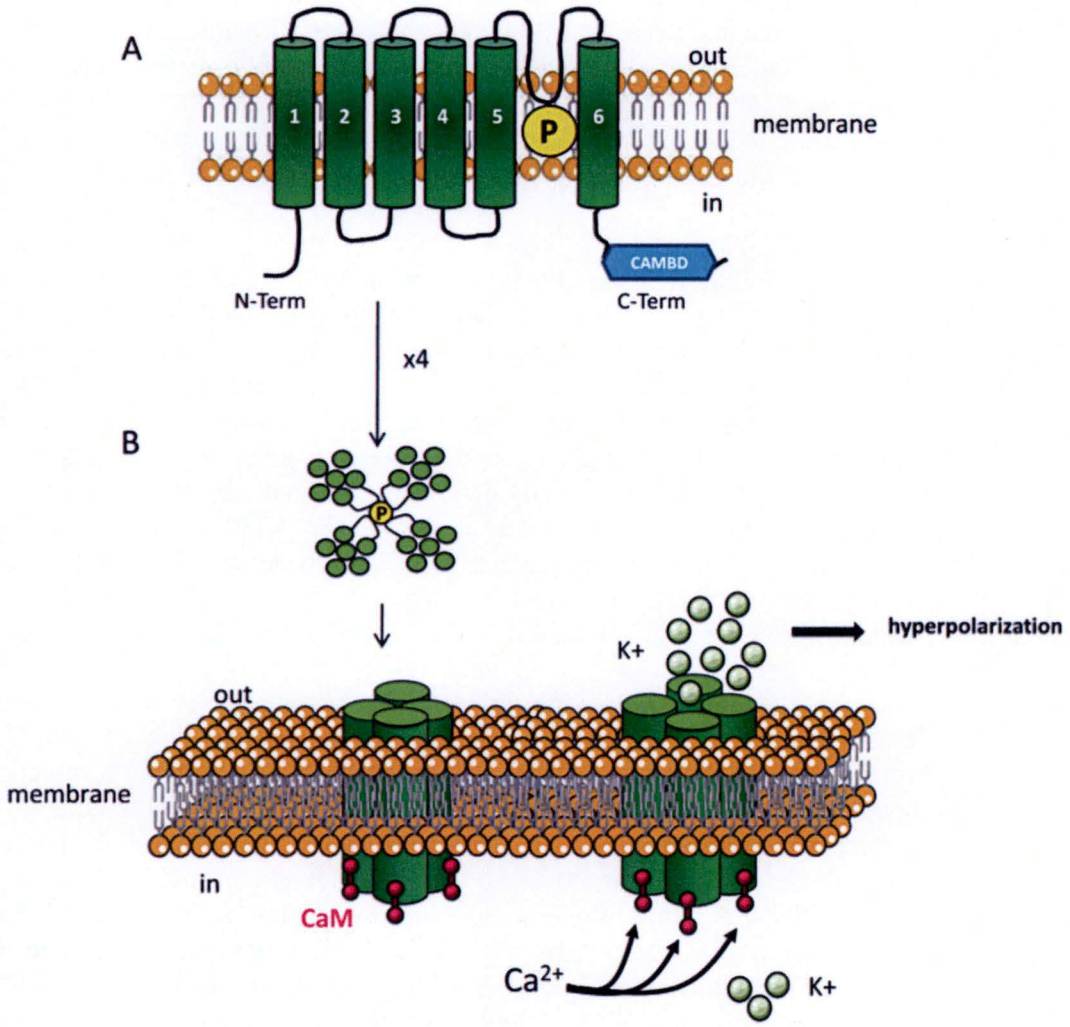

Figure 1.3. Schematic diagrams of small conductance Ca^{2+}-activated K^+ channel structure and its opening mechanism. A, The SK3 channel expressed in endothelial cells is composed of six transmembrane domains. **B**, Calmodulin is constitutively bound to the C-terminal cytoplasmic tail and mediates the opening of the channel in response to intracellular Ca^{2+} ions to allow the selective passage of K^+ ions out of the cell (Girault et al., 2012).

the vasodilation due to shear stress, too. Indeed, SK3 suppression leads to impaired wall shear stress-induced dilator responses (Brähler et al., 2009).

1.1.2.2 Small conductance Ca^{2+}-activated K^+ channel-3 (SK3): necessary for EDH?

The human SK3 gene, located on chromosome 1q21.3, just like its mouse paralog located on the mouse chromosome 3, encodes a 731 amino acid long integral membrane protein with six transmembrane domains and intracellular C- and N-terminal tails. Four of these subunits associate to form a homotetrameric channel with a high sensitivity to intracellular Ca^{2+}, mediated by calmodulin (Fig. 1.3) (Girault et al., 2012). The channel activity increases with negative membrane potential and is made of a selective permeability for potassium ions (Lancaster et al., 1991; Kohler et al., 1996; Xia et al., 1998; Wittekindt et al., 1998; Ledoux et al., 2006).

Initially, SK3 was considered to play an important role in the afterhyperpolarization (or undershoot phase) of vertebrate neurons and to be thus implicated in the development of neurological diseases such as schizophrenia or bipolar disorder (Kohler et al., 1996; Chandy et al., 1998; Wittekindt et al., 1998). However, as described above, SK3 is also associated with EDH mediated vasodilation and this latter role may be more important. For instance, the phenotype of SK3 knockout mice is mostly cardiovascular although these mice also suffer from complex alteration in emotional behaviors. Crane et al. (2003) studied the role of Ca^{2+}-activated K^+ channels by selectively blocking small or intermediate potassium channels and suggested that EDH of mesenteric arteries, a model resistance bed for studies of vasodilator function especially for EDH, is mainly due to SK3 whereas IK1 plays a role in the repolarization phase following depolarization. This functional difference between IK1 and SK3 can be correlated with differential spatial arrangements of SK3, located throughout the endothelial cell membrane but especially in adjacent endothelial cell gap junctions, and IK1, concentrated at myoendothelial gap junctions (Sandow et al., 2006; Dora et al., 2008). The involvement of SK3 in EDH mediated vasodilation could be further confirmed by direct modulation of SK3 expression. A conditional transgenic mouse model ($SK3^{T/T}$) was designed to suppress the expression of a functional SK3 protein with conserved tissue distribution when exposed to dietary doxycycline (DOX) (Taylor et al., 2003). The suppression of SK3 expression by DOX did cause a high decrease in apamin-sensitive K^+ currents, considered to be specific of SK3 channels, and thus indicating that SK3 causes the observed hyperpolarization of endothelial cells in the EDH pathway. Additionally, SK3 suppression enhanced the constriction of arteries in response to phenylephrine and led to increased blood pressure. Taylor et al. (2003) concluded that the SK3 channel is fundamental in the regulation of vascular tone and blood pressure.

The discovery of the upregulating effect of 17β-estradiol on SK3 mRNA expression in the guinea pig brain led to further transcriptional regulation studies, which revealed that the estrogen hormone 17β-estradiol (E2) has an effect on SK3 gene expression mediated by the specificity protein (Sp) transcription factors (Bosch et al., 2002). *In vitro* studies using an ER-α- and SK3-expressing rat skeletal muscle cell line showed that ER-α enhances the affinity of the transcription factor Sp1 to bind to the 33 bp enhancer region adjacent to the SK3 promoter (Jacobson et al., 2003). The effect of estrogens on SK3 was assessed indirectly *in vivo* by surgical removal of ovaries (ovariectomy). This lead to a rapid reduction of estrogen plasma levels which caused enhanced vasoconstrictive responses to phenylephrine as well as attenuated EDH mediated vasodilation (Liu et al., 2001). Interestingly, chronic administration of E2 after ovariectomy rescued all changes in EDH mediated vasodilation (Nawate et al.,

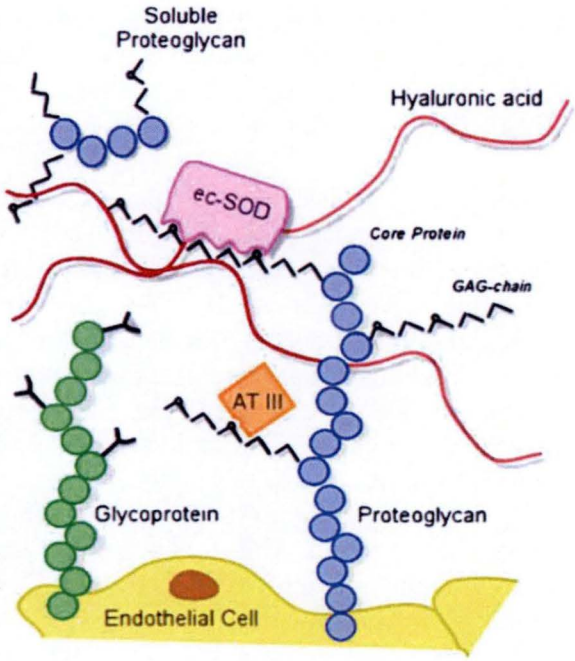

Figure 1.4. Schematic representation of the glycocalyx network lining the luminal surface of endothelial cells. The main components of the EG are glycoproteins and proteoglycans. The glycoproteins are characterized by relatively small and branched carbohydrate side chains and are attached to the endothelial cell by transmembrane domains, whereas the proteoglycans are composed of protein cores to which long linear glycosaminoglycans such as chondroitin sulfate, keratan sulfate, and heparan sulfate are attached causing the negative charge under physiological conditions. The GAG hyaluronan does not form a proteoglycan but is able to interact with other EG components. Several proteoglycans are secreted by the cells as a soluble form and retained in the endothelial glycocalyx. Furthermore, soluble molecules of the blood stream can be incorporated into the endothelial glycocalyx and contribute to its highly dynamic structure. *GAG: glycosaminoglycan, ec-SOD: extracellular superoxide dismutase, AT III: antithrombin III* (Reitsma, 2007).

2005). Yap et al. (2014) linked the decreased EDH mediated vasorelaxation to the reduction in SK3 channel expression and resulting decreased contribution to the EDH vasodilation. Based on these studies, the regulation of SK3 expression by estrogens in endothelial cells, inducing vasodilating effects, may be the key to the cardioprotective effects of E2 in females. However, no studies have investigated the direct effect of estrogen on SK3 protein expression in endothelial cells, with a putative contribution to the EDH mediated vasodilation mechanism.

1.1.3 Endothelial glycocalyx (EG): an additional barrier

1.1.3.1 Endothelial glycocalyx thickness: a challenging question

It was already known for years that many cell types are coated by a polysaccharide layer when Danielli gave the first evidence of a polysaccharide-protein coat on the luminal surface of endothelial cells, by studying the capillary permeability in frogs in 1940 (Danielli, 1940). This structure was named glycocalyx (Greek for « sweet husk ») in 1962 by Bennett, who also provided the first electron microscopy images showing the glycocalyx on endothelial cells (Bennett, 1962). Many different approaches including electron microscopy techniques using various types of solvents and dyes to minimize the collapse of the EG caused by the fixation technique, or intravital microscopy techniques, for example based on mathematical predictions compared to experimental distributions, have been used to study the thickness of the EG. They are reviewed in Pries et al. (2000). Actually, the different techniques led to the estimation of an EG thickness ranging from 45 nm to 4.5 μm, which is a huge range probably not achieved *in vivo*. EG thickness may also increase with vascular diameter in the arterial system (Reitsma et al., 2007). It should be noted that some of these studies referred solely to the glycocalyx structure whereas others measured the whole endothelial surface layer where soluble plasma components interact with the membrane-bound glycocalyx, which is responsible for plasma motion retardation *in vivo* (Pries et al., 2000).

1.1.3.2 Structure of the endothelial glycocalyx: carbohydrates in the leading role

The EG can be defined as a carbohydrate-rich layer that lines the endothelium on its luminal surface. It is composed of molecules either attached to the endothelial membrane or soluble, originating both from the endothelial cells themselves and from the plasma (Fig. 1.4). The EG network is mainly composed of glycoproteins and proteoglycans attached to the endothelial membrane, enabling the incorporation of soluble molecules which are in a dynamic equilibrium with the flowing blood. Thus, the EG can be considered as a dynamic structure that continuously changes its composition and thickness rather than a static object (Reitsma et al., 2007; Alphonsus and Rodseth, 2014).

Glycoproteins are regarded as EG backbone molecules because of their connection to the endothelial cell membrane. They are characterized by relatively small and branched carbohydrate side chains of 2 to 15 monosaccharide residues. All of the glycoproteins found in the EG have in common a transmembrane domain that enables their integration in the endothelial membrane. The main families are selectins (e. g. E-selectin, P-selectin), integrins (specific combination of α- and β-subunits) and the immunoglobulin superfamily (ICAM-1 and -2, VCAM-1, and PECAM-1), with a major role in cell signaling or immune cell recruitment from the bloodstream, as well as in coagulation or fibrinolysis. Importantly, the glycoproteins vary considerably in response to different cellular stimuli and are not expressed constitutively and in a similar expression over time. Therefore, they contribute to the highly dynamic character of the EG (Reitsma et al., 2007).

Proteoglycans, the main constituents of the EG, are glycoproteins with covalent O-glycosyl linkages between core proteins and long, linear carbohydrates containing sulfate and uronic acid groups, leading to a negatively charged molecule under physiologic conditions (Reitsma et al., 2007; Labat-Robert and Robert, 2012; Alphonsus and Rodseth, 2014). The protein cores differ in size and in their connection with the endothelial membrane. Indeed, whereas the syndecan family of core proteins is attached to the membrane by a transmembrane domain (Carey, 1997), glypicans are attached to the endothelial membrane by a phosphatidylinositol (GPI) anchor (David et al., 1990), and other proteoglycans, including perlecan, versican, decorin, biglycan, and mimecan, are not attached to the endothelial membrane but secreted after their assembly to form soluble proteoglycans which are retained in the EG or released in the blood stream. The carbohydrate chains attached to the core protein of a proteoglycan are called glycosaminoglycans (GAG), long linear polysaccharides (from 10 to over 100 kDa) with a repeating disaccharide backbone containing derivatives of amino sugar. One protein core is able to bind different types of GAGs and changes in the proportion of GAGs in one proteoglycan can occur in response to specific stimuli (Rapraeger, 1989). The four types of GAGs are heparin sulfate, chondroitin sulfate, keratin sulfate, and hyaluronan or hyaluronic acid (HA). They differ in the incorporated uronic acid and hexosamine, the disaccharide link between them, their branching or not, and last but not least, their sulfation pattern. It is important to note that HA differs from the other GAGs as it is almost never covalently linked to a core protein, and is unbranched and unsulfated. This will be detailed below (cf. 1.2). Interestingly, some proteoglycans such as aggrecan have HA binding domains to retain HA in the EG (Watanabe et al., 1997).

Often considered as a fifth type of GAG, dermatan sulfate is, strictly speaking, no more than a subtype of chondroitin sulfate where the glucuronic acid is replaced by an iduronic acid through an epimerization reaction (Trowbridge and Gallo, 2002). The most common proteoglycan of the EG is heparan sulfate, representing 50% to 90% of the total proteoglycans in the vascular endothelium, although the proportions of each proteoglycan vary in response to various stimuli (Ihrcke et al., 1993). Despite the fact that heparan sulfates are the major GAGs of the EG, it could be shown that the different GAGs are not distributed evenly throughout the glycocalyx and that HA has a major influence on EG permeability (Gao and Lipowsky, 2010; Lennon and Singleton, 2011).

Together, GAGs, proteoglycans, and glycoproteins form a negatively charged mesh, whose composition affects its interactions with plasma constituents and has various impacts on vascular function (cf. 1.4). For example, enzymatic digestion of the EG with hyaluronidase in rats causes myocardial tissue edema, making the EG an important component in the permeability barrier function of vascular endothelium (van den Berg et al., 2003). Interestingly, the EG is composed of molecules triggering adhesion of cells such as leukocytes on one hand, and preventing their binding by shielding them from their ligands on the other hand (Constantinescu et al., 2003). Furthermore, the EG is associated with, and even thought to be the sensor of, mechanotransduced vasodilation (Tarbell et al. , 2014).

Considering these findings, the EG is a highly dynamic and important structure on the surface of the endothelium. The EG has an impact on the functions fulfilled by endothelial cells. As expected, cardiovascular diseases such as diabetes can be linked with an impaired EG. For example, it could be shown that hyperglycemia leads to increased permeability of the EG (Zuurbier et al., 2005).

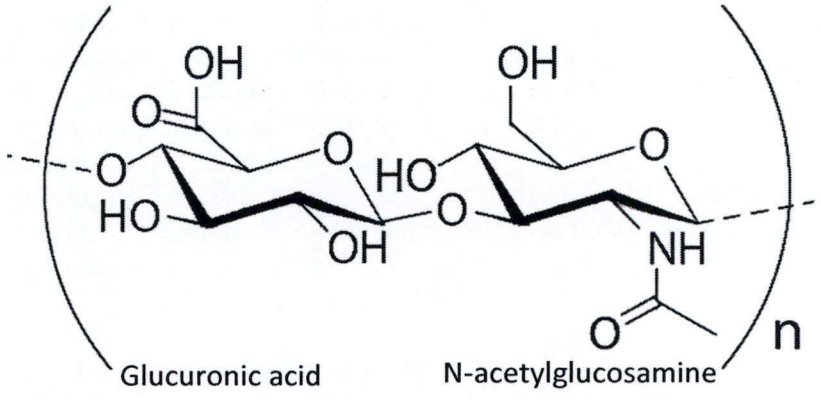

Figure 1.5. Biochemical structure of hyaluronan (HA). HA is composed of D-glycuronic-acid-[β-1→3]-N-acetyl-D-glucosamine disaccharides linked together up to 25,000 times by β-1→4 glucosydic links to form a large polysaccharide charged negatively under physiological conditions and reaching a size of 10^7 Da (Stridh et al., 2012).

1.2 Hyaluronan (HA)

1.2.1 Historical basis and evolution theories

According to the literature, HA is a molecule of increasing interest. During the last decades it was shown to be implicated in multiple cellular processes including maintenance of tissue hydration and lubrication, morphogenesis, wound healing, angiogenesis, tumor metastasis, as well as in various pathological states, although sometimes with controversial functions (Dicker et al., 2014). The history of HA began in 1934, when Meyer and Palmer discovered a polysaccharide acid of high molecular weight by precipitating the vitrous humour of bovine eyes. They named it hyaluronic acid (Palmer and Meyer, 1934). Under physiologic conditions, however, HA associates with cations to form a polyelectrolyte, frequently as a sodium salt. The term hyaluronan has later been used as a more appropriate and general nomenclature (Balazs et al., 1986; Dicker et al., 2014). Exactly 20 years passed before Meyer and Weissmann were able to determine the chemical structure of HA (Weissmann and Meyer, 1954). They showed that HA is a repetition of the (→3]-N-acetyl-D-glycosamine-[β-1→4]-D-glucoronic acid-[β1→) disaccharide, up to 25,000 times, to form a polysaccharide that can reach a molecular weight up to 10,000 kDa (Fig. 1.5) (Weissmann and Meyer, 1954). As explained above (cf. 1.1.3.2), HA belongs to the GAG family of polymers and is found ubiquitously in the extracellular matrix of vertebrate tissues and several microorganisms. Despite the principal localization of HA at the cell surface and extracellular matrix, it can also be found inside cells (Evanko and Wight, 1999; DeAngelis, 2002). In contrast to the other GAGs, heparin/heparan sulfate, chondroitin sulfate, and keratin sulfate, which are synthesized in the Golgi lumen, HA synthases are located at the inner surface of plasma membrane where they translocate the HA chain directly into the extracellular matrix (ECM) without passing through the secretory pathway. This may be the explanation for their high molecular weight compared to the other GAGs (DeAngelis, 1999). Further differences between HA and the other GAGs are that the latter are often linked covalently to a core protein to form proteoglycans and are often modified post-synthetically by sulfation or epimerization of glucuronic acid to iduronic acid (Stern et al., 2006).

Despite the simplicity of the HA molecule, which suggests that it emerged relatively early during evolution, its evolutionary appearance remains unclear (DeAngelis, 2002). The findings that no candidates for HA synthases have been found either in *Caenorhabditis elegans* or in *Drosophila melanogaster* genomes are in favor with the theory that HA is a relative recent innovation in the evolution of metazoans (Lee and Spicer, 2000; DeAngelis, 2002). However, HA could be detected in some invertebrates as well as in the GAG capsules of highly virulent bacterial pathogens, such as *Pasteurella*, *Escherichia*, and *Streptococcus*, or even in viruses, such as the *Chlorella* virus, as a result of a combination of horizontal gene transfer and functional convergent evolution (DeAngelis, 1999). In fact, it is suggested that HA appeared later in evolution than other GAGs such as chondroitin and that the enzymes catalyzing the HA and chondroitin syntheses arose through distinct evolutionary paths. Unfortunately, no animal could be identified as ancestor of HA synthase and thus of HA (DeAngelis, 2002).

1.2.2 HA: a simple but multifaceted molecule

HA plays a decisive role in many biological processes because of its biophysical and biomechanical properties on one hand and its interactions with a broad spectrum of proteins on the other hand.

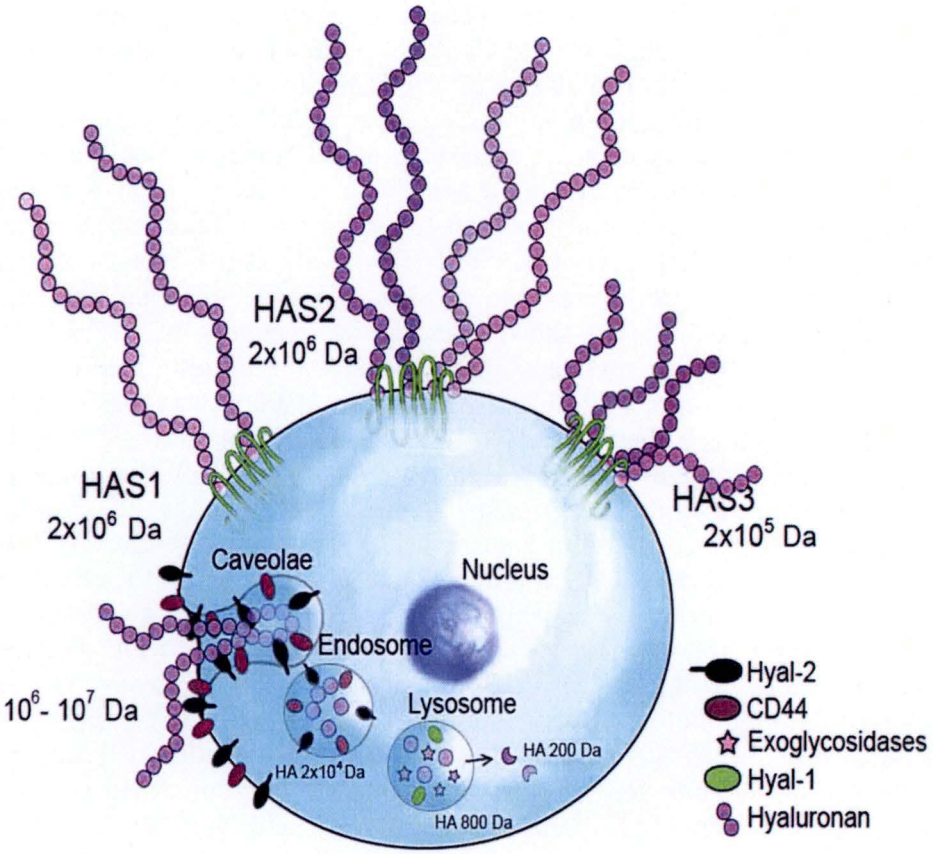

Figure 1.6. Schematic representation of hyaluronan turnover. Hyaluronan is synthesized and directly extruded into the extracellular matrix by three membrane located hyaluronan synthases producing HA molecules of different sizes. The cellular HA catabolic cascade as proposed by Stern et al. (2004) suggests in a first step the cleavage of HA by HYAL2 into smaller fragments, followed by binding to the CD44 receptor and internalization of HA fragments into the cell. Further fragmentation is catalyzed by in concert acting lysosomal HYAL1, and the exoglycosidases β-glucuronidase and β-N-acetylglucosaminidase. Monosaccharides are the result of a complete degradation of HA. *HA: hyaluronan, HYAL: hyaluronidase, CD44: cluster of differentiation antigen 44* (Stridh et al., 2012).

Firstly, the HA polymer, through intramolecular hydrogenic bonds between adjacent saccharides as well as through its polyanionic properties in physiological conditions and neutral pH, forms an expanded helical structure in solutions and occupies a high hydrodynamic volume (Scott, 1989; Laurent and Fraser, 1992; Garg and Hales, 2004). The high molecular weight of HA is responsible, amongst other, for its hydration capacities that are achieved by mechanically immobilizing water molecules in its physical structure, as well as for its viscoelastic behavior which is crucial, e.g., in synovial joints (Scott, 1989; Tamer, 2013).

Secondly, numerous proteins, termed HA-binding proteins or hyaladherins, such as the HA receptor cluster of differentiation antigen 44 (CD44) and the tumor necrosis factor-stimulated gene-6 (TSG-6), interact with HA through different types of HA-binding motifs to fulfill many cellular functions depending on factors such as the cellular localization of the hyaladherins or the cell type (Day and Prestwich, 2002). Based on these properties, HA impacts tissue organization, water homeostasis, cell proliferation, cell adhesion, and locomotion, to name a few. Consequently, many diseases, including cancer or vascular diseases caused by diabetes, can be associated with differences in HA compared to healthy state, where HA can act in both ways, i.e. as a stimulator or an inhibitor (Lennon and Singleton, 2011; Dicker et al., 2014). Taken together, the seemingly simple HA molecule can be associated with a high degree of complexity in the stimulation of biological responses, mainly based on the size of the implicated HA fragments. In general it has been shown that high-molecular-weight HA has an anti-angiogenic and immunosuppressive role whereas low-molecular-weight fragments of HA stimulate inflammation, immune response, and angiogenesis (Stern et al., 2006).

1.2.3 HA turnover: fine tuning between biosynthesis and degradation

Compared to other GAG molecules, HA turnover is incredible high, especially if one considers that HA is sometimes believed to fulfill solely a structural function in connective tissues (Laurent and Fraser, 1992). Nowadays, after the discovery of the wide spectrum of biological functions of the HA polymer and its fragments, its high turnover seems to be a logical consequence. HA half-life ranges from 2.5 to 5.5 min in blood up to 18 d in cartilage. All in all, about one-third of the total HA, estimated to be around 15 g in an average adult human, is turned over daily (Fraser et al., 1984; Triggs-Raine and Natowicz, 2015).

Three forms of HA turnover have been described to contribute, even though in different degrees and in a tissue-dependent manner, to this high rate. One part of HA is degraded directly *in situ*. This local degradation is probably most prominent in densely structured tissues (Fig. 1.6) (Fraser et al., 1997; Stridh et al., 2012). The remaining HA is drained by lymphatic vessels and removed by lymph nodes. HA that reaches the blood stream is taken up by the hepatic sinusoidal endothelial cells, mostly in the liver, and only a minority is taken up by the spleen or the kidneys and eliminated in the urine (Fraser et al., 1983). In fact, only small HA fragments between 4,000 and 12,000 Da can pass the glomerular filtration and thus be eliminated in the urine (Laurent et al., 1987).

HA internalization into the cell is an indispensable step for HA degradation. HA endocytosis can be receptor mediated or independent of endocytosis receptors (Racine and Mummert, 2012). Several key receptors have been reported to be implicated in HA endocytosis such as CD44, lymphatic vessel endothelial-1 (LYVE-1), receptor for HA-mediated motility (RHAMM), or HA receptor for endocytosis (HARE). However, one of the difficulties involved in analyzing HA receptor mediated endocytosis is that binding of HA to

the receptor and HA uptake are separate events that do not necessarily take place at the same time and do not necessarily give rise to the same cellular response. Indeed, the association of HA with its receptor may only have in impact on the signaling capacity and modulate cell response. So far, only CD44, LYVE-1 and HARE are suggested to involve HA endocytosis, although only under certain conditions in specific cell types. For example, CD44 enables HA internalization when it is associated with a cholesterol-rich microdomain of the plasma membrane termed 'lipid raft', which in turn depends on acetylation of the CD44 cytoplasmic tail (Thankamony and Knudson, 2006). The mechanism of HA endocytosis by LYVE-1 is less clear but this receptor probably acts similarly as CD44, thus in a clathrin-independent manner with an activation step, in this case consisting in the cleavage of inhibitory sialyl moieties on the glycosylated region, triggering its activation (Jackson, 2009; Racine and Mummert, 2012). Unlike the ubiquitously expressed CD44, LYVE-1 expression is restricted almost entirely to lymphatic tissues. The third key HA receptor, HARE, also known as stabilin 2, is primarily found in sinusoidal endothelial cells of the liver, lymph node, and spleen. HARE possesses a high affinity for HA; HA uptake is mediated by a clathrin coated pit pathway (Harris et al., 2007). HA endocytosis can also be receptor-independent, at least in B16-F10 melanoma cells, where HA probably interacts non-specifically with the cell surface and gets into the cell through macropinocytosis (Greyner et al., 2010).

Essential for a rapid turnover of HA is a high rate of HA biosynthesis combined with a high rate of HA breakdown.

1.2.3.1 HA biosynthesis: exceptional in the 'GAG-field"

As mentioned above, HA is a GAG that is produced by a family of enzymes called HA synthases (HAS). Three human and mouse HASs named HAS1, 2, and 3, have been described to catalyze HA synthesis at the plasma membrane. These enzymes differ from other GAG synthesizing proteins firstly because of their plasma membrane localization, which is enabled by their multiple transmembrane domains, and secondly because of their ability to extrude the HA polymer without any primer to trigger polymerization and without the requirement of an anchor protein or lipid (Weigel and DeAngelis, 2007). The human HAS encoding genes *HAS1, HAS2* and *HAS3*, located on the 19q13.3–q13.4 chromosome boundary and the chromosomal loci 8q24.12 and 16q22.1, respectively, are highly conserved and related with the mouse *Has1*, *Has2* and *Has3* genes located on the mouse chromosomes 17, 15 and 8, respectively (Spicer et al., 1997). The human and mouse HAS isozymes are 55-70% identical, and within their own species isoenzyme family, are about 90% identical. They all use cytoplasmic UDP-GlcNAc and UDP-GlcUA in the presence of divalent cations Mg^{2+} or Mn^{2+} to form β-1→4 as well as β-1→3 glycosidic bonds. The glycosyltransferases HASs are an exception in the GAG-field in as much as they perform multiple functions including catalyzing the transfer of two different monosaccharides into two different glycosidic linkages, thus executing repetitive sugar polymerization at the reducing terminus, as well as extruding HA through the plasma membrane into the ECM (Weigel and DeAngelis, 2007). HAS1, HAS2 and HAS3 differ in their catalytic activity as measured by different K_M for both of the substrates and by different biochemical properties such as enzyme stability and elongation rate (Itano et al., 1999; Itano and Kimata, 2002). Whereas HAS3 is the most active enzyme and produces polymers of low molecular weight (~ 2 x 10^5 Da), HAS1 is the less active one but, together with HAS2, produces polymers of high molecular weight (~ 2 x 10^6 Da and even higher). Moreover, the different HASs are expressed at different levels in embryonic or adult tissues (Törrönen et al., 2014). Indeed, it could be shown that only HAS2 is crucial as the deficiency in *Has2* is lethal during embryonic development, whereas the *Has1/3* double KO mice are viable and fertile although they show alterations in brain

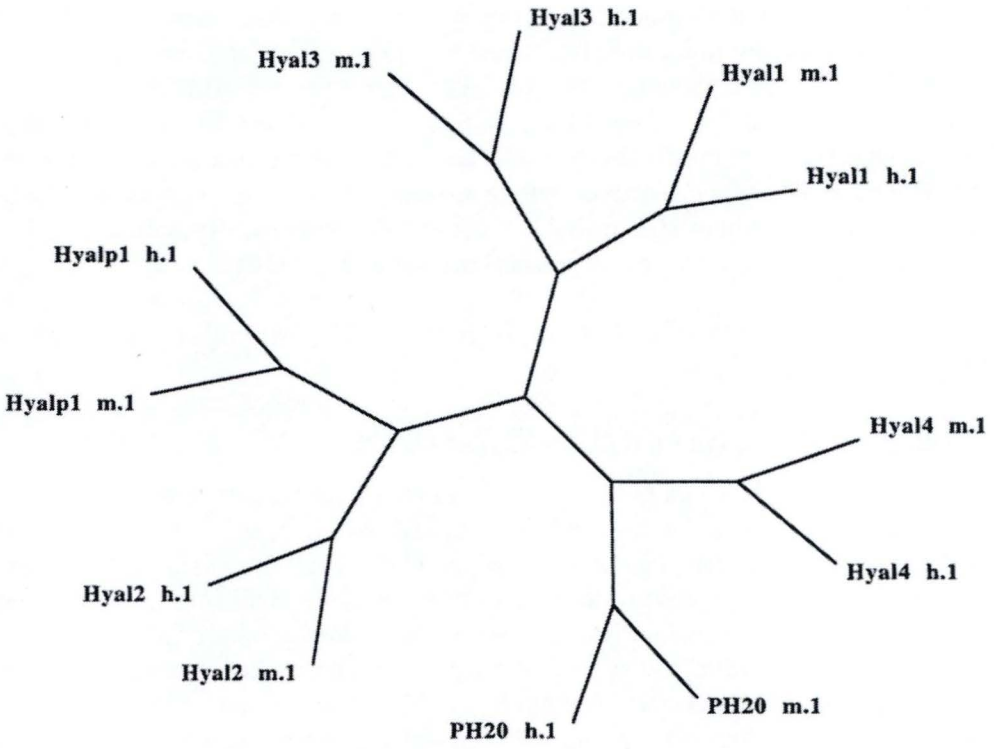

Figure 1.7. Dendrogram of the phylogenetic analysis of the human and mouse genome hyaluronidase-like genes. The divergence between the parlogous genes must have occurred long before the divergence of mouse and human. These events result in higher identity degrees between the human paralogs than between human and mouse orthologs (Csoka et al., 2001).

functioning (Camenisch et al., 2000; Mack et al., 2012; Triggs-Raine and Natowicz, 2015). Additionally, many exogenous stimuli such as growth factors, cytokines, or the general energy level of the cell contribute to HAS regulation (Racine and Mummert, 2012; Vigetti et al., 2014).

1.2.3.2 HA degradation: a focus on enzymatic catabolism

The degradation of HA is essential to ensure HA homeostasis. It has become clear that HA fragments trigger diverse and even sometimes contradictory cellular responses. Thus, understanding the mechanisms of HA degradation becomes increasingly important. From a historical point of view, the first enzyme able to degrade HA was discovered in 1928 and called "spreading factor" as it favored the spreading and virulence of bacterial pathogens (Duran-Reynals, 1933). The discovery of their substrate later became responsible for the name assignment "hyaluronidases" (Chain and Duthie, 1940). According to our present state of knowledge, HA can be cleaved by three principal types of HA degrading enzymes that can be grouped based on their mechanism of action or numerous non-enzymatic reactions:

(1) Bacterial hyaluronidases, which are known as β-endoglycosidases, HA eliminases or HA lyases (E.C.4.2.99.1), are found in several species of *Streptococcus, Streptomyces* and other member of the bacterial genus. Their mechanism of HA cleavage is based on an acid/base processive type, as they slide freely down the HA polysaccharide. This is termed proton acceptance and donation (PAD). This reaction is made possible by specific amino acids in the active side of the enzyme that act on the glucoronic acid residues of the HA chain (Li et al., 2000; Rigden and Jedrzejas, 2003; Stern et al., 2007).

(2) Hyaluronidases that are β-endoglucuronidases (E.C.3.2.1.36) are found in certain annelids (e.g., leech *Herudo medicinalis*) and crustaceans (e.g., krill *Euphasia superba*). They cleave the HA polymer at the β-(1→3) glycosidic bond between β-D-glucuronate and N-acetyl-D- glucosamine residues in a random fashion using a hydrolysis mechanism, unlikely the other main HA-degrading families, which cleave the β-(1→4) glycosidic bond (Karlstam and Ljunglöf, 1991; Hovingh and Linker, 1999). The generated end products are tetra- and hexasaccharides.

(3) Endo-β-n-acetylhexosaminidases (E.C.3.2.1.35), also known as mammalian-type hyaluronidases (Hyals), are O-Glycosyl hydrolases (EC 3.2.1.), which hydrolyse glycosidic bonds in a specific mechanism of action that has been extensively studied and will be described in detail below (Rye and Withers, 2000; Zechel and Withers, 2000). The human and the mouse genomes contain six hyaluronidase-like genes, which are considered as homologous genes, and more precisely as paralogs, because they are suggested to have a common ancestor (Csóka et al., 2001). The human Hyals are grouped in two blocks of three genes on chromosome 3p21.3 (telomere <*HYAL1, HYAL2* and *HYAL3*> centromere) and chromosome 7q31.3 (telomere <*HYAL4, SPAM1* or *PH20,* and *HYALP1*> centromere). This arrangement led to the hypothesis that the Hyals were generated by an ancient gene duplication, followed by an 'en masse' block duplication (Csóka et al., 1999). The mouse Hyal encoding genes are positioned in the same manner on chromosomes 9 (*Hyal1, Hyal2* and *Hyal3*) and 6 (*Hyal4, Spam1,* and *Hyalp1*) (Csóka et al., 1998, 2001). The mouse Hyal amino acid sequences are between 68% and 80% identical to the human orthologous genes, and thus the degree of identity between mouse and human orthologs is greater than between the human paralogs, which are identical to about 40%. By phylogenetic analyzes of the human and mouse Hyals, the divergence between the paralogs must have occurred long before the divergence of mouse and human (Fig. 1.7) (Csóka et al., 1999).

The six mammalian Hyals differ in many respects, including their unique tissue-specific expression pattern, their activity level and their optimal activity conditions, their subcellular location, or their biological functions. Indeed, whereas *HYAL2* and *HYALP1* are widely expressed, *HYAL1* is expressed differentially in the liver, heart, spleen and kidney, *HYAL3* in the bone marrow and testis, *HYAL4* in the placenta and skeletal muscle, and *SPAM1* (*PH20*) in the testis (Csóka et al., 1999; Shuttleworth et al., 2002). Hyals may not only be involved in HA breakdown because only HYAL1, HYAL2 and SPAM1 have been shown as enzymatically active. The remaining Hyals may thus be involved in other cellular processes and functions (Stern et al., 2007). The maximal activity of SPAM1 at neutral pH and of HYAL1 and HYAL2 at an acidic pH (pH ~3.7) reflects the wide range of pH optima in the Hyal family (Afify et al., 1993; Frost et al., 1997; Oettl et al., 2003). Whereas HYAL2 and SPAM1 are attached to the plasma membrane by a glycosylphosphatidylinositol (GPI) anchor, HYAL1 is a free-form enzyme that can be found either inside the cell or in the ECM.

The functions fulfilled by all six Hyals have mostly been clarified during the last decades. HYAL1 and HYAL2 are involved in the cellular pathway of HA degradation (Fig. 1.6). HYAL2 is responsible for the cleavage of high-molecular-weight polysaccharides into approximately 20 kDa fragments in acidic microenvironments created by a Na+/H+ exchanger (Stern, 2003, 2004; Bourguignon et al., 2004). Then, HYAL1 further fragments HA into low-molecular-weight HA fragments, which are principally tetrasaccharides. The breakdown of extracellular high-molecular-weight HA into its individual monosaccharides can be represented as a cascade carried out by CD44, HYAL2, HYAL1, as well as the two lysosomal enzymes β-glucuronidase and β-N- acetylglucosaminidase acting in concert (Stern et al., 2006). Because of the failure to detect an *in vitro* HA degrading activity of HYAL3, the third gene on chromosome 3p21.3, the longstanding issue of its function remained unsolved until it could be shown that *Hyal3* overexpression leads to increased *Hyal1* activity in cultured cells (Harada and Takahashi, 2007; Hemming et al., 2008). The main localization of SPAM1 (sperm adhesion molecule), previously called PH20, on the acrosomal sperm membrane and its function during fertilization have been extensively studied (Sabeur et al., 1997; Sabeur, Foristall and Ball, 2002). HYAL4 has no capacity to degrade HA because of its absolute specificity for chondroitin sulfate (ChS) degradation, another member of the GAG family differing from HA by the replacement of N-acetylglucosamine by N-acetylgalactosamine typically sulfated at the C-4 and C-6 positions (Kaneiwa et al., 2012; Mikami and Kitagawa, 2013). *HYALP1*, considered as pseudogene, contains two mutations that encode premature termination codons, leading to a transcribed but non-translated or active protein, in contrast to an intact *Hyalp1* sequence and functional Hyalp1 enzyme in mice (Frost et al., 1997; Csóka et al., 2001).

Most of Hyals in all organisms have a preference for β-(1→4) glycosidic bonds, which is probably due to the extended helical conformation of HA polymers (cf. 1.2.2) leading to a more accessible β-(1→4) glycosidic bond compared to a more hidden β-(1→3) glycosidic bond (Haxaire et al., 2000). In addition, most Hyals do not have absolute specificity for HA. Indeed, they digest other substrates such as Ch and ChS, although often at a lower rate and in a more random fashion. For example, bacterial HA lyases cleave HA in a processive way, whereas the structurally very similar Ch/ChS are broken down in a non-processive and random mode depending on the sulfation position and degree of the sugar unit (Rigden and Jedrzejas, 2003; Stern and Jedrzejas, 2006). This substrate tolerance of Hyals may be caused by their evolutionary origin. As explained above, HA appeared relatively early during evolution (cf. 1.3.1) and, thus, Hyals may have evolved from the already existing

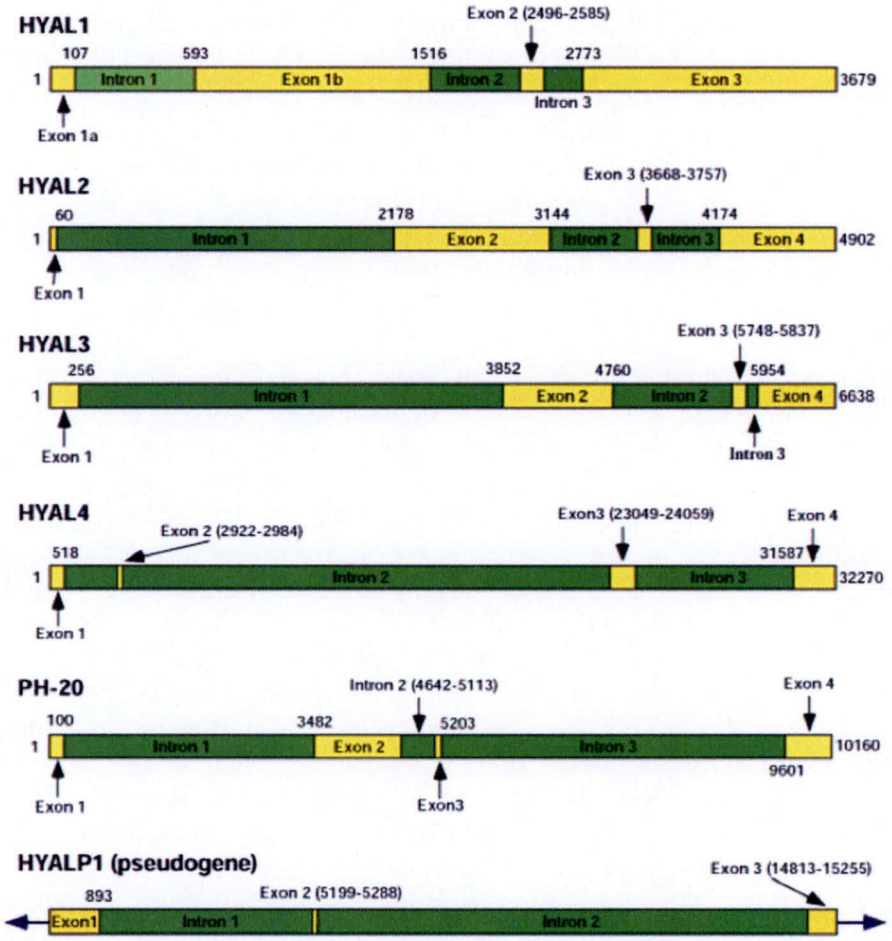

Figure 1.8. Genomic structure of the hyaluronidase genes in the human genome. *HYAL1*, *HYAL2*, and *HYAL3* are located on chromosome 3p21.3 and have similar exon and intron structures, whereas the second block of HA of hyaluronidase-like genes including *HYAL4*, *SPAM1* or *PH20*, and *HYALP1* is located on the 7q31.3 chromosome and does not preserve the exon-intron similarities between the homologous genes. In the alternative spliced variant of HYAL1 the exon 1b is removed with the intron 1 as indicated by the light green rectangle. *Yellow rectangles indicate exons, dark green rectangles indicate introns, numbers indicate the beginning and end of exons* (Csoka et al., 2001).

chondroitinases, which would explain their capacity to break down Ch/ChS. Finally, there is a major difference between bacterial and mammalian-type Hyals. Whereas bacterial HA lyases generate primarily disaccharide end products, mammalian-type Hyals break down HA to form principally tetra- or hexasaccharides (Stern et al., 2007).

Another protein, KIAA1199, also known as HYBID (HYaluronan Binding protein Involved in hyaluronan Depolymerization) has been discovered recently to be involved in HA depolymerization in a clathrin-coated pit pathway, independently of CD44 binding and subsequent cleavage by HYAL1 and HYAL2. KIAA1199 could be the long sought-for answer to the question why HYAL1 and HYAL2 are completely absent in the HA rich ECM of the brain (Yoshida et al., 2013; Nagaoka et al., 2015).

Beside the enzymatic ways to break down the HA polysaccharide catalyzed by Hyals, HA can be cleaved without the intervention of enzymes including acidic and alkaline hydrolysis reactions, ultrasonic and thermal degradation, degradation by oxidants (reactive oxygen species), and miscellaneous degradations, as reviewed by Stern (Stern et al., 2007).

1.3 Mammalian hyaluronidase 1: important insights

1.3.1 Genomic characterization

The mammalian HYAL1 was the first somatic hyaluronidase discovered. This was in the human plasma, so HYAL1 is often referred to as the plasma hyaluronidase. Later expression studies showed HYAL1 expression in many organs, and to a higher extent in the liver, the heart, and the spleen (Csóka et al., 1999). Cloning, sequencing, and characterization studies of *HYAL1* revealed that its genomic structure is similar to that of the other Hyal encoding genes located on the human chromosome 3, thus composed of 4 exons (1a, 1b, 2, and 3) and 3 introns (1, 2, and 3) (Fig. 1.8). At the transcriptional level, an isoform of HYAL1 mRNA could be detected, corresponding to alternative splice variants, where intron 1 is retained with the exon 1b, leading to a non-translated mRNA (Csóka et al., 2001).

1.3.2 Mechanism of action and intracellular localization

The basic mechanism of action of O-glycosyl-hydrolases is well studied. However, the studies to investigate the mechanism of action of the endoglycosidase hyaluronidases are based on the only hyaluronidase with a known three-dimensional structure: the hyaluronidase of the bee venom, homologous to the six Hyals of the human genome such as HYAL1. Additionally and contrary to bacterial Hyals described above, no unsaturated bond is produced during HA cleavage by eukaryotic Hyals, making the use of spectrophotometric assays impossible (Li et al., 2000; Stern et al., 2007). Hydrolysis of HA can be summarized in four steps as reviewed in Stern (2006, 2007) (Fig. 1.9). The first step consists in binding of the hyaluronidase to its substrate HA: that is enabled by a large cleft traversing the enzyme. Then, the nucleophile N-acetyl of the N-acetylglucosamine attacks its own C-1 carbon and the carboxylic acid residue of a glutamic acid of the enzyme acts as acid/base catalyst, resulting in a covalent link between them as well as the cleavage of the β-(1→4) glycosidic bond. Additionally, the C-1 anomeric configuration is inversed during this step. The third step requires a water molecule to hydrolyse the covalent link between C-1 and the carbonyl, leading to the re-protonation of Glu and a subsequent displacement of the C-1 carbon to its initial position. Finally, HA is released from the active side of the enzyme.

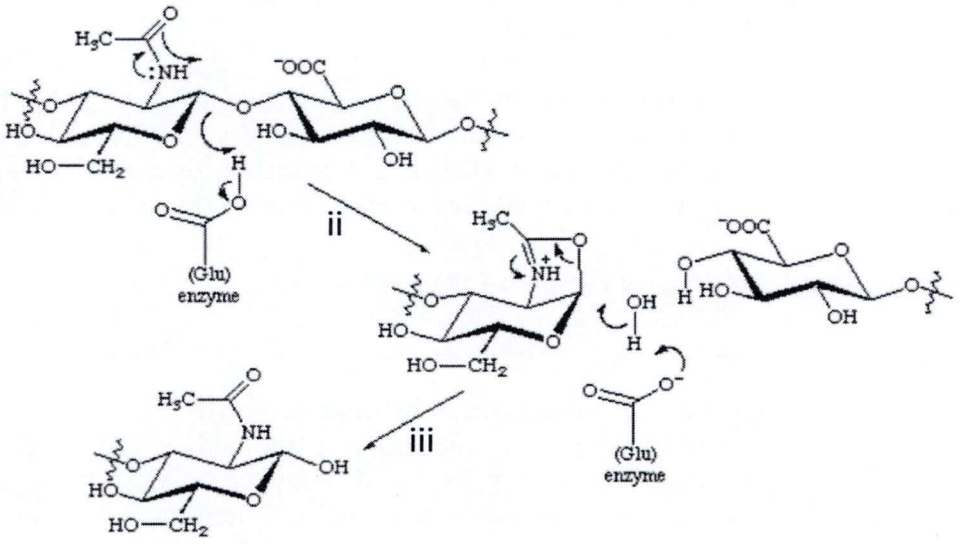

Figure 1.9. Schematic representation of hyaluronan hydrolysis by HYAL1. In a first step, HYAL1 binds to its substrate. (ii) Secondly, the C-1 carbon of N-acetyl-glucosamine is attacked by its own nucleophilic N-acetyl. The carboxylic acid residue of glutamic acid (Glu) of the enzyme acts as acid/base catalyst, resulting in a covalent link between the carbonyl group and C1 as well as in the cleavage of the β-1→4 glycosydic bond. (iii) In the third step, a water molecule hydrolyses the covalent link between C-1 and carbonyl , leading to the reprotonation of the Glu amino acid and the displacement of C-1 to its initial position. Finally, HA is released from the active side of the enzyme.

The subcellular localization and trafficking of HYAL1, which is a protein composed of 435 amino acids, has only been determined recently. It has long been suggested that the HYAL1 enzyme is localized in lysosomes because of its pH-optimum at ~ 3.7. However, because of the detection of the highest activity at a much lower pH than in the lysosome (pH 4.5), the most acid cellular compartment, it has also been suggested to be the result of an *in vitro* artifact (Stern, 2003). However, the fact that the deficiency of serum HYAL1 activity results in a lysosomal storage disorder further supports the hypothesis of the lysosomal localization of HYAL1 (Natowicz et al., 1996; Triggs-Raine et al., 1999). By the use of a subcellular fractionation approach, it could finally be proved that HYAL1 resides in the lysosomal compartments. In fact, HYAL1 differs from most newly synthesized GAG-degrading enzymes in that its lysosomal localization is not mediated by the acquisition of mannose-6-phosphate signals during the transport in the Golgi apparatus followed by signal recognition at the trans-Golgi network to concentrate these enzymes in endo/lysosomes, but by a Man-6-P independent secretion and recapture mechanism with the intervention of a mannose receptor that has the capacity to bind to terminal mannose and N-acetylglucosamine residues of GAGs (Puissant et al., 2014). The detection of two HYAL1 isozymes in human urine, one of which corresponds to a glycolysated form of 57 kDa and the other one to a non-glycosylated form of 45 kDa, was seen as an indicator for endoproteolytical processing (Csóka et al., 1997, 1998; Frost et al., 1997). Further studies performed in the URPhyM laboratory in Namur revealed that the proteolytical cleavage of a premature form into the mature form, both having a HA degrading activity, occurs in endosomes during the transport of HYAL1 to the lysosomes. The mature form may contain non-covalent associations or may require closely linked partners, at least in the mouse liver and macrophages (Boonen et al., 2014; Puissant et al., 2014).

1.3.3 HYAL1 deficiency

Due to the importance of HYAL1 in HA catabolism and homeostasis, as well as its wide expression throughout the body, it was suggested that a deficiency of this enzyme causes lethal diseases or at least severe pathologies. However, clinical and biochemical manifestations of HYAL1 deficiency in one patient could only be related with a relatively mild phenotype, including mildly dysmorphic facial features, nodular intraarticular soft-tissue masses, increased number of lysosomes with excess in mucopolysaccharide content, and highly increased plasma HA. The disease was later termed mucopolysaccharidosis IX (Natowicz et al., 1996). Genomic analysis revealed that this patient contained two mutations in its HYAL1 encoding gene. One mutation encoded a premature termination codon, whereas the other mutation caused an amino acid substitution of an amino acid putatively important in the cleavage mechanism, 136del37ins14 and 1412G→A (Glu268Lys), respectively (Triggs-Raine et al., 1999). A second case study of HYAL1 deficiency could be explained by a homologous deletion c.104delT causing a premature termination codon and no HYAL1 enzymatic activity (Imundo et al., 2011). To conclude, the observed phenotypes of HYAL1 deficiency had less severe effects than presumed.

To further study the effect of HYAL1 deficiency, a Hyal1$^{-/-}$ mouse model has been characterized and compared to the human mucopolysaccharidosis IX phenotype. Actually, 753 bp of the coding region in exon 1b, predicted to contain the active site of *Hyal1*, were replaced by a neomycine resistance cassette (Fig. 3.2) (Martin et al., 2008). Surprisingly, even though Hyal1 was revealed to be inactive, an elevation of HA could be detected neither in the serum nor in non-skeletal tissues. These findings led to the hypothesis that other enzymes involved in the HA catabolism may compensate in HA degradation. Consistent with this theory were the increased *Hyal3* expression in *Hyal1* null mice as well as the significantly

higher HA accumulation in tissues of *Hyal1*$^{-/-}$*Hexa*$^{-/-}$*Hexb*$^{-/-}$ mice compared to *Hyal1*$^{-/-}$ or *Hexa*$^{-/-}$*Hexb*$^{-/-}$ mice (Gushulak et al., 2012). However, as explained above, HYAL3 is a protein without enzymatic activity that simply enhances the activity of HYAL1 (cf. 1.2.3.2). Interestingly, the Hyal1$^{-/-}$ mice in our laboratory, having the same genetic background as the mice described by Martin (2008) but further backcrossed, display a significantly increased serum HA concentration compared to wild type mice (Dogné, submitted data).

1.4 HA and HYAL1: contribution to vascular integrity

EG-covered endothelial cells are essential for proper vascular integrity (cf. 1.1.2). The EG contains a large amount of HA. Thus it is not surprising that the vascular glycocalyx influences endothelial cells and fulfills a number of vital roles in the cardiovascular system such as vasodilation. Indeed, it could be shown that the EG contributes to the vascular wall shear stress-induced vasodilation, shortly described above (cf. 1.1.2.1), by playing a mechanosensing and mechanotransducing role, as reviewed in (Tarbell and Pahakis, 2006; Tarbell et al., 2014). Studies performed to investigate the role of the glycocalyx in mechanotransduction are mainly performed by the use of GAG degrading enzymes, such as heparinase, hyaluronidase, or chondroitinase, on either cultured endothelial cells, isolated vessels, or, less frequently, *in vivo*. Based on these methods, several studies attributed a role to HA in the EG-initiated vasodilation. For instance, isolated canine femoral arteries used by Mochizuki et al. (2003) had different reactions to flow-induced shear stress, more precisely with regard to the production of the vasodilator NO, with or without pretreatment with hyaluronidase. Hyaluronidase treatment caused a significant decrease in NO production in response to shear stress, which led to the conclusion that HA detects or amplifies blood flow mediated vasodilation. However, the downstream signaling events underlying vasodilation mediated by the EG remain to be elucidated, as well as whether other vasodilating pathways may be involved. This could be surmised if one considers that Hyal1 deficient mice have a thicker EG and a partially preserved EDH mediated vasodilation response to ACh after streptozotocin-induced diabetes mellitus (Dogné, submitted data).

Objectives

2 Objectives

According to the International Diabetes Federation diabetes is a major health problem that concerns more than 387 million people around the world and is thought to increase to over 592 million by 2035 (IDF Diabetes Atlas 2014). In Belgium, about 4,000 individuals died due to the consequences of diabetes in 2014. In fact, more than 50% of people diagnosed with diabetes die prematurely. One of the main causes of death is the cardiovascular complications associated with diabetes. These facts show that research, and even basic research, in this topic is without doubt necessary to resolve current and future public health problems.

This master thesis was carried out as part of a larger study conducted by the laboratory of Physiology & Pharmacology investigating the effect of a deficiency in the hyaluronidase Hyal1 on the cardiovascular alterations induced by diabetes in mice (Sophie Dogné, dissertation currently in progress). Strikingly, Hyal1 deficiency is associated with partially preserved endothelial function in diabetic mice compared to highly abolished endothelial function in diabetic wild-type mice. Further investigations have revealed that the upregulation of the SK3 channel, a key element of the endothelium derived hyperpolarization (EDH) vasodilation pathway, might contribute these observations.

The objective of this master thesis is to test two different hypotheses to elucidate by which mechanisms Hyal1 deficiency leads to SK3 overexpression in Hyal1 deficient mice.

The first hypothesis suggests that the Hyal1 enzyme directly impacts SK3 expression, so that Hyal1 suppression *per se* leads to SK3 overexpression. This hypothesis will be tested through several *in vitro* approaches investigating the effect of Hyal1 on ER-α, a known stimulator of SK3, or using different methods of Hyal1 overexpression to test the effect on SK3 expression.

The second hypothesis is based on the observation that Hyal1 deficient mice display a thicker endothelial glycocalyx compared to wild-type mice. The increase in glycocalyx thickness might indirectly increase SK3 expression in Hyal1 deficient mice. This suggestion will be tested using *in vivo* studies based on endothelial glycocalyx degradation through the heparinase enzyme.

Material and Methods

	EA.hy926	HMEC-1	MCF7
Culture medium	DMEM: 4.0 mM L-glutamine; 5.5 mM glucose (life technologies #31600-034)	MCDB 131 (life technologies #10372-019)	DMEM (Lonza #BE12-604F)
	DMEM: 4.0 mM L-gutamine; 25 mM glucose (life technologies #52100-021)		
Supp-lements	25 mM $NaHCO_3$ 10% inactivated FBS (Lonza #DE14-801E)	10 ng/ml EGF (R&D systems #236-EG) 1 μg/ml hydrocortisone (Stemcell technologies #07904) 10 mM glutamine (Lonza BE17-605E) 15% inactivated FBS (PAA #A11-151)	0.01 mg/ml recombinant human insuline (Sigma #91077C) 10% inactivated FBS (PAA #A11-151)
Other solutions	Phosphate Buffer Saline (PBS): 136 mM NaCl, 2.68 mM KCl, 8.1 mM Na_2HPO_4, 1.5 mM KH_2PO_4		
	Trypsin - 0.2 g/L Versene® (EDTA: ethylenediaminetetraacetic acid) (Lonza #BE02-007E)		

Table 3.1. Table representing the culture media and supplements as well as other solutions required for cell culture of EA.hy926, HMEC-1, and MCF7 cells. FBS (Fœtal Bovine Serum) has been inactivated previously by incubation for 30 min at 50 °C.

3 Material and Methods

3.1 Cell culture

Three cell lines were used in this project: EA.hy926 and HMEC-1 as endothelial cell models, and MCF7 as a non-endothelial cell line.

3.1.1 EA.hy926

EA.hy926 (ATCC #CRL-2922™) is an adherent immortalized human umbilical vein cell line obtained by the fusion of primary human umbilical vein cells with A549 lung carcinoma cells.

EA.hy926 cells are cultured in DMEM culture medium containing either 5.5 or 25 mM glucose (Table 3.1). The cells are cultured at 37 °C in 5% CO_2 in T75 culture flasks (75 cm^2) and passaged three times a week. The adherent cell monolayer is rinsed twice with 10 ml of PBS (Table 3.1), then incubated with 2 ml Trypsin-EDTA for 2 min at 37 °C to detach cells from the flask surface. The cells are then resuspended in 5 ml of culture medium and centrifuged at 1,200 rpm for 5 min with an ALC 4236 centrifuge. The supernatant is subsequently removed. The pellet composed of cells is resuspended in 4 ml of complete culture medium and one third or one fifth is transferred in a T75 flask. The volume is adjusted to 12 ml.

High glucose treatment is realized by exposing confluent EA.hy926 cells for an additional 24 h to DMEM containing 25 mM glucose.

3.1.2 HMEC-1

HMEC-1 (ATCC #CRL-3243™) is an adherent human dermal microvascular endothelial cell line, immortalized by introducing a plasmid encoding the SV40 large T-antigen, overcoming cell cycle arrest. HMEC-1 cells, kindly provided by the URBC laboratory, are cultured at 37 °C in 5% CO_2 in T75 culture flasks containing 12 ml of MCDB 131 medium (Table 3.1). Passaging is limited to about 30 times. Two to three times a week, cells are passaged by rinsing them twice with 10 ml PBS, followed by incubation with 2 ml of Trypsin-EDTA for 3 to 5 min at 37 °C. Then, the cells are resuspended in 5 ml of complete culture medium and the solution is centrifuged at 1,200 rpm for 5 min with an ALC 4236 centrifuge. The pellet is resuspended in 4 ml of culture medium and one third is seeded per T75 flask.

3.1.3 MCF7

MCF7 (ATCC #HTB-22™) is an adherent human mammary gland epithelial cell line derived from a metastatic site of adenocarcinoma.

MCF7 cells are cultured in T75 culture flasks with 12 ml of DMEM culture medium (Table 3.1) at 37 °C in 5% CO_2. Cells are passaged once or twice a week by rinsing them twice with 10 ml PBS, followed by incubation with 2 ml of Trypsin-EDTA for 3 to 5 min at 37 °C. Then, the cells are resuspended in 5 ml of complete culture medium and the solution is centrifuged at 1,200 rpm for 5 min with an ALC 4236 centrifuge. The pellet is resuspended in 4 ml of culture medium and the cells are seeded at the desired density.

3.2 Analysis of messenger RNA abundance

The production of a protein starts with the transcription of the gene (DNA) into a messenger RNA molecule. The first approach to see whether a cell expresses a protein, and in what amount, is to analyze the abundance of its mRNA. The detection of RNA expression and its quantification includes three major steps. The total RNA extraction from cells is followed by reverse transcription into its DNA complement, and finally the newly reverse transcribed cDNA of the target protein is quantified using a real-time polymerase chain reaction and a

Target	Forward primer (5'-3')	Reverse primer (3'-5')
hHYAL1	TCCAGATCTTCTATGACACGAC	TCCTTGATGGCCTGACATGA
hHYAL2	GCACTCCCAGTCTACGTCTTC	GCACTCTCGCCAATGGTAGAG
hHYAL3	GATCTGGGAGGTTCCTGTCC	AGAGCTGGAGAGGCTCAGGT
hHAS1	CACCTCACCAACCGCATGCT	GTCTGCTGGCTCAGCCACCG
hHAS3	GCCCTCGGCGATTCG	TGGATCCAGCACAGTGTCAGA
hSK3*	TGGGAAAGGTGTCTGTCTCC	TGGTGAGCTGAGTGTCCATC
mSK3	GCCAACTCTACCGCCATC	GGCTGTGGAACTTGGAGAG
hTBP	TCAAACCCAGAATTGTTCTCC	CCTGAATCCCTTTAGAATAGG

Table 3.2. List of the forward and reverse primers used in quantitative PCR reactions. *h: human; m: mouse*; **: personally designed.*

marker fluorescent molecule, SYBR Green. This technique is called the reverse transcription quantitative polymerase chain reaction, abbreviated RT-qPCR.

3.2.1 RNA extraction

The culture medium of eighty percent confluent cells (in T75, T25, or 6-well plates) is completely removed by using a vacuum pump, then cells are rinsed with ice-cold PBS. Depending on the culture flask size, cells are scraped with 1 or 4 ml of ice-cold PBS, transferred into an Eppendorf-tube and centrifuged for 5 min at 1,500 rpm at 4 °C. The supernatant is thrown away and the next steps of total RNA extraction are performed with the RNeasy Mini Kit (Qiagen #74104) in RNase free conditions. First, 350 µl of RLT buffer are added and mixed by pipetting the sample, then 350 µl of 70% ethanol are added and mixed well by pipetting. If the sample gets viscous, another 350 µl of RLT and ethanol are necessary. Seven hundred µl of the sample are transferred to an RNeasy spin column placed in a 2-ml collection tube and centrifuged for 15 s at 8,000 x g. To digest genomic DNA, 10 µl DNase mixed with 70 µl RDD buffer are added and incubated for 15 min at RT. Subsequently, 350 µl of RW1 buffer are added and the column is centrifuged for 15 s at 8000 x g. The next steps include the addition of 350 µl of RW1 buffer to the spin column and centrifugation for 15 s at 8,000 x g, the addition of 500 µl of RPE and centrifugation for 15 s at 8000 x g, and the addition of 500 µl of 80% ethanol and centrifugation for 2 min at 8,000 x g. The spin column is placed on a new collection tube and centrifuged for 5 min at 12,000 x g with open lid. The column is placed on a 1.5 ml collection tube, and 20 µl of H_20 are added and incubated for 1 min, followed by a centrifugation during 1 min at 12,000 x g. The flow-through is reapplied to the spin column to repeat the last step and ensure the elution of all the RNA into the collection tube. The extracted RNA is quantified using the Nanodrop spectrophotometer, which determines the concentration on the basis of absorbance at 260 nm. The sample is either used directly or stored at -80 °C until needed.

3.2.2 Retro-transcription

Before the PCR reaction can be performed, the mRNA needs to be reverse transcribed into its complementary DNA (cDNA). For this purpose, a volume corresponding to 1 µg of RNA and the appropriate amount of RNase free H_2O are mixed to reach a final volume of 13 µl, which are incubated for 10 min at 70 °C to obtain linear single stranded RNA before being placed on ice. The reverse transcription is carried out by adding 1 µl of the enzyme M-MLV RTase (Promega #29473115), 4 µl of M-MLV RT 5x buffer (Promega #M1531A), 1 µl of dNTP (Promega #U1511), and 1 µl of random primers previously diluted 10 times (Invitrogen #48190-011). The 20 µl samples are placed into the thermocycler to perform the RT reaction including 5 min at 25 °C, followed by 1 h at 42 °C, and 5 min at 95 °C. The resulting cDNA samples are stored at -20 °C or used directly for qPCR.

3.2.3 Quantitative PCR

The cDNA is diluted in RNase free H_20 to 1 ng/µl. Five ng of the diluted cDNA are added per well of the 96-well PCR plate previously filled with 10 µl of SYBR Green (FastStart Universal SYBR Green Master Rox: Roche #0491385000, FastStart Essentiel DNA Green Master: Roche #06402712001, or Takyon™ Rox SYBR® MasterMix dTTP Blue: Eurogentec #UF-RSMT-B0101), 2.5 µl of forward primer and 2.5 µl of reverse primer. These primers are listed in Table 3.2 and used at a final concentration of 0.3 µM. The plate is centrifuged at 337 x g for 3 min and placed into the LightCycler® 96 Real-Time PCR System (Roche) thermocycler for 2 min at 50 °C, 10 min at 95 °C, and 40 cycles of 15 s at 95 °C and 1 min at 60 °C.

RIPA				
Tris HCl	NaCl	Triton X-100	SDS	DOC
100 mM pH 7.4	240 mM	2%	0.2%	2%
DLA–ASB-14				
Urea	Thiourea	CHAPS	ASB-14	Tris
7 M	2 M	2%	2%	30 mM

Table 3.3. Composition of RIPA lysis buffer 2 x and DLA–ASB-14 lysis buffer.
ASB-14: amidosulfobetaine-14; CHAPS: 3-[(3-cholamidopropyl)dimethylammonio]-1-propanesulfonate; DOC: sodium deoxycholate; SDS: sodium dodecyl sulfate; Tris: Tris(hydroxymethyl)aminomethane.

3.3 Protein extraction

3.3.1 Cultured cells

Eighty percent confluent cells are rinsed with 5 ml of ice-cold PBS. To collect the cells, 5 ml or 1 ml of ice-cold PBS are added and the cells are scraped from the T75 or T25 culture flask/6-well plate, respectively. Then, they are centrifuged at 430 x g for 5 min at 4 °C after which the supernatant is removed. The cells are resuspended in 100 to 400 µl of sucrose-imidazole lysis buffer (0.25 M sucrose, 3 mM imidazole), depending on the pellet size, supplemented with Complete Protease Inhibitor Cocktail (Roche #11697498001) and transferred into an ice-cold dounce homogenizer where the pestle is pressed down and lifted 12 times at 4 °C. The sample is further homogenized by incubation in an ultrasonic bath for 3 min or with the ultrasonic homogenizer twice during 5 to 10 s.

3.3.2 Mesenteric arteries

Liquid nitrogen frozen tissue samples are placed into a porcelain mortar. Mortar and pestle are cleaned prior to use and liquid nitrogen is poured over in order to cool them down. The tissue is ground by firmly pressing on the sample while twisting. A small amount of powder remains once the grounding is completed. The pistil is scraped with a forceps in order to recover a maximum of the grounded sample.

3.3.2.1 RIPA lysis buffer

A. RIPA lysis buffer preparation (Table 3.3)

First, Tris-HCl and NaCl are added to approximately 100 ml of distilled water and mixed. Then, Triton X-100, SDS and DOC are added step by step. The pH of the solution is controlled at 7.4. Finally, the solution is heated at 37 °C for 10 min and stored at 4 °C while protected from light.

B. Method

Fifty µl of the RIPA lysis buffer are added to the grounded sample and transferred into a Potter-Elvehjem homogenizer. This step is repeated. The pestle is lifted and pressed down 20 times on ice to avoid an increase in temperature. The sample is finally transferred into an Eppendorf-tube and centrifuged at 1,500 x g for 3 min. The supernatant containing the proteins is removed and stored at -20 °C.

3.3.2.2 DLA–ASB-14 lysis buffer

A. DLA lysis buffer preparation (Table 3.3)

To prepare 25 ml of DLA–ASB-14 lysis buffer, urea and thiourea are solubilized in a volume slightly below 25 ml of Milli-Q water. Then, the zwitterionic detergents CHAPS and ASB-14 are added. Finally, tris(hydroxymethyl)aminomethane is added and the volume is brought to 25 ml. The pH is adapted to 8.5. The solution is divided into 1-ml aliquots and stored at -20 °C.

B. Method

The sample is directly transferred into an Eppendorf-tube, placed into a thermomixer at 12 °C to avoid DLA precipitation and 100 µl of DLA–ASB-14 lysis buffer are added. The sample is sonicated twice for 5 to 10 s before being incubated in the thermomixer for 30 min at 12 °C and 1,200 rpm. Then, the sample is centrifuged for 10 min at 12,500 x g. The supernatant containing the proteins is stored at -20 °C and 10 µl are stored as an aliquot to determine protein concentration.

3.4 Evaluation of protein concentration

3.4.1 Bio-Rad protein assay

3.4.1.1 Principle

The total protein concentration of lysed samples is determined with the Bio-Rad Protein Assay Dye Reagent (Bio-Rad #1-800-424-6723). This colorimetric assay is based on a shift in the absorbance maximum of the dye (Coomassie® Brilliant Blue G-250) when it binds to the protein. Thus, after adding the solution to the samples, absorbance is measured with a spectrophotometer at the new maximum, which is at 595 nm, and compared to a standard curve. Especially arginine and other basic or aromatic amino acid residues are bound by the Coomassie blue dye (Compton and Jones, 1985).

3.4.1.2 Method

900 µl of Bio-Rad Protein Assay Dye Reagent (diluted 10 times) are added to 100 µl of solution in standard polystyrene semi-micro cuvettes (Sarsteadt #67.742). One tube containing 100 µl of distilled water will set the spectrophotometer to read zero absorbance. To obtain a standard curve, bovine serum albumin (BSA) is used as protein concentration standard. Thirty µl, 40 µl, 50 µl, 60 µl, or 70 µl of BSA at a concentration of 1 µg/10 µl is diluted in distilled water in 100 µl final volume. Then, 900 µl of the Bio-Rad agent are added and the absorbance is read at 595 nm after 5 min reaction time. Sample protein concentration is determined and based on the standard curve.

3.4.2 Pierce protein assay

3.4.2.1 Principle

The Pierce Protein Assay (Life technologies #22660) is used to measure total protein concentration compared to a protein standard. As for the Bio-Rad Protein Assay it is a colorimetric assay based on a shift in the absorbance maximum of the dye when it binds to basic amino acid residues and to a lesser extend to aromatic acid residues. This assay allows measurement of tissue or cell samples when a lysis buffer has been used.

3.4.2.2 Method

First, the accessory Ionic Detergent Compatibility Reagent (IDCR) is dissolved in Pierce™ 660 nm Protein Assay Reagent to obtain a final concentration of 0.05 g/ml. Ten µl of each replicate of standard (0.1 µg/µl, 0.25 µg/µl, 0.5 µg/µl, 0.75 µg/µl and 1.0 µg/µl), 2.5 or 5 µl of the sample, and lysis buffer blank sample are added to a microplate well. Distilled H_2O is added to each well to obtain a final volume of 10 µl, and finally, 150 µl of prepared Pierce Reagent are added. The microplate is covered and mixed on a plate shaker for 1 min, incubated for 5 min, and absorbance at 660 nm is read with the SoftMaxPro software. To determine the protein concentration of each unknown sample, the standard curve, obtained by plotting the average blank-corrected standard BSA measure at 660 nm vs. its concentration, is used.

3.5 Western blot

The Western blot is an analytical technique to detect proteins in a semi-quantitative manner. The main steps consist in (1) electrophoresis to separate the proteins of a tissue or cell sample by size, (2) transfer onto a membrane (solid support) that (3) allows the detection of proteins or protein modifications with specific primary antibodies and visualization with secondary antibodies. The use of secondary antibodies labeled with fluorescent dyes allows protein detection with a scanner in the near-infrared spectrum without adding any substrate.

Solution	Running gel	Stacking gel
1.5 M Tris-HCl 0.4% SDS pH 8.8	1.25 ml	/
0.5 M Tris-HCl 0.4% SDS pH 6.8	/	625 µl
Acrylamide/bisacrylamide 40%	1.25 ml	237.5 µl
dH_2O	2.25 ml	145 µl
APS (Ammonium Persulfate)	250 µl	187.5 µl
TEMED (tetramethylethylenediamin)	5 µl	2.5 µl

Table 3.4. Table representing the solutions necessary for a 10% SDS-PAGE (Sodium Dodecyl Sulfate PolyAcrylamide Gel Electrophoresis) gel.

Component	Function(s)
SDS	denaturating and negatively charging the resulted polypeptide (equal charge densities per unit length)
β-mercaptoethanol	reduce disulphide bridges to allow random coil configuration
Glycerol	increase the density of the sample to avoid overflow and uneven gel loading
Bromophenol blue	migration visualisation (small molecules that migrates fast)
1.25 M Tris-HCl pH 6.8	

Table 3.5. List of the components of Laemmli's sample buffer and their function.

Buffer	Components
Migration buffer	25 mM Tris-HCl pH 8.3 192 mM Glycine 0.1% SDS
Transfer buffer	25 mM Tris-HCl pH 8.3 192 mM Glycine 20% Methanol

Table 3.6. Buffers used for western blot electrophoresis and transfer to membrane.

3.5.1 Polyacrylamide gel preparation

The polyacrylamide gel used for western blotting consists of a running gel part and a stacking gel part whose components are summarized in Table 3.4. The running gel and stacking gel solutions are prepared without adding TEMED and APS, responsible for rapid polymerization. After checking the leak tightness of the assembled rack that has a 0.75 mm space between the glass plates, TEMED and APS are added to the running gel solution. This solution is then added to reach a level of 4/5 between the glass plates and separated from oxygen, which inhibits polymerization, by a layer of ethanol. The gel solidifies within 30 min, the ethanol is removed with distilled water, being removed with a paper. TEMED as well as APS are added to the stacking gel solution, which is then added over the polymerized gel. The comb is inserted in order to create tracks in which the protein samples can be loaded. After 30 min of polymerization the gel can be directly used or wrapped in cling film and aluminum foil to be stored at 4 °C for later use (up to one week of storage).

3.5.2 Sample preparation

To detect the target protein (SK3 or ER-α), between 10 µg and 60 µg of proteins are used, diluted in the appropriate amount of distilled water, and 1/5 of the final volume of Laemmli's sample buffer (Table 3.5) is added. The final volume depends on the protein concentration but cannot exceed 40 µl because of the track size and gel thickness. The samples are mixed by vortexing to be used immediately or stored overnight at 4 °C. Shortly before loading the samples in the wells, they are boiled for 3 min at 100 °C, vortexed and briefly spinned.

3.5.3 Protein loading and electrophoresis

The comb is removed carefully from the SDS-PAGE gel when it has been placed into the electrophorator and the migration buffer (Table 3.6) is added. Six µl of the protein marker (Lonza #5510) is loaded in one of the wells, whereas the protein samples are loaded in the remaining wells. One well is left empty between the protein marker and the first protein sample to avoid interference in the detection step. The tank is connected to a power supply and the gel is run at a low voltage of 80 V during the first 10 min and at a higher voltage of 120 to 130 V for another 60 min. The migration is stopped when the dye front runs off the bottom of the gel.

3.5.4 Transfer onto membrane

After weight-specific separation of the proteins during electrophoresis, the proteins are transferred onto a polyvinylidene membrane. In advance, 6 Whatman papers and 2 thin sponges are cut to fit the measurements of the gel (6 cm x 9 cm) and soaked in ice-cold transfer buffer (Table 3.6). The polyvinylidene difluoride membrane (PVDF) (Hybond™ GE Healthcare #RPN303-LFP), with the same measurements, is plunged in methanol for 1 min and soaked in ice-cold transfer buffer. The glass plates are separated and the gel is detached. On the white grid of the transfer apparatus, one sponge is placed, then 3 of the Whatman papers, followed by the PVDF membrane, the gel, 3 Whatman papers, the second sponge, and the black grid. Air bubbles are avoided by rolling over the sandwich with a pipet. Then, the sandwich is introduced into the transfer tank filled with ice-cold transfer buffer and a block of ice. The tank is connected to a power supply and the transfer is performed during 90 min at 60 V.

3.5.5 Protein detection with IRDye fluorescent secondary antibodies

The detection of the target proteins, now located on the PVDF membrane, is based on a primary antibody that recognizes the target protein and a secondary antibody labeled with fluorescent dyes, which can be detected in the near-infrared spectrum.

Target protein		**SK3**	**ER-α**	**β-actin**
MW (kDa)		70	66	42
Primary antibody	*Dilution*	1: 200	1: 1,000	1: 5,000
	Incubation	1-2 h at RT or overnight 4 °C	overnight at 4 °C	1 h at RT
	Origin	Rabbit (Santa Cruz #sc-28621)	Mouse (Abcam #ab9269)	Mouse (Sigma-Aldrich A5316)
Secondary antibody	*Dilution*	1: 4,000	1: 4,000	1: 5,000
	Incubation	1 h at RT	1 h at RT	30 min at RT
	Origin	goat (IRDye 800CW Li-Cor #926-32211)	goat (IRDye 680RD Li-Cor #926-68070)	goat (IRDye 680RD Li-Cor #926-68070)

Table 3.7. Summary of target proteins, their primary and secondary antibodies, antibody dilutions, and incubation durations.

The membrane is placed into a 50 ml falcon and blocked with 10 ml of blocking solution (Li-Cor Odyssey Infrared Imaging System blocking buffer #927-40000) for 1 h at RT. The membrane is incubated with the primary antibody diluted in Li-Cor PBS containing 0.1% Tween for 1 to 2 h at RT or overnight at 4 °C. The primary and secondary antibodies with their appropriate dilutions are listed in Table 3.7. Then, the membrane is washed with PBS containing 0.1% Tween four times for 5 min. During the following steps the falcon is deprived of light. The secondary antibody is diluted in Li-Cor PBS 0.1% Tween and added to the membrane. After 1 h of incubation, the membrane is washed again with PBS 0.1% Tween 4 times for 5 min. The membrane is scanned with the Odyssey CLx Infrared Imaging System and analyzed with Odyssey Software. In order to control the protein loading, incubation with primary and secondary antibodies as well as all washing steps are repeated with antibodies to detect β-actin. The relative quantity of the target protein can be calculated with the Odyssey Software after normalization with β-actin.

3.6 Hyaluronidase activity assay: Zymography

3.6.1 Principle

Zymography is a technique generally used for enzyme detection or 'measuring' enzyme activity. This technique is based on the direct incorporation of the substrate into the polyacrylamide gel, thus avoiding its migration during electrophoresis. The enzyme is separated from its inhibitors in the electrophoresis step. The gel is then incubated in pH optimal conditions (here, pH 3.7) and physiological temperature (37 °C) allowing the enzymatic reaction to occur. The last step consists in staining the undigested gel to allow the visualization of the clear digested area. The zymography assay can be done in 'native' conditions where the enzyme stays in its initial structure, or in 'renaturated' conditions, where the enzyme is first denaturated and renaturated after electrophoresis. The zymography assay has been used in this study to detect the activity of HYAL1. For this purpose, the substrate HA has been incorporated into the gel.

3.6.2 Method

Eighty percent confluent cells are lysed and the proteins are extracted; their concentration is determined as described previously (cf. 3.3.1; 3.4.1 or 3.4.2).

3.6.2.1 Renaturated zymography

To measure hyaluronidase activity, the HA-substrate zymography as described by Guntenhöner et al. (1992) is applied. A 10% polyacrylamide gel is prepared the day before use as described in 3.5.1 with the difference that 850 µl of H_2O of the running gel are replaced by 850 µl rooster comb HA (1 mg/ml) (Sigma-Aldrich #H-5388), corresponding to a final concentration of HA of 0.17 mg/ml, and stored at 4 °C. Cell lysates equivalent to 5 µg of proteins are prepared by using SDS-free Leammli's sample buffer and directly loaded on the gel. Mouse serum (1 µl) is used as positive control. Electrophoresis is conducted at 4 °C for 10 min at 85 V and about 3½ h at 110 V. 30 min after the blue has migrated out of the gel, the gel is incubated twice in Triton X-100 3% for 1 h at RT to allow renaturation of HYAL1. Next the gel is incubated in a buffer containing 0.1 M sodium formate and 0.1 M NaCl at pH 3.7 for 30 min at RT followed by a 20 h incubation in a shaking water bath at 37 °C to allow HA digestion. Then, the gel is rinsed with water 5 to 10 times for 10 min at RT. The gel is incubated for 2 h with 40 ml of pronase (0.1 mg/ml) in order to eliminate proteins that are located in the gel and could inhibit the penetration of the dye. After washing the gel several times with water, it is incubated with 50% formamide for 30 min at RT. Finally the 50% formamide is replaced with the staining solution (20 ml H_2O, 14 ml 100% formamide, 6 ml Stains-All at 1 mg/ml 100% formamide). Stains-All is a cationic carbocyanine dye that stains

Plasmid	Dual-luciferase reporter assay			Transient transfection
	Transfection control	Protein control	Experimental condition	
pRL-TK	x	x	x	
pERE TATA luc (addgene #11354).	x	x	x	
pcDNA3.1	x			
peGFP		x		
pHYAL1			x	x
ptGFP				x

Table 3.8. Plasmids used for the three different conditions to perform dual-luciferase reporter assays and plasmids used for tansient transfection. *eGFP: enhanced green fluorescent protein, ERE: estrogen response element, luc: firefly luciferase, RL-TK: renilla luciferase-thymidine kinase promoter, tGFP: turbo green fluorescent protein, x: used.*

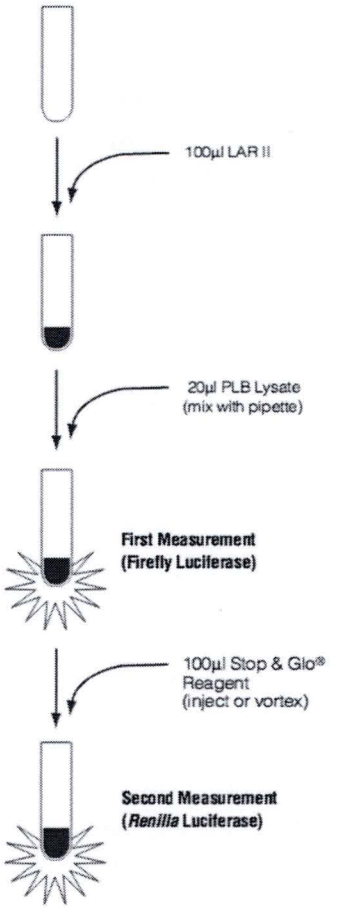

Figure 3.1. Manufacturers protocol of dual-luciferase reporter gene assay (Promega #E1910). Luminometer tube (Sarstedt #55.476.005); FB12 Single Tube Luminometer (Berthold).

anionic molecules such as anionic proteins, nucleic acids, or polysaccharides such as HA (Green et al., 1973). After at least 16 h of incubation under dark conditions the gel can be placed in water to visualize enzymatically digested and non-digested parts of the gel.

3.6.2.2 Native zymography

In contrast to the renaturated zymography, the whole experiment is performed under non-reducing conditions, which means that all solutions are SDS-free, including the Laemmli's sample buffer, the migration buffer, as well as the polyacrylamide gel. The other steps are similar to renaturated zymography with the difference that the incubation with Triton X-100 3% is not necessary and the gel is directly incubated in sodium formate buffer at pH 3.7.

3.7 Dual-Luciferase reporter gene assay

3.7.1 Principle

The aim of a reporter gene assay is to evaluate the regulatory potential of a DNA sequence on downstream gene expression. This technique is based on the simple principle that cells are transiently transfected with a plasmid containing the DNA sequence of interest linked to a reporter gene, whose activity is easily detectable. A dual-luciferase assay consists in the simultaneous expression of two individual reporter enzymes in a single system. The advantage of this technique is that one of the luciferases can be used as experimental reporter whereas the other one serves as transfection control and baseline response measurement. In this study, the dual-luciferase assay has been used to test the possible impact of HYAL1 on ERE.

3.7.2 Method

3.7.2.1 Transient transfection

EA.hy926 cells are plated in 12-well plates at 150,000 cells/well. Twenty-four hours later, they are co-transfected with three plasmids in order to obtain three different experimental conditions (Table 3.8). The appropriate plasmids for each condition are incubated with 100 µl of Opti-MEM (life technologies #11058021) per plasmid for 5 min at RT. Four µl of Lipofectamine are incubated per 100 µl Opti-MEM for 5 min. Then, Lipofectamine-Opti-MEM is added to the plasmid-Opti-MEM tube in a 1:1 ratio and incubated for 20 min at RT. Culture medium is added to obtain a final volume of 1 ml per well and mixed gently by pipetting. The medium of each well is removed and replaced with the mix. The 12-well plate is incubated for 4 h at 37 °C. Then, the cells are rinsed twice with PBS and 1 ml of normal growth medium is added.

3.7.2.2 Cell lysis and dual luciferase assay

The culture medium is removed, 250 µl of passive lysis buffer are added to lyse cells and the 12-well plate is placed on a rocking platform for 15 min at RT. Cells are transferred into an Eppendorf-tube and used directly or stored at -80 °C. Luciferase activities are measured using the Dual-Luciferase® Reporter Assay System (Promega #TM040) and a FB12 Single Tube Luminometer (Berthofl) following the manufacturers instructions (Fig. 3.1). *Firefly*-luciferase luminescence is normalized using *renilla*-luciferase data after subtraction of background.

3.8 Transient transfection

3.8.1 Principle

The simple transient transfection assay is a method to overexpress a protein by introducing a plasmid encoding this protein. In this study, the transient transfection has been

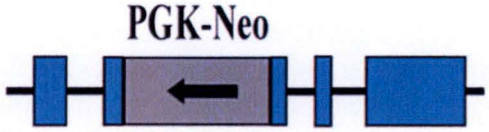

Figure 3.2. Schematic representation of the Hyal1 gene in Hyal1$^{-/-}$ mice. The neomycine resistance cassette has been inserted in exon 1b (the arrow indicates its orientation). *Exons are represented in blue, introns as lines. PGK : phosphoglycerate kinase promotor* (Martin et al., 2008).

used to overexpress HYAL1 in the different cell types and investigate the effect on SK3 expression.

3.8.2 Method

EA.hy926, HMEC-1 and MCF7 cells are plated in 6-well plates to reach 80% confluence after 24 h. Two wells are used as control and do not receive any plasmid, two wells are transfected with a tGFP encoding plasmid (only for EA.hy926 cells), and other two wells are transfected with the *HYAL1*-HA (hemagglutinine) plasmid. To perform the transfection, 4 µg of *HYAL1*-HA plasmid (Table 3.8) per 250 µl of Opti-MEM and 8 µl of Lipofectamine per 250 µl of Opti-MEM are incubated for 5 min at RT. Then, Lipofectamine-Opti-MEM is added to the plasmid-Opti-MEM tube in a 1:1 ratio and incubated for 20 min at RT. Culture medium is added to obtain a final volume of 2 ml per well and mixed gently by pipetting. The medium of each well is removed and replaced with the mix. The 6-well plate is incubated for 4 h at 37 °C. Then, the cells are rinsed once with PBS and 2 ml of normal growth medium is added. Cells are lysed 24 h after the replacement of growth medium as described previously (cf. 3.3.1) with the difference that after the first centrifugation of two pooled wells the pellet is resuspended in PBS. One third of the sample is levied in order to extract mRNA (cf. 3.2) whereas the rest is used to extract proteins. Protein concentration is determined as described above (cf. 3.4.2.).

3.9 Endocytosis assay

3.9.1 Principle

It has been shown *in vitro* and *in vivo* that HYAL1 can be endocytosed by several cell types (Gasingirwa et al., 2010; Puissant et al., 2014). Thus, incubation of cells in HYAL1 containing medium in order to allow endocytosis can be considered as another method beside the transfection of an HYAL1 encoding plasmid to overexpress HYAL1 *in vitro*.

3.9.2 Method

This experiment has been described previously by Puissant et al. (2014) and slightly adapted in this study. Cells are plated in 6-well plates in order to reach 80% confluence 24 h later. Then, they are incubated with 4 µg of human recombinant HYAL1 with or without 75 µM leupeptin (Sigma #2884), to inhibit HYAL1 processing proteases, for 2 h at RT. The incubation with rhHYAL1 is followed by culture in rhHYAL1 free medium for 15 min at 37 °C. Finally, cells are lysed as described above (cf. 3.3.1) and concentration of proteins determined using the Pierce protein assay (cf. 3.4.2).

3.10 Mouse model

For this study, C57BL/6(N10) *Hyal1*$^{-/-}$ mice previously obtained from the Mutant Mouse Regional Resource Center (MMRRC, University of California, Davis, USA) were raised at the UNamur animal facilities. The Animal Ethics Committee of UNamur gave their agreement and supervised all experimental procedures. Martin et al. (2008) characterized this mouse model and revealed that a neomycin resistance cassette had been inserted into the exon 1b of *Hyal1* as described in the introduction (Fig. 3.2).

3.10.1 Degradation of endothelial glycocalyx

Twelve weeks old homozygous *Hyal1* KO mice are injected intravenously with 1 U of heparinase III (Sigma-Aldrich #H8891) in order to remove heparin sulfates from the endothelial glycocalyx and thus degrade it.

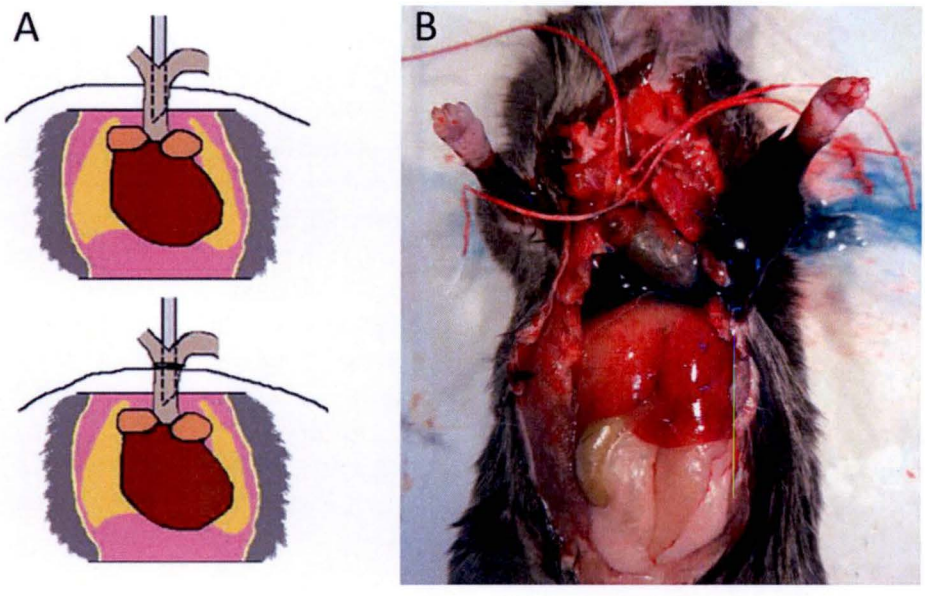

Figure 3.3. A, Schematic representation of the retrograde cannulation at the aorta/brachiocephalic trunk and fixation of the catheter with a node. B, Photograph of a retrogradely cannulated mouse during coloration with 1% glutaraldehyde - 1% paraformaledhyde containing 0.05% Alcian Blue 8GX in order to colour and fix the endothelial glycocalux.

Component	**Concentration (mM)**
NaCl	114
KCl	10
KH_2PO_4	1.15
$NaHPO_4$	25
Hepes	5
EDTA	0.025
$MgSO_4 . 7H_2O$	1.17

Table 3.9. Composition of calcium-free cardioplegic solution CCS.

Alcohol content (in H_2O)	**Repetitions**	**Time (min)**
30%	2	5
50%	2	5
70%	2	5
90%	2	10
100%	3	15

Table 3.10. Summary of the dehydration steps used to prepare the tissue samples for transmission electron microscopy.

3.10.2 Transmission electron microscopy

Twenty-four h after enzyme injection, the mice are anesthetized with an intraperitoneal injection of 0.5 mg/kg Domitor and 150 mg/kg Ketamine. Several minutes later the rear foot and tail reflexes are tested before any incision is made. After opening the thorax and cutting off the rib cage to access the heart, the aorta is cannulated retrogradely at the aorta-brachiocephalic trunk bifurcation as represented in Figure 3.3. The next steps include the perfusion with fixation and coloration media, which are performed as described previously in rats (van den Berg et al., 2003) with slight adjustments for mice. The hearts are washed of blood using an oxygenated calcium-free cardioplegic solution (CCS, Table 3.9) supplemented with 0.1% BSA and 0.1% glucose at 0.4 ml/min for 3 min, followed by 2-min fixation using a 1% glutaraldehyde - 4% paraformaldehyde solution at pH 7.4 containing 30 mmol/l $MgCl_2$, and finally the same solution supplemented with 0.05% Alcian Blue 8GX for 30 min. The left ventricles are cut into 2x2-mm segments, fixed for an additional hour in the glutaraldehyde-paraformaldehyde solution, and rinsed 3 times with 84 mM phosphate buffer for 10 min. Post-fixation is realized with 1% osmium tetroxide and 1% lanthanum nitrate in water for 1 h, followed by three rinsing steps with H_20 for 10 min, and incubation in H_20 overnight at 4 °C. Then, 1% uranyl acetate in H_20 is added for 1 h to enhance contrast. Dehydration steps are performed using increasing concentrations of ethanol (Table 3.10). Then, the tissue segments are incubated twice with propylene oxide for 10 min, 50% propylene oxide and 50% LX 112 resin for 30% under agitation, and 100% LX 112 for 1 h at 37 °C under agitation. Finally, the tissue segments are embedded into LX 112 resin over night at 37 °C, for 24 h at 45 °C, and 48 h at 60 °C. The consolidated resin blocks are cut and digital pictures are taken with a FEI Tecnai Transmission Electron Microscope. Glycocalyx thickness is measured using ImageJ software.

Results and Discussion

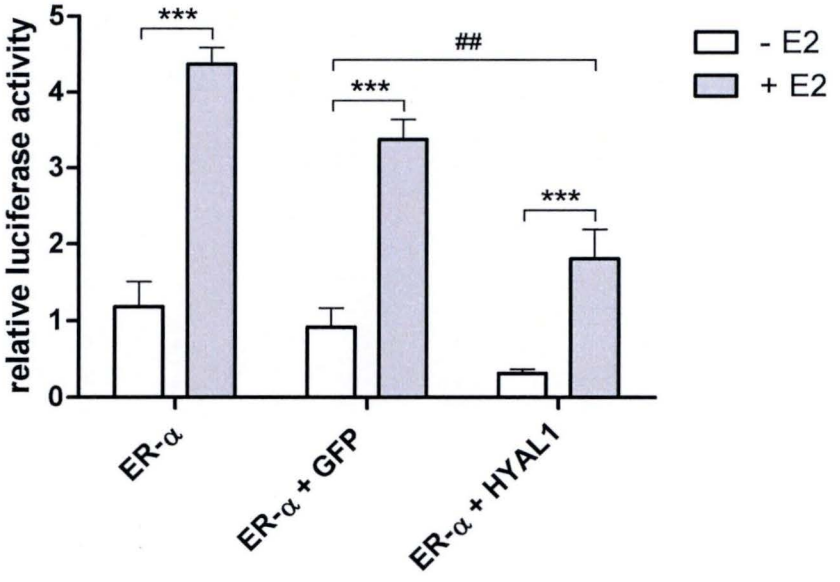

Figure 4.1. Effect of hyaluronidase 1 on estrogen response element (ERE)-luciferase activity in MCF7 cells. Transient co-transfection of estrogen response element (*ERE*)-*firefly*-luciferase reporter construct, either *GFP* or *HYAL1*, *renilla*-TK luciferase as normalization plasmid and stimulation or not with E2 (10 nM) in MCF7 cells. Effect of E2 on ERE-luciferase activity (***, $p<0.001$); effect of *HYAL1* on ERE-luciferase activity compared to *GFP* (##, $p<0.01$). All quantitative values show mean ± SEM normalized by *renilla*-luciferase-TK plasmid, n=3, statistical analysis: two-way ANOVA.

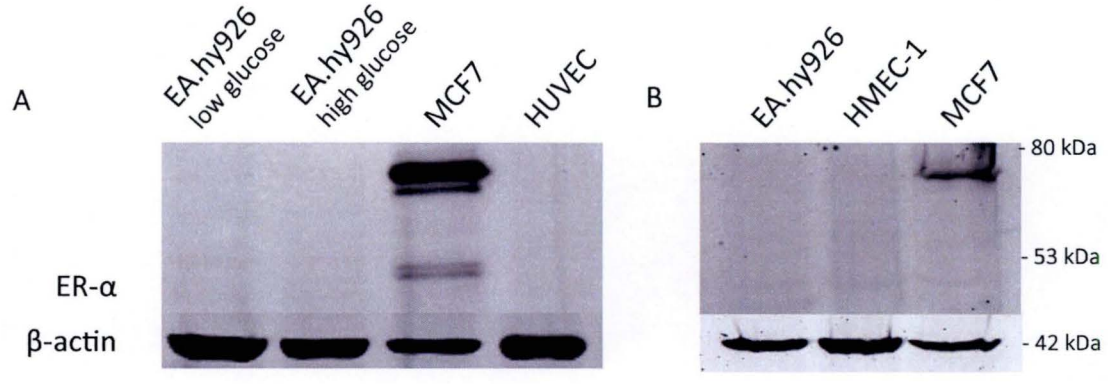

Figure 4.2. Expression of estrogen receptor alpha (ER-α) protein. Expression of ER-α was tested by western blotting EA.hy926 cells grown in low glucose (5.5 mM) or high glucose (25 mM) conditions, its primary cell line HUVEC (human umbilical vein endothelial cells) both homogenized with the dounce homogenizer and in MCF7 cells lysed with RIPA buffer **(A)** and EA.hy926, HMEC-1, or MCF7 cells homogenized with RIPA lysis buffer **(B)**. MCF7 cells, descended from an ER-α positive breast cancer cell line were used as a positive control. Forty or twenty micrograms of total proteins were loaded in A and B, respectively. β-actin was used as loading control. No expression of ER-α with a size of 66 kDa, as in MCF7 cells, could be detected in any of the tested endothelial cell lines.

4 Results and Discussion

4.1 *In vitro*: HYAL1 and SK3

4.1.1 Effect of HYAL1 expression on ERE activity

Observations in Hyal1 deficient mice show increased SK3 levels in mesenteric arteries. Furthermore, SK3 can be upregulated by estrogens in rat myoblasts and kidney fibroblasts (Jacobson et al., 2003; Tang et al., 2015). Therefore, we decided to test the effect of HYAL1 on the estrogen response element (ERE) using transient transfection assays in the endothelial cell line EA.hy926. First, preliminary assays were performed using MCF7 cells because these cells had been shown to respond to estrogens in previous experiments in our laboratory. MCF7 cells were co-transfected with the reporter plasmids *ERE-firefly*-luciferase, containing three copies of vitellogenin ERE, and *renilla*-luciferase-TK for normalization. Additionally, a HYAL1 encoding plasmid, or a GFP encoding plasmid as a negative control, were co-transfected with the two reporter plasmids. The dual luciferase assays performed in MCF7 cells, described in the literature to express ER-α, reveal significant changes in the relative luciferase activity in different conditions, which are analyzed by two-way ANOVA (n=3) (Fig. 4.1). Firstly, the relative luciferase activity increases significantly with 17β-estradiol (E2) stimulation as expected (10 nM; two-way ANOVA, $p<0.0001$). Secondly, the transfection with *HYAL1* leads to a significant decrease of ERE-luciferase activity in both E2 stimulated and non-stimulated cells (two-way ANOVA, $p<0.01$). However, by individually analyzing the activity of *renilla*-luciferase used for normalization, which should be stable, we observed that its activity varied highly between the different transfection conditions (data not shown). Thus, it may be suggested that the overexpression of a protein *per se* diminishes either the cell proliferation, which automatically leads to a decrease in luciferase signal, or the luciferases themselves, resulting in different activities. The decrease of relative luciferase activity following *HYAL1* transfection observed in this preliminary study might be an artifact because it is not only due to the decrease in ERE-luciferase activity but also to changes in the *renilla*-luciferase activity used for normalization between the compared conditions.

The endothelial cell line EA.hy926, also described to express ER-α, was then used to test whether ERE may be a regulation mediator between HYAL1 and SK3 in endothelial cells. However, several circumstances hindered the performance of the dual luciferase assay in this cell line. A high mortality rate was observed during the first hours of transfection when using more than 1 µg of DNA per 100,000 cells. Yet, by adapting the amount of transfected DNA, ERE-luciferase could not be activated sufficiently to be differentiated form background luminescence. The expression of ER-α protein in EA.hy926 cells, as well as in its primary cell line HUVEC, was thus checked using western blot to find a cause of the *ERE*-luciferase activation failure.

4.1.2 Expression of ER-α in endothelial cells

The ER-α protein with a molecular weight of about 66 kDa, although clearly detected as expected in MCF7 cells (see below), could not be detected in EA.hy926 and HUVEC cells (Fig. 4.2. A). However, as the MCF7 cells were lysed using RIPA lysis buffer whereas EA.hy926 and HUVEC cells were lysed using the dounce homogenization method, a difference in protein extraction might explain the non-detection of ER-α in these cell lines. For this purpose, new cell lysate samples of MCF7 and EA.hy926 cells, as well as cells of another endothelial cell line, HMEC-1, were prepared using the RIPA lysis buffer to perform another blot to detect ER-α (Fig. 4.2. B). Again, ER-α with a size of about 66 kDa could be

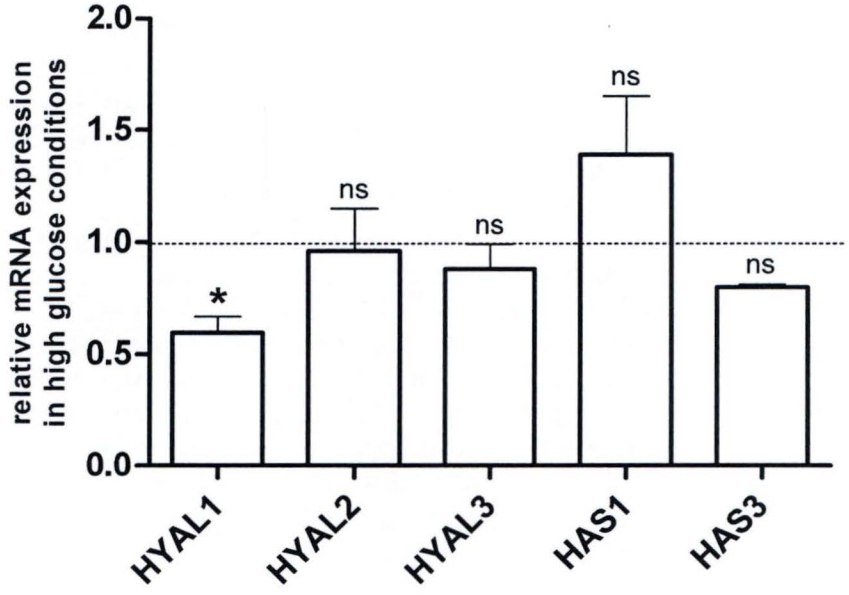

Figure 4.3. Effect of glucose on enzymes involved in the HA metabolism. The effect of glucose on mRNA expression of enzymes involved in HA synthesis (HAS1 and HAS3) and HA degradation (HYAL1, HYAL2, and HYAL3) is assessed by RT-qPCR on EA.hy926 cells exposed to high glucose levels (25 mM) for 24 h compared to cells grown in control glucose conditions (5.5 mM). HYAL1 decreases significantly (*, unpaired t-test, $p<0.05$, $n=3$) with high glucose exposure whereas no alterations could be observed for the other tested mRNAs. TBP is used as reference gene for normalization. Mean ± SEM are shown.

detected in MCF7 cells but neither in EA.hy926 nor in HMEC-1 cells. β-actin was used as a loading control in both experiments. A second band with a molecular weight of about 46 kDa, with a much lower intensity than the 66 kDa signal, could be detected in MCF7 cells in the first experiment (Fig. 4.2.A) but not in the second western blot (Fig. 4.2.B). The lower signal of the ER-α 46 kDa variant may be due either to lower expression of this variant in MCF7 cells compared to the 66 kDa protein or to a lower recognition by the monoclonal antibody used in this experiment. Indeed, the region recognized by the antibody is unknown. Actually, MCF7 cells have been proven in previous studies to express both the 66 kDa and the N-terminal truncated 46 kDa receptor variants, whose detection were antibody-dependent (Flouriot et al., 2000). As it became clear that estrogen has an effect on the cardiovascular system, researchers got also interested in the question of the presence of estrogen receptors in endothelial cells (Mendelsohn and Karas, 1999). Several authors could show that both variants of ER-α, the 66 kDa form and the 46 kDa protein, are present in endothelial cells such as in the HUVEC cell line whereas other endothelial cells seem to express only one of the ERs such as the 66 kDa form of ER-α in immortalized ovine pulmonary artery endothelial cells or the 46 kDa variant in the immortalized human endothelial cell line EA.hy926 (Chambliss et al., 2000; Russell et al., 2000; Ihionkhan et al., 2002; Li et al., 2003). Our failure to detect any of the ER-α forms in the endothelial cell lines may be due to antibody recognition.

Controversial information is available on the correlation between the receptor variants and their function in the generation of genomic or rapid, non-genomic, responses to E2. Indeed, Flouriot et al. (2000) reported that the 46 kDa ER-α acts as a competitive inhibitor of the full ER-α form, whereas Russell et al. (2000) suggest a role of the 46 kDa isoform in the generation of rapid responses without the capacity to induce ERE-mediated transcription.

When applying these findings to the observed failure of *ERE*-luciferase activation in the dual luciferase assay, it is suggested that the 66 kDa form may be necessary to activate ERE-luciferase reporter gene and that the shorter variant of ER-α may not be able to bind to the *ERE*-sequence or to activate the *ERE*-luciferase reporter gene.

In conclusion, the experimental assay using a dual luciferase reporter system based on an ERE-luciferase reporter gene may not be appropriate for testing the effect of HYAL1 on ER-α in endothelial cells.

4.1.3 Effect of high glucose on HA metabolizing enzymes in EA.hy926 cells

The recommended cell culture medium for EA.hy926 contains glucose at a high concentration of 25 mmol/L, whereas the physiological blood glucose level to which the endothelial cells are exposed is around 5.5 mmol/L in an average adult (Güemes et al., 2015). High glucose exposure (25 mmol/L) has been used in previous studies on different cell types as an *in vitro* model for hyperglycemia as observed in diabetes (Singh et al., 2011; Manea et al., 2013). Thus, EA.hy926 cells were grown in a low glucose medium (5.5 mmol/L) before being exposed to high glucose concentrations for 24 h. mRNA expression of enzymes involved in HA synthesis and degradation was tested using RT-qPCR reactions in independent triplicates and analyzed using the $e^{-\Delta\Delta Cq}$ method with TBP as normalization mRNA (Fig. 4.3). The mRNA of two HA synthases, HAS1 and HAS3, could be detected in EA.hy926 cells, as well as those of the three hyaluronidases HYAL1, HYAL2 and HYAL3. High glucose exposure did not have any effect on the mRNA levels of HA synthases (HAS1 and HAS3) or hyaluronidases HYAL2 and HYAL3, with the exception of HYAL1 mRNA

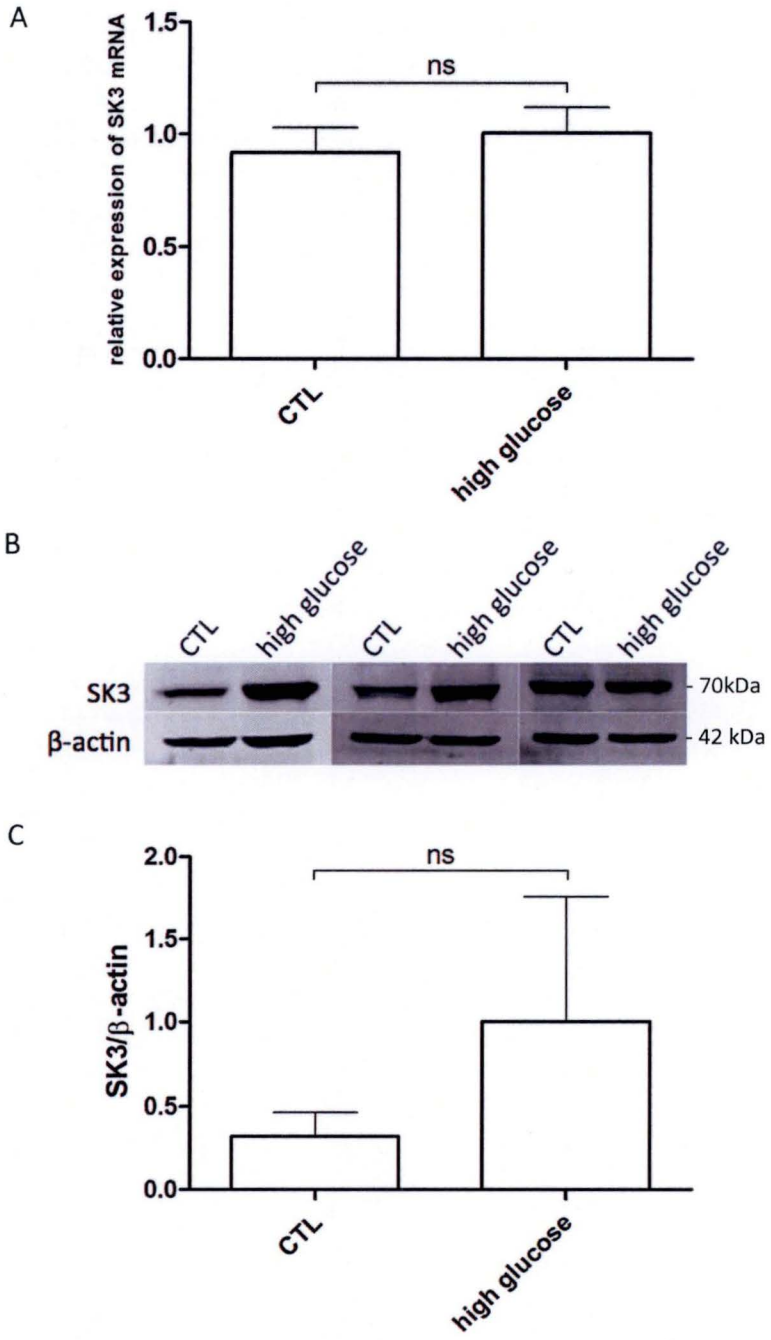

Figure 4.4. Effect of glucose on SK3 mRNA expression or on SK3 protein levels in EA.hy926 cells. The effect of glucose on SK3 mRNA and protein expression were assessed by RT-qPCR (A) and quantification of western blot (B and C), respectively. EA.hy926 cells were grown in high glucose conditions for 24 h (25 mM) compared to control glucose levels (5.5 mM). **A**, quantitative PCR of SK3, using new designed and validated primers, was normalized by TBP and analyzed using the $e^{-\Delta\Delta Cq}$ method. (n=3, unpaired t-test, $p>0.05$). **B**, Western blot of SK3 of twenty micrograms of total proteins extracted from EA.hy926 cells grown in high glucose concentration for 24 h compared to control glucose levels. **C**, Quantification of SK3 protein levels obtained by western blot, β-actin was used as reference for normalization (n=3, unpaired t-test, $p>0.05$). Means ± SD are shown.

whose expression decreased significantly after a 24 h exposure to high glucose concentrations when analyzed statistically with unpaired t-test ($p<0.05$). Previous studies on patients with type 1 diabetes mellitus showed a perturbation of HA metabolism consisting in increased plasma levels of HA and HYAL1 that could be correlated with the development of vascular complications (Nieuwdorp et al., 2007). The downregulation of *HYAL1* expression or the decreased stability of HYAL1 mRNA in the endothelial cells grown in hyperglycemic conditions does not necessarily contradict the increased level of HYAL1 in the plasma of T1DM patients. Indeed, endothelial cells are known to perform endocytosis of plasma HYAL1 (Gasingirwa et al., 2010), and thus, the intrinsic expression of HYAL1 by the endothelial cell itself may be of secondary importance. Additionally, *in vivo* studies using diabetic mice models or *in vitro* studies based on hyperglycemia growth conditions to mimic diabetes show an increase in HA in the ECM of glomerular mesangial cells and pancreatic islets but a decrease in HYAL1 expression (Wang and Hascall, 2004; Nagy et al., 2015).

Furthermore, the activity of HYAL1 in EA.hy926 cells could be detected in none of the conditions, by performing native zymography assays. This indicates a low expression and activity of endogenous HYAL1 (data not shown). It is important to note that the measured mRNA expressions do not necessarily reflect protein expression, when considering that elements such as miRNAs have a supplemental regulation capacity on the translation of mRNA into the protein, or that other post-translational mechanisms implicated in protein turnover can occur (Kendrick 2004).

4.1.4 Effect of high glucose on SK3 in EA.hy926 cells

To test whether the decrease in HYAL1 mRNA caused by a 24 h exposure to high glucose could have an effect on the mRNA expression and protein expression of SK3 in EA.hy926 cells, RT-qPCR and western blot assays were performed, respectively. Using a newly designed set of primers, validated and tested for efficacy, RT-qPCR was repeated in three independent replicates of EA.hy926 cells grown for 24 h in high glucose concentrations (Fig. 4.4. A). No statistically significant difference in SK3 mRNA levels was obtained comparing control cells grown exclusively in low glucose with high glucose growth for 24 h by unpaired t-test analysis. To determine SK3 protein expression in response to high glucose exposure western blots were performed using the same samples as for RT-qPCR assays (Fig. 4.4. B) and quantified by normalization with the protein expression of β-actin (Fig. 4.4. C). Here again, no statistically significant difference in SK3 protein expression between both conditions could be detected using unpaired t-test ($n=3$, $p>0.05$). These findings are in concordance with the unaltered mRNA and protein expression of SK3 in mesenteric arteries of STZ-induced diabetic WT and Hyal1$^{-/-}$ mice (Dogné, submitted data). However in the STZ-induced Apolipoprotein E (ApoE)-deficient diabetic mouse model of atherosclerosis a decrease of SK3 mRNA has been suggested to be implicated in the observed increased endothelial dysfunction (Ding et al., 2005), which may be related to the diabetes-related dyslipidemia rather than to hyperglycemia.

In summary, the decrease of HYAL1 mRNA in high glucose growth conditions did not result in an increase of SK3 mRNA or protein expression as it could be imagined when considering that Hyal1$^{-/-}$ mice show a significant increase of SK3 mRNA and protein expression. Given the low endogenous expression of HYAL1 in EA.hy926 cells, the decrease of HYAL1 in this cell type may not be serious enough to provoke expression changes in SK3.

Thus, the endothelial cell model EA.hy926 may not be adapted for testing the putative correlation between HYAL1 and SK3 by the mean of hyperglycemia studies. Taken into

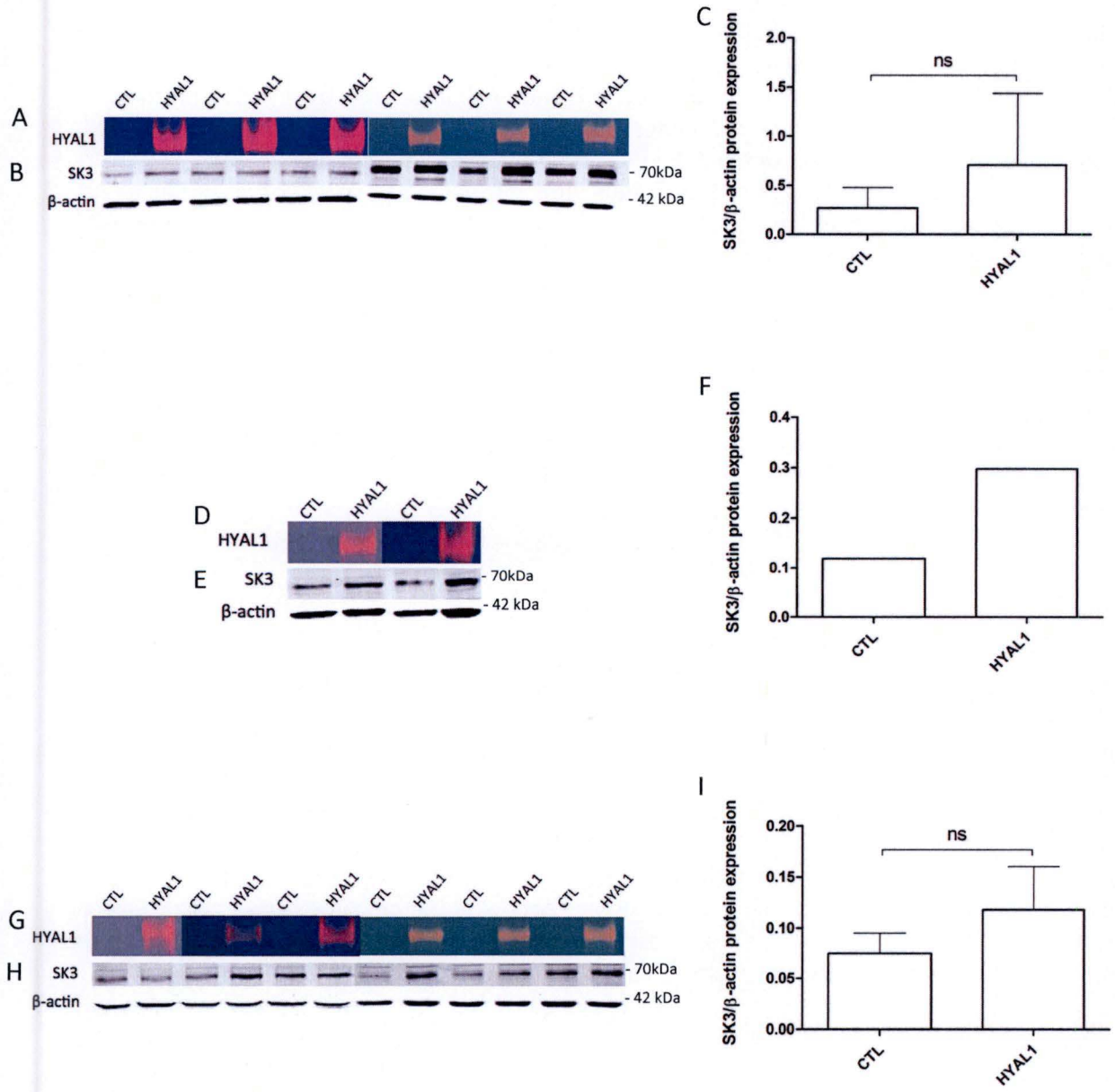

Figure 4.5. Effect of *HYAL1* transfection on SK3 protein expression. EA.hy926 (A, B, C), HMEC-1 (D, E, F), and MCF7 (G, H, I) cells were transfected during 4 hours with a HYAL1 encoding plasmid (4 µg)-Lipofectamine (8 µl) mix or exclusively Lipofectamine as transfection reagent control. The success of transfection was tested by native zymography (A, D, G) and the expression of SK3 protein was tested by performing western blots (B, E, H) and quantified (C, F, I). **A, D, G**, five micrograms of total proteins were loaded on each lane of an SDS-free 10% polyacrylamide gel with incorporated HA. The gel was incubated for 20 h in formate. **B, E, H**, ten micrograms of total proteins were loaded on each lane of a 10% SDS-PAGE gel, SK3 was detected with the appropriate antibody and β-actin was used as loading control. **C, F, I**, SK3 has been quantified and normalized with β-actin (n=6, except for HMEC-1 where n=2; unpaired t-test; $p>0.05$). Means ± SD are shown. Cells were lysed and proteins extracted 24 h after transfection. Pink bands represent digested HA by HYAL1.

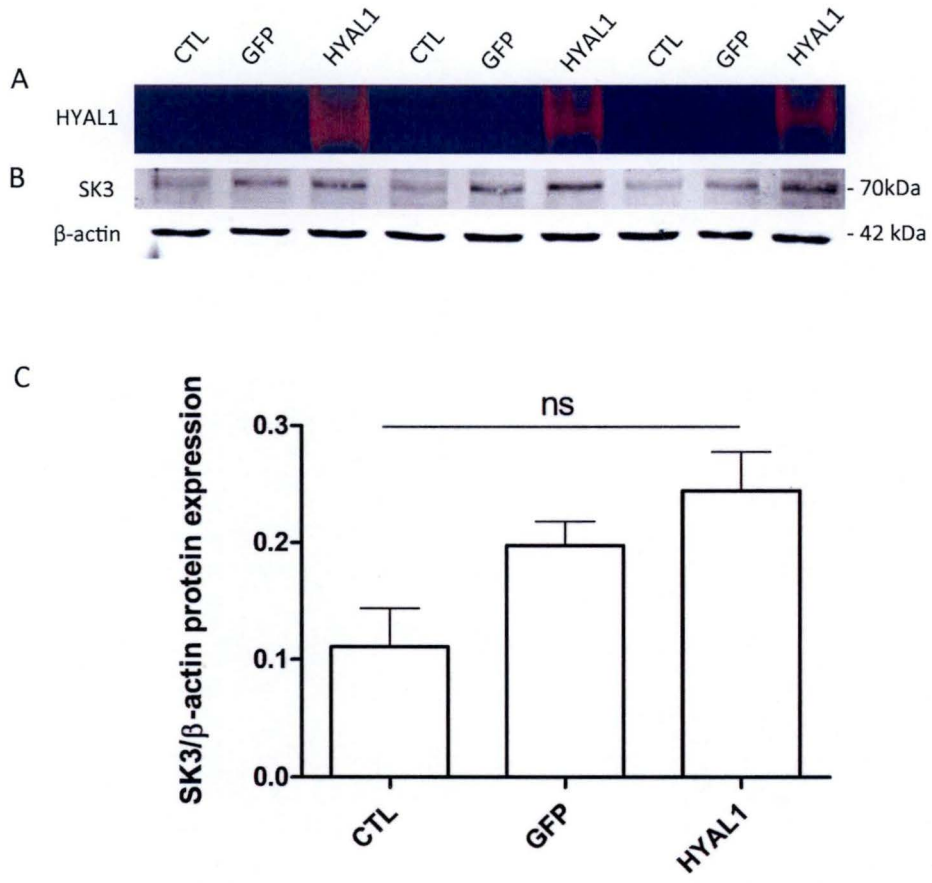

Figure 4.6. Effect of a *GFP* transfection control in the *HYAL1* transfection assay. EA.hy926 cells were transfected during 4 hours with a HYAL1 encoding plasmid (4 µg)-Lipofectamine (8 µl) mix or exclusively Lipofectamine as transfection reagent control, as well as with a GFP encoding plasmid. The success of transfection was tested by native zymography (A) and the expression of SK3 protein was tested by performing western blots (B) and subsequent quantification (C). **A**, five micrograms of total proteins were loaded on each lane of an SDS-free 10% polyacrylamide gel with incorporated HA. The gel was incubated for 20 h in formate. **B**, ten micrograms of total proteins were loaded on each lane of a 10% SDS-PAGE gel, SK3 was detected with the appropriate antibody and β-actin was used as loading control. **C**, SK3 has been quantified and normalized with β-actin (n=3, paired t-test, $p>0.05$). Means ± SD are shown. Cells were lysed and proteins extracted 24 h after transfection. Pink bands represent digested HA by HYAL1.

account the fact that (a) high glucose neither had an effect on the HAS enzymes, nor on HYAL2 and HYAL3, (b) HYAL1 activity in EA.hy926 cells could be detected in none of the growth conditions, EA.hy926 cells were henceforward grown in their optimal growth conditions containing high levels of glucose.

4.1.5 Overexpression of HYAL1

Another *in vitro* approach to test whether HYAL1 may have an impact on SK3 expression is by directly modifying HYAL1 expression. Because of the low endogenous expression in the EA.hy926 cell line, as well as in the HMEC-1 and MCF7 cell lines (data not shown), the use of siRNAs or shRNAs to specifically knock down *HYAL1* was not applicable. On the contrary, HYAL1 could be overexpressed in a transient manner by either transfecting a HYAL1 encoding plasmid or by enabling HYAL1 endocytosis.

4.1.5.1 Transient transfection of different cell lines with HYAL1

HYAL1 overexpression was performed by introducing a HA-tagged HYAL1 encoding plasmid into the cells using the transfection reagent Lipofectamine 2000, in parallel to a transfection reagent control. The transfection assay was performed in the human endothelial cell line EA.hy926 (Fig. 4.5. A, B, C), in the human dermal microvascular cell line HMEC-1 (Fig. 4.5. D, E, F), as well as in the MCF7 breast cancer cell line (Fig. 4.5. G, H, I), the latter being used to see whether the expression of the 66 kDa variant of ER-α may influence the results. None of these cell lines express HYAL1 at a level that HYAL1 activity could be detected by zymography. The transfections with the *HYAL1-HA* plasmid were repeated six times in all of the three cell types; HYAL1 expression and activity in *HYAL1* transfected cells were confirmed by performing native zymography assays compared to no HYAL1 activity in control (Fig. 4.5. A, D, G), then the protein expression of SK3 was examined applying western blot technique (Fig. 4.5. B, E, H) with β-actin as normalization protein for quantification (Fig. 4.5. C, F, I). As a general conclusion, no difference of SK3 expression in either endothelial cell line lacking the 66 kDa variant of ER-α or the MCF7 cell line expressing both ER-α variants could be measured by quantifying SK3 protein levels and performing unpaired t-test statistical analysis ($n=6$, $p>0.05$). The analysis of SK3 in HMEC-1 cells could only be performed twice because of transfection problems, not allowing statistical analysis. Altogether, these findings seem to indicate that the increase in SK3 expression as observed in Hyal1$^{-/-}$ mice is not solely the result of Hyal1 deficiency.

An additional control, by introducing a GFP encoding plasmid, was performed in the EA.hy926 cell line to test whether the excessive production of a protein may have an effect *per se* on the results of transfection with *HYAL1* (Fig. 4.6.). It could be shown that, as for the transfection reagent control, the GFP transfection control did not have any statistically significant effect on the expression of SK3 by performing paired t-test analysis (t-test, $p>0.05$). However, the transfection of GFP did have an influence on SK3 expression. Overloading the cell with a plasmid encoding a protein that needs transcription, translation and transportation within the cell may therefore impact SK3 expression. Thus, correct interpretation of the findings in HMEC-1 and MCF7 cells requires the performance of the GFP transfection control.

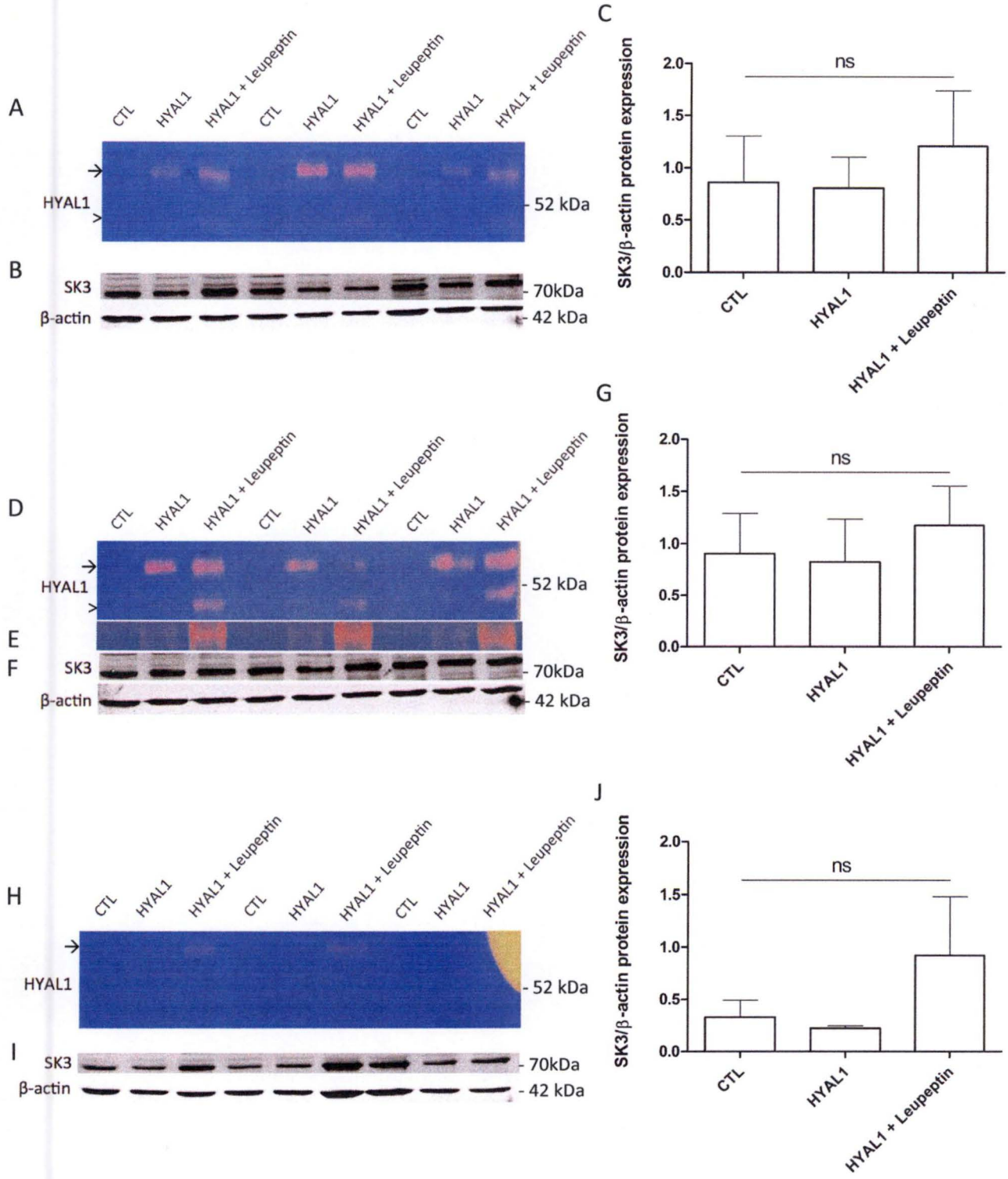

Figure 4.7. Effect of rhHYAL1 endocytosis on SK3 mRNA and protein expression. The effect of rhHYAL1 endocytosis on SK3 protein expression was tested in EA.hy926, (A, B, C), HMEC-1 (D, E, F, G), and MCF7 cells (G, H, I). Cells were incubated in presence of human recombinant HYAL1 during 3 hours with or without incubation of the protease inhibitor leupeptin. The efficacy of endocytosis was assessed by renatured zymography (A, D, H), or native zymography (E) and expression of SK3 protein was tested by performing western blots (B, F, I) and subsequent quantification (C, G, J). **A, D, H**, five micrograms of total proteins were loaded on each lane of a 10% SDS-PAGE gel with incorporated HA. The gel was incubated for 2 h in Triton X-300 and 20h in formate. **E**, five micrograms of total proteins were loaded on each lane of an SDS-free 10% polyacrylamide gel and the gel was incubated for 20 h in formate. **B, F, I**, ten micrograms of total proteins were loaded on each lane of a 10% SDS-PAGE gel. SK3 was detected with the appropriate antibody and β-actin was used as loading control. **C, F, J**, SK3 was quantified and normalized with β-actin and values are represented ± SD (n=3, One-way ANOVA, $p>0.05$). Cells were lysed and proteins extracted 24 h after endocytosis.

4.1.5.2 Endocytosis of HYAL1 in different cell lines

The effect of 3-h endocytosis (pulse) of recombinant human HYAL1 on the expression of SK3 was studied in the macrovascular endothelial cell type EA.hy926 (Fig. 4.7. A, B, C) and the microvascular cell line HMEC-1 (Fig. 4.7. D, E, F, G.), as well as in the breast cancer cell line MCF7 (Fig. 4.7. H, I, J). Protein level of SK3 was assessed by western blotting 24 h post-endocytosis.

Endocytosis success was tested by renaturated zymography assay of three replicates of each cell line. It should be reminded that none of these cell lines has an intrinsic HYAL1 expression detectable by zymography as shown by the control condition. The activity of rhHYAL could be revealed in all cell lines when incubated with recombinant rhHYAL1 compared to incubation with normal culture medium (Fig. 4.7. A, D, H). This experiment aims to determine whether HYAL1, in its unprocessed or processed form, has an impact on SK3 protein expression. The detection of the premature (unprocessed) 57 kDa form of rhHYAL1 after a 24-h chasing time was unexpected because previous studies of rhHYAL1 endocytosis conducted by Puissant et al. (2014) demonstrated that already after 2 h of chase, only the mature (processed) 47 kDa form could be detected in a murine macrophage cell line. Indeed, with increasing chasing time, the unprocessed form of rhHYAL1 disappears continuously and is transformed into the processed form of rhHYAL1. Several hypotheses could explain these unexpected results showing solely the unprocessed form of rhHYAL1 after 24 h of chasing time. Firstly, the presence of an rhHYAL1 precursor form could be the result of its retention in early endosomes so that rhHYAL1 does not reach the lysosomes. This is rather improbable when considering that endothelial cells have been described to express the mannose receptor implicated in the capture of HYAL1 in macrophage cells (Elvevold et al., 2008). However, the capture of HYAL1 by the cell surface mannose receptor might not trigger the same subcellular trafficking in both cell types. Secondly, the detection of the proteolytically processed form of rhHYAL1 may have been hampered by the zymography technique used here, consisting in SDS-PAGE resolution followed by subsequent renaturation. Actually, Puissant et al. (2014) showed that renaturated zymography fails to detect the processed form of rhHYAL1 in contrast to native zymography enabling the visualization of both the premature and the processed form; the latter has the disadvantage that the two forms cannot be distinguished.

One suggestion explaining why renaturated zymography fails to detect the processed form of HYAL1 in our experiments is that a lysosomal thiol reductase (Arunachalam et al., 2000) reduces one or more of the five disulfide bonds present in the HYAL1 enzyme that may not be reconstructed during the renaturation step of renaturated zymography (Zhang et al., 2009; Puissant et al., 2014). Another suggestion is that HYAL1 may require closely linked partners to support processed HYAL1 activity, which are not present when performing SDS-PAGE (Boonen et al., 2014). Thus, the band of HA digestion produced by the rhHYAL1 precursor form could be minor compared to the non-detected mature form. However, by performing a native zymography on the same HMEC-1 cell lysates, but with an additional freezing stage, rhHYAL1 activity could only be observed when rhHYAL1 was incubated simultaneously with leupeptin and not in the rhHYAL1 alone endocytosis (Fig. 4.7. E). The only possible explanation for this observation is that the processed form of rhHYAL1 detected in renaturated zymography is more stable and thus responsible for the observed signal in the native zymography. Finally, the rinsing steps performed before chasing and before protein extraction could have been inefficient to completely eliminate the rhHYAL1 that partly attaches to the cell surfaces during pulse.

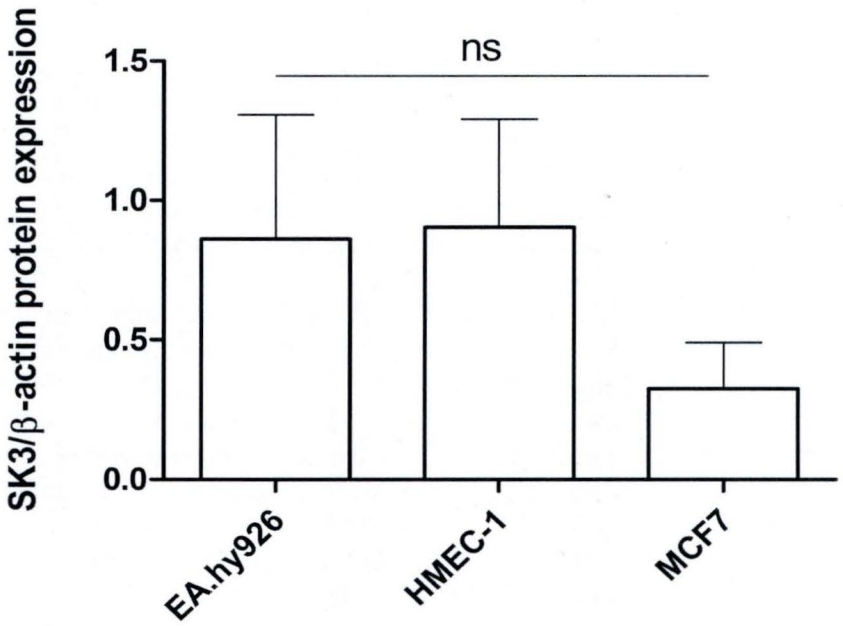

Figure 4.8. Protein expression of SK3 in different cell lines. The expression of SK3 protein was been assessed by western blot in the endothelial cell lines EA.hy926, HMEC-1, and the breast cancer cell line MCF7. Ten micrograms of total proteins were loaded on each lane of a 10% SDS-PAGE gel. SK3 was detected with the appropriate antibody and quantified by normalization with β-actin. Means ± SD are shown (n=3, One-way ANOVA, $p>0.05$).

In order to test whether the unprocessed form *per se* impacts SK3 protein expression, the cells were incubated with the thiol protease inhibitor leupeptin with the aim to inhibit the processing of HYAL1 in the lysosomes (Furuno et al., 1982). The transfection success was tested by renaturated zymography (Fig. 4.7. A, D, H). Contrary to our expectations, leupeptin failed to inhibit HYAL1 processing and led to different findings between the cell types. In the endothelial cell types, both the unprocessed and processed form of rhHYAL1 could be detected (Fig. 4.7. A, D, indicated with arrows). In general, the processed form of rhHYAL1 is less important than the unprocessed form. There are several theories to explain the detection of the cleaved form of HA using renaturated zymography. One explanation suggests that the observed processed form is only an active cleavage intermediate with a molecular weight close to the end product of cleavage, which in turn, as explained above, cannot be detected using renaturated zymography. Thus, the formation of a processed rhHYAL1 from a precursor rhHYAL1 could be the result of successive cleavage steps. A second suggestion is that the incubation with leupeptin for 24 h has side effects on lysosomes. Previous studies could reveal that leupeptin inhibits the fusion between the lysosome and amphisome, resulting from the fusion of autophagosomes with endosomes (Berg et al., 1998). Here, it could be suggested that leupeptin acts in an indirect way to inhibit the putative reduction of disulfate bridges by a lysosomal thiol reductase, leading to the detection of processed rhHYAL1 in renaturated zymography.

In contrast to the endothelial cell lines, the HA digestion by endocytosed rhHYAL1 in MCF7 cells is barely detectable (Fig. 4.7. H). In general, it could be observed that the MCF7 cell line has less rhHYAL1 activity following rhHYAL1 endocytosis compared to the endothelial cell lines, which is probably due to a lower endocytic capacity of this cell line. Thus the absence of the processed rhHYAL1 enzyme when incubated with leupeptin may simply be the result of an insufficient amount of total protein loaded on the gel compared to the other cell lines. The high capacity of rhHYAL1 endocytosis by endothelial cells may highlight the important role attributed to HA turnover, at least in sinusoidal endothelial liver cells, suggesting that lysosomal HYAL1 is the result of endocytosis of serum HYAL1 (Gasingirwa et al., 2010).

The detection of SK3 protein expression by western blot (Fig. 7. B, F, I) after HYAL1 endocytosis performed in triplicates in the three cell lines did not result in a statistically significant difference when normalized with β-actin and analyzed using unpaired t-test, $p>0.05$ (Fig. 4.7. C, G, J). On the basis of the results obtained by zymography assay where the presence and quantity of premature and processed forms of rhHYAL1 could not be fully elucidated, further interpretation of SK3 protein expression in response to rhHYAL1 transfection is not possible.

Another interesting observation could be made by comparing the three cell lines in their SK3 protein expression levels relative to β-actin expression (Fig. 4.8). Actually, MCF7 cells have a much lower expression of SK3 protein compared to both endothelial cell lines. This result is not surprising since SK3 is known to play a crucial role in endothelial cell function. However the few studies about SK3 function in human mammary cancer cell lines suggest a role of SK3 in cancer cell migration in combination with other voltage-gated ion channels but considered MCF7 cells as lacking SK3 (Potier et al., 2006, 2011; Le Guennec et al., 2007).

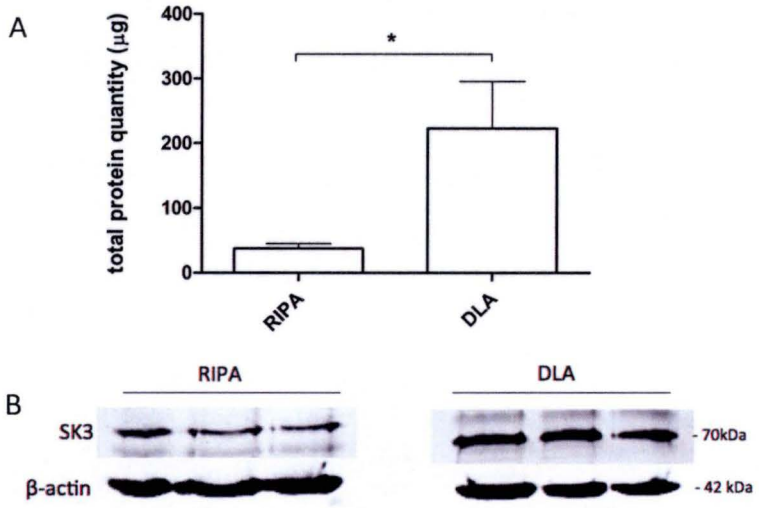

Figure 4.9. Comparison of two methods to extract proteins from mesenteric arteries. Proteins of mesenteric arteries of mice were extracted either by using the RIPA lysis buffer and Potter-Elvehjem homogenizer or DLA lysis buffer without Potter-Elvehjem homogenizer. **A**, Total protein quantity was determined based on protein concentration and final sample volume and analyzed (*, $p<0.05$, unparied t-test, n=3). Means ± SD are represented. **B**, Ten micrograms of total proteins were loaded on each lane of a 10% SDS-PAGE gel, SK3 was detected with the appropriate antibody and β-actin was used as loading control.

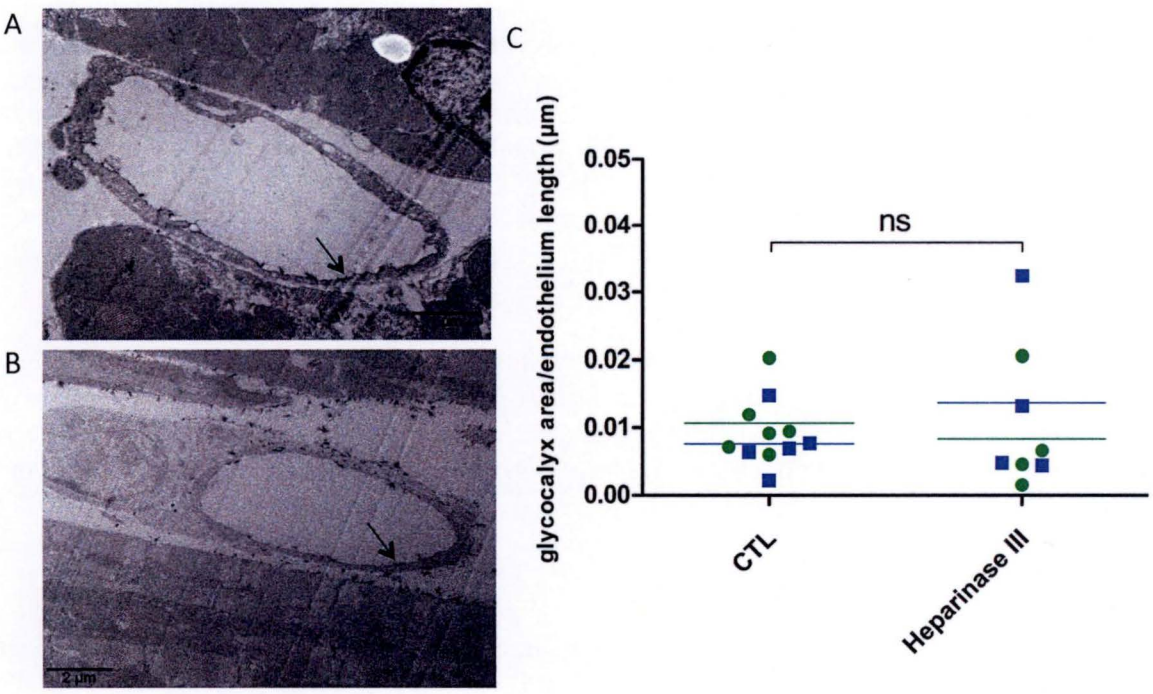

Figure 4.10. Endothelial glycocalyx thickness after heparinase III (1 U) treatment. One enzymatic unit of heparinase or 100 µl of physiological salt solution as control was administered as a single tail vein bolus injection in Hyal1$^{-/-}$ mice. Twenty-four hours later, the heart of these mice was fixed and simultaneously stained with Alcian Blue 8GX. Segments of the left ventricle were prepared for electron microscopy and observed with the transmission electron microscope. **A**, Electron microscopic overview of a control mice left ventricular blood vessel (bar=2 µm). **B**, Electron microscopic overview of a heparinase-treated left ventricular blood vessel. **C**, Quantification of glycocalyx thickness by dividing the glycocalyx area with the endothelium length of the measured vessel segment. Data were statistically analyzed by non parameric Mann Whitney test ($p>0.05$). Single dots represent the mean of one series of analyzed pictures. Blue and green dots differentiate the two mice of each treatment. Arrow points to the glycocalyx located at the luminal surface of endothelial cells.

4.2 *In vivo*: endothelial glycocalyx and SK3

4.2.1 Protein extraction from mesenteric arteries

The extraction of proteins from the mouse mesenteric arteries is the limiting step for further analysis because it determines not only the quantity of tissue lysate but also its quality. The extraction method using RIPA lysis buffer combined with mechanical grinding of the tissue using the Potter-Elvejehm homogenizer has been compared with the method consisting in lysis based on DLA lysis buffer followed by sonication. By analyzing the protein concentrations determined by Pierce protein assay as well as the final volume of tissue lysate prepared with the RIPA and DLA homogeneization method, the DLA protein extraction method enables a statistically significant increase in the final protein quantity according to an unpaired t-test analysis ($p<0.05$) (Fig. 4.9. A). This finding can be explained by the fact that the recovered volume of tissue lysate using the DLA homogeneization of mesenteric arteries is higher than using the Potter-Elvejehm homogenizer, where the loss of a part of the sample is unavoidable, and also by the higher protein concentration of the sample, considering that both samples were lysed in the same volume of lysis buffer.

Western blot analysis shows that both extraction methods enable the liberation of the membrane protein SK3, but indicate that the DLA method may be more efficient (Fig. 4.9. B).

In conclusion, the DLA protein extraction could be adapted to the mouse mesenteric arteries enabling an easier, faster and more powerful protein extraction.

4.2.2 Heparinase injection in Hyal1$^{-/-}$ mice

Hyal1 deficiency in mice leads to SK3 overexpression in mesenteric arteries as well as to an increase in the thickness of endothelial glycocalyx (Dogné, submitted data). To test whether these two findings may correlate, we decided to test the effect of the degradation of endothelial glycocalyx. For this purpose, one enzymatic unit of the heparinase III enzyme was injected intravenously 24 h before staining of the endothelial glycocalyx in order to cleave heparin sulfates and thus degrade the endothelial glycocalyx in Hyal1 deficient mice.

The endothelial glycocalyx was stained with Alcian Blue 8GX and visualized by transmission electron microscopy. Electron views of left ventricular blood vessels representative for control or heparinase-treated mice are represented in Fig. 4.10. A and B. The quantification of the endothelial glycocalyx thickness, by dividing glycocalyx area with endothelium length of the measured region (Fig. 4.10 C), reveals no change in endothelial glycocalyx thickness of cardiac vessels following the injection of heparinase III. This result was somewhat surprising as previous studies had shown that heparinase efficiently degrades the endothelial glycocalyx (Bruegger et al., 2005; Potter et al., 2009; Strunden et al., 2012). However, there may be technical differences between our experiments and those of previous investigators. For instance, Bruegger et al. (2005) used a short treatment with a high quantity of heparinase on isolated and perfused guinea pig hearts. Strunden et al. (2012) also performed *ex vivo* studies to provoke endothelial degradation with heparinase. Thus, we may suggest that *in vivo* heparinase administration 24 h before glycocalyx thickness measurements may have additional effects on the glycocalyx structure, its degradation and synthesis. In contrast to this hypothesis are the findings obtained by Potter et al. (2010) who showed that 1 U of heparinase efficiently degrades the endothelial glycocalyx in mice, an effect that persists as long as 7 days. However, these authors did not visualize the endothelial glycocalyx by

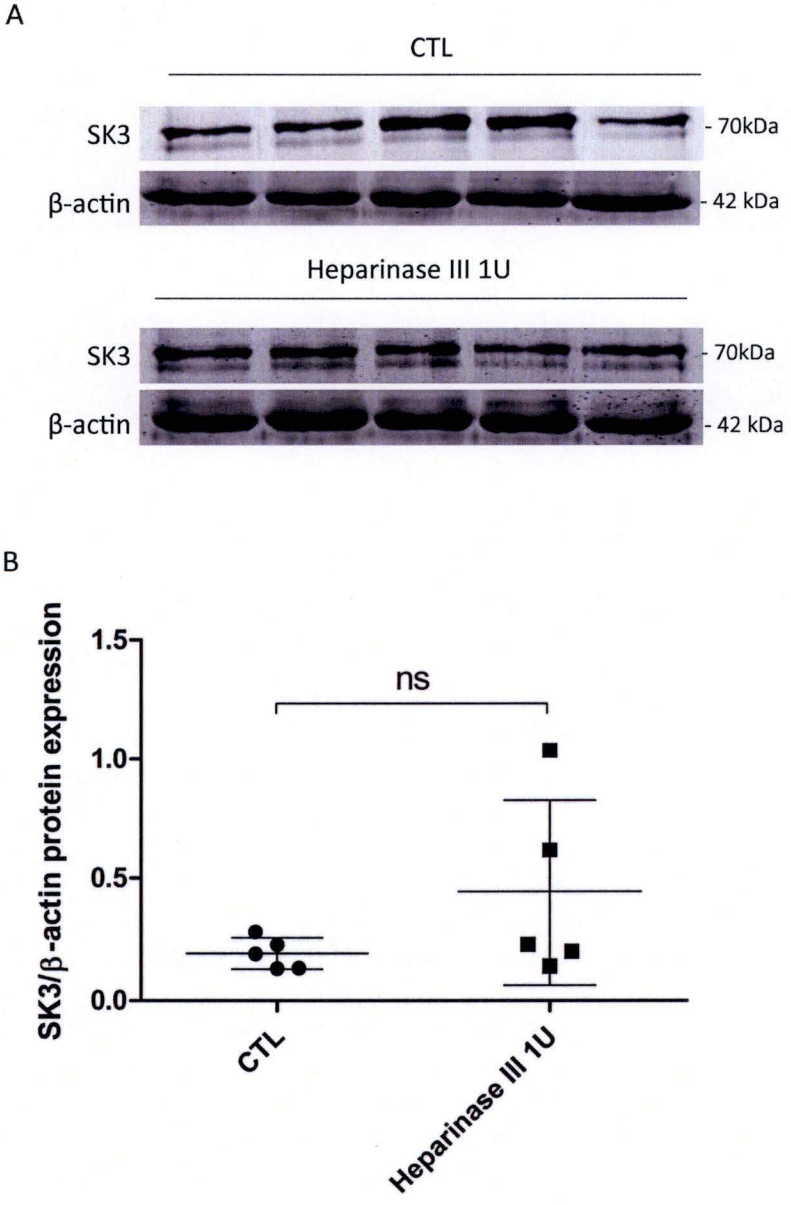

Figure 4.11. Effect of Heparinase III on SK3 protein expression in Hyal1$^{-/-}$ mice. The expression of SK3 protein of five Hyal1 deficient mice injected with 1 U of Heparinase III or physiological salt solution (NaCl 0.9%) 24 h before dissection was assessed by western blot (A) and quantified (B). **A**, ten micrograms of total proteins were loaded on each lane of a 10% SDS-PAGE gel, SK3 was detected with the appropriate antibody and β-actin was used as loading control. **B**, SK3 was quantified and normalized with β-actin (n=5, unpaired t-test, $p>0.05$).

electron microscopy but used a velocity determination method to indirectly estimate endothelial glycocalyx.

A second hypothesis to explain the absence of change in endothelial glycocalyx thickness in response to heparinase treatment is that, compared to the other studies based on heparinase mediated endothelial glycocalyx degradation, we used a mouse model deficient for HYAL1. The organization and the proportion of the different components of the endothelial glycocalyx of Hyal1$^{-/-}$ mice have not been elucidated yet. Thus, the reaction of Hyal1$^{-/-}$ mice may not be comparable to the reaction of wild-type mice following heparinase treatment.

4.2.3 SK3 expression after heparinase treatment

In order to see whether heparinase-induced endothelial glycocalyx degradation influences SK3 protein expression in mesenteric arteries of Hyal1$^{-/-}$ mice, western blot (Fig. 4.11. A) and quantification of SK3 normalized with β-actin (Fig. 4.11. B) were performed on mesenteric artery tissue lysates 24 h after heparinase III injection. No significant difference in SK3 protein levels could be observed between mice injected with heparinase III and those injected with a physiologic salt solution (control group) using unpaired t-test analysis ($n=5$, $p>0.05$). expression. As explained above, the heparinase III injection failed to degrade endothelial glycocalyx structure, thus further interpretations of SK3 expression after heparinase administration are not possible.

Conclusion and Perspectives

5 Conclusion and Perspectives

5.1 *In vitro*: HYAL1 and SK3

Two different endothelial cell lines, EA.hy926 as a macrovascular cell line and HMEC-1 as a microvascular cell model, were used to test the hypothesis that the observed increase of SK3 in Hyal1 deficient mice can directly be linked to the loss of Hyal1 activity. Several approaches were used in this study to investigate this question.

Firstly, based on the findings that SK3 gene expression is enhanced by estrogen through the estrogen receptor alpha as discovered by Jacobson et al. (2003), a reporter gene construct was used to test the effect of *HYAL1* expression on estrogen response element binding and transcription of the luciferase reporter gene located downstream to *ERE*. The experiment was first performed in MCF7 cells, described in the literature to express a full length 66 kDa and an N-terminal truncated 46 kDa variant of ER-α. HYAL1 expression could be shown to lead to a decrease in ERE-luciferase activity as well as generally increased ERE-luciferase activity following stimulation with 17β-estradiol. However, the experiment should be repeated using additional controls to validate the results, such as the transfection with a plasmid encoding a truncated or non-active form of HYAL1. Additionally, these results should be regarded with caution because the expression of the normalization plasmid was not stable in the different conditions. Thus, the assay should be repeated using another normalization gene because previous studies already discovered that the activity of pRL-TK is affected by hormone treatment (Ibrahim et al., 2000).

Then, the same dual luciferase reporter assay was performed with endothelial EA.hy926 cells. However, the activity of ERE-luciferase was insufficient to be differentiated from background levels. By testing the expression of ER-α we could show that MCF7 cells express both ER-α receptor variants (46 kDa and 66 kDa) but EA.hy926 cells do not, rather surprisingly. This result prompted us to examine the scientific literature in more details. Actually, controversial information is available on ER-α expression in EA.hy926 cells. Whereas its primary cell line, human umbilical vein cells (HUVEC), was shown to have both ER-α variants, only the 46 kDa form could be detected by western blot assays in EA.hy926 cells. The use of a C-terminal antibody is required to get a final answer on the expression of different ER-α variants in the EA.hy926 used in this study. The capacity of EA.hy926 cells to activate ERE-luciferase reporter gene is another debated question in the literature. Whereas a study by Russell et al. (2000) showed that the ERE-luciferase construct is not inducible in EA.hy926 cells, another study led by Figtree et al. (2003) detected ERE-luciferase activity and responsiveness to E2 in EA.hy926 but concluded the ER-α 46 kDa to be only a weak transcriptional activator and to rather play a role in acute estrogen signaling. HMEC-1, another endothelial cell line, was tested for ER-α expression in our experiments but the results were similar to those of EA.hy926 cells.

In conclusion, the dual luciferase assay based on *ERE*-luciferase transcriptional activation may not be the ideal experimental model to study the effect of HYAL1 on SK3 in endothelial cells.

Secondly, it is known that diabetes and especially the hyperglycemia feature of diabetes impact HA and HYAL1 levels. The plasma levels of HYAL1 increase in diabetic patients but decreases in different cells and tissues when exposed to high glucose, mimicking hyperglycemia and diabetes *in vitro* (Wang and Hascall, 2004; Nagy et al., 2015). The

recommended culture medium for EA.hy926 cells contains high levels of glucose (25 mM) compared to physiological glucose levels (5.5 mM). It was thus necessary to test whether the genes involved in HA metabolism (*HASs* and *HYALs*, especially *HYAL1*) in cultured EA.hy926 cells are influenced by high glucose exposure for 24 h because they are the basis of this study. *HYAL1* expression (but not the other genes tested) decreased significantly in high glucose medium. Thus, the exposure of EA.hy926 cells to high glucose could be used as an indirect model to test the effect of the decrease of *HYAL1* expression on SK3 gene and protein expression. As a result, high glucose exposure impacted neither *SK3* mRNA expression nor SK3 protein levels. In conclusion, high glucose may not sufficiently impact HYAL1 expression to be a good model to test whether Hyal1 deficiency in mice is responsible for the increase in SK3 expression.

The last two approaches testing the effect of HYAL1 on SK3 in this study were not based on the direct modification of HYAL1 expression nor on ER-α as a possible mediator between HYAL1 and SK3. As a next step, overexpression studies were performed using either a simple transfection with a HYAL1 encoding plasmid or endocytosis of recombinant human HYAL1. These assays were performed in macrovascular endothelial cells, EA.hy926, and microvascular endothelial cells, HMEC-1. The use of these two cell lines was important knowing that the behavior and response to HYAL1 overexpression and SK3 expression may be different due to the different functions of macro- versus micro-vascular endothelial cells, as well as their contribution to macro- or micro-vascular complications in diabetes. The breast cancer cell line MCF7 cells was chosen as a control to test whether the expression of the two ER-α variants leads to the generation of similar results compared with endothelial cells.

The transfection of *HYAL1* did not have an effect on SK3 expression in any of the tested cell lines. However, the transfection with *HYAL1* led to an almost statistically significant increase in SK3 protein expression ($p=0.05$) in MCF7 cells. The control used in this study was a simple transfection agent, which may not be sufficient to control the effects of transfection *per se*. Thus, an additional control, consisting in the transfection with a gene coding for a protein (GFP) that is thought *a priori* not to have any effect on the target proteins, was tested in a first assay in EA.hy926 cells. Even though no statistically significant results were obtained, it could be shown that the transfection of GFP generates intermediate levels of SK3 between the transfection agent control and HYAL1 transfection. Thus, transfection of GFP is considered a better control and should absolutely be performed in HMEC-1 and MCF7 cells to confirm the results obtained in the previous experiments. Ideally, the transfection with a *HYAL1* plasmid generating a truncated or inactive HYAL1 enzyme should be performed.

Endocytosis assays of rhHYAL1 did not lead to statistically significant differences in SK3 expression. Importantly, testing the success of endocytosis by renaturated zymography revealed firstly only a rhHYAL1 enzymatic activity at a molecular weight of 57 kDa, leading to the suggestion that rhHYAL1 may not be processed in the endothelial cell lines and may stay in an unprocessed form or that the processed form of rhHYAL1 is not stable enough to be detectable 24 h after endocytosis. Secondly, the incubation of cells with leupeptin in addition to rhHYAL1 in order to block rhHYAL1 processing resulted in the observation of a processed from of rhHYAL1 with a molecular weight of around 47 kDa. Several suggestions have been made to explain these unexpected results (cf. 4.1.5.2). A more complete understanding of HYAL1 processing is required to control the experimental conditions and to produce interpretable results of SK3 expression.

If we compare the transfection assay using a *HYAL1*-HA plasmid with the endocytosis assay where the cells are incubated with a growth medium supplemented with rhHYAL1, we may conclude that the latter approach is closer to physiological conditions because less variables can interfere with the results and lead to experimental artifacts.

As a general conclusion for the *in vitro* studies using the endothelial cell lines EA.hy926 and HMEC-1, or the non-endothelial cell line MCF7, we observed no effect of HYAL1 on SK3 expression. The dual luciferase reporter gene assay based on ERE-luciferase as well as the effect of high glucose do not seem to be the ideal models to test the effect of HYAL1 on SK3. The transfection and endocytosis assays are, on the other hand, better models to test the effect of HYAL1 on SK3 but it should be kept in mind that the optimization of these assays as well as the final completion of the analyses are necessary to draw final conclusions on the question whether HYAL1 deficiency *per se* is responsible for increased SK3 expression.

5.2 *In vivo*: endothelial glycocalyx and SK3

Beside the increased expression of SK3, Hyal1 deficient mice have thicker endothelial glycocalyx compared to wild-type mice. Thus, it was suggested that the increased endothelial glycocalyx thickness causes an increase in the expression of SK3. An *in vivo* approach has been chosen to test this hypothesis, which is based on enzymatic degradation of endothelial glycocalyx in Hyal1 deficient mice followed by the evaluation of SK3 protein levels. Although it is known that cultured endothelial cells have an endothelial glycocalyx, the great contrast between measured glycocalyx thickness in *ex vivo* and *in vivo* measurements as well as the generation of conflicting results make *in vivo* studies the most valid model to study endothelial glycocalyx (Drake-Holland and Noble, 2012).

Before the actual test of the effect of endothelial degradation on SK3 expression, another method for mesenteric artery homogeneization to extract proteins was developed and tested. This method is based on DLA as a lysis buffer rather than the previously developed method of protein extraction based on RIPA lysis buffer. It could be shown that the total quantity of proteins extracted with DLA is significantly higher compared to extraction with the RIPA lysis protocol. This increase is due on one hand to higher concentrations of total proteins and on the other hand to a lower loss of lysate volume compared with the RIPA lysis method. Additionally and most importantly, it seems that the DLA method extracts SK3 more efficiently compared to RIPA. Thus, the DLA extraction method turns out to be faster, more efficient, and to achieve higher yields of total protein quantity. It should be noted that it remains to be tested whether these cell lysates can be used to perform RT-qPCR assays or zymography assays to assess Hyal1 enzymatic activity.

Endothelial glycocalyx degradation was the goal of the injections of heparinase III or, as control, physiological salt solution in Hyal1$^{-/-}$ mice 24 h before tissue fixation. The observation of left ventricle segments in transmission electron microscopy and the subsequent analysis of endothelial glycocalyx thickness revealed that the heparinase III treatment did not result in the disappearance of the glycocalyx. This observation is surprising in the sense that several studies used heparinase III *in vivo* or *ex vivo* and demonstrated endothelial glycocalyx degradation (Potter et al., 2009; Strunden et al., 2012). However, we should point out that Hyal1 KO mice were used in this study and, contrary to wild-type mice, their endothelial glycocalyx composition and organization have not been elucidated yet. The injection of heparinase III should be repeated in wild-type mice. In parallel to the microscopic analysis of heparinase III-treated mice, SK3 protein expression in mesenteric arteries was tested. No statistical significant difference in SK3 expression could be observed compared to Hyal1

deficient mice injected with physiological salt solution. These results are difficult to interpret in the absence of any significant change in glycocalyx thickness.

In conclusion, the *in vivo* assay to test the hypothesis that increased SK3 expression is linked to thicker endothelial glycocalyx, based on endothelial glycocalyx degradation by heparinase III, did not lead to a final confirmation or a final rejection of this theory. Indeed, further studies are necessary to find an efficient method of endothelial glycocalyx degradation *in vivo* and study its effect on SK3 gene expression.

Brief summary

In summary, neither the *in vitro* approaches to test the hypothesis that Hyal1 deficiency causes increased SK3 expression in Hyal1$^{-/-}$ mice nor the *in vivo* approach to test the hypothesis that increased SK3 expression in Hyal1$^{-/-}$ mice is caused by thicker endothelial glycocalyx could be confirmed or rejected during the current experiments. The final conclusion of this master's thesis is that future studies based on both hypotheses are necessary to elucidate the mechanism leading from Hayl1 deficiency to increased expression of SK3, an effect that may be cardioprotective in diabetic mice.

References

6 References

Afify, A.M., Stern, M., Guntenhöner, M. and Stern, R. (1993) Purification and characterization of human serum hyaluronidase. *Archives of Biochemistry and Biophysics*, **305**, 434–41.

Alphonsus, C.S. and Rodseth, R.N. (2014) The endothelial glycocalyx: A review of the vascular barrier. *Anaesthesia*, **69**, 777–784.

Arunachalam, B., Phan, U.T., Geuze, H.J. and Cresswell, P. (2000) Enzymatic reduction of disulfide bonds in lysosomes: characterization of a gamma-interferon-inducible lysosomal thiol reductase (GILT). *PNAS*, **97**, 745–750.

Balazs, E.A., Laurent, T.C. and Jeanloz, R.W. (1986) Nomenclature of hyaluronic acid. *The Biochemical Journal*, **235**, 903.

Bennett, H.S. (1962) Morhological aspects of extracellular polysaccharides. *Journal of Histochemistry & Cytochemistry*, **11**, 14–23.

Berg, T.O., Fengsrud, M., Strømhaug, P.E., Berg, T. and Seglen, P.O. (1998) Isolation and Characterization of Rat Liver Amphisomes. *Journal of Biological Chemistry*, **273**, 21883–21892.

van den Berg, B.M., Vink, H. and Spaan, J.A.E. (2003) The endothelial glycocalyx protects against myocardial edema. *Circulation Research*, **92**, 592–594.

Boonen, M., Puissant, E., Gilis, F., Flamion, B. and Jadot, M. (2014) Mouse liver lysosomes contain enzymatically active processed forms of Hyal-1. *Biochemical and Biophysical Research Communications*, **446**, 1155–1160.

Bosch, M.A., Kelly, M.J. and Rønnekleiv, O.K. (2002) Distribution, neuronal colocalization, and 17beta-E2 modulation of small conductance calcium-activated K(+) channel (SK3) mRNA in the guinea pig brain. *Endocrinology*, **143**, 1097–1107.

Bourguignon, L.Y.W., Singleton, P.A., Diedrich, F., Stern, R. and Gilad, E. (2004) CD44 Interaction with Na+-H+ Exchanger (NHE1) Creates Acidic Microenvironments Leading to Hyaluronidase-2 and Cathepsin B Activation and Breast Tumor Cell Invasion. *Journal of Biological Chemistry*, **279**, 26991–27007.

Brähler, S., Kaistha, A., Schmidt, V.J., Wölfle, S.E., Busch, C., Kaistha, B.P., et al. (2009) Genetic deficit of SK3 and IK1 channels disrupts the endothelium-deerived hyperpolarizing factor vasodilator pathway and causes hypertension. *Circulation*, **119**, 2323–2332.

Bruegger, D., Jacob, M., Rehm, M., Loetsch, M., Welsch, U., Conzen, P., et al. (2005) Atrial natriuretic peptide induces shedding of endothelial glycocalyx in coronary vascular bed of guinea pig hearts. *American Journal of Physiology. Heart and Circulatory Physiology*, **289**, H1993–H1999.

Camenisch, T.D., Spicer, A.P., Brehm-Gibson, T., Biesterfeldt, J., Augustine, M. Lou, Calabro, A., et al. (2000) Disruption of hyaluronan synthase-2 abrogates normal cardiac morphogenesis and hyaluronan-mediated transformation of epithelium to mesenchyme. *Journal of Clinical Investigation*, **106**, 349–360.

Carey, D.J. (1997) Syndecans: multifunctional cell-surface co-receptors. *The Biochemical Journal*, **327**, 1–16.

Chain, E. and Duthie, E.S. (1940) Identity of hyaluronidase and spreading factor. *British Journal of Experimental Pathology*, **21**, 324–338.

Chambliss, K.L., Yuhanna, I.S., Mineo, C., Liu, P., German, Z., Sherman, T.S., et al. (2000) Estrogen receptor alpha and endothelial nitric oxide synthase are organized into a functional signaling module in caveolae. *Circulation research*, **87**, E44–E52.

Chandy, K.G., Fantino, E., Wittekindt, O., Kalman, K., Tong, L.L., Ho, T.H., et al. (1998) Isolation of

a novel potassium channel gene hSKCa3 containing a polymorphic CAG repeat: a candidate for schizophrenia and bipolar disorder? *Molecular Psychiatry*, **3**, 32–7.

Chen, G., Suzuki, H. and Weston, A.H. (1988) Acetylcholine releases endothelium-derived hyperpolarizing factor and EDRF from rat blood vessels. *British Journal of Pharmacology*, **95**, 1165–1174.

Compton, S.J. and Jones, C.G. (1985) Mechanism of dye response and interference in the Bradford protein assay. *Analytical Biochemistry*, **151**, 369–374.

Constantinescu, A.A., Vink, H. and Spaan, J.A.E. (2003) Endothelial Cell Glycocalyx Modulates Immobilization of Leukocytes at the Endothelial Surface. *Arteriosclerosis, Thrombosis, and Vascular Biology*, **23**, 1541–1547.

Corriu, C., Félétou, M., Canet, E. and Vanhoutte, P.M. (1996) Endothelium-derived factors and hyperpolarization of the carotid artery of the guinea-pig. *British Journal of Pharmacology*, **119**, 959–964.

Crane, G.J., Gallagher, N., Dora, K.A. and Garland, C.J. (2003) Small- and Intermediate-Conductance Calcium-Activated K^+ Channels Provide Different Facets of Endothelium-Dependent Hyperpolarization in Rat Mesenteric Artery. *The Journal of Physiology*, **553**, 183–189.

Csóka, A.B., Frost, G.I., Heng, H.H., Scherer, S.W., Mohapatra, G. and Stern, R. (1998) The hyaluronidase gene HYAL1 maps to chromosome 3p21.2-p21.3 in human and 9F1-F2 in mouse, a conserved candidate tumor suppressor locus. *Genomics*, **48**, 63–70.

Csóka, A.B., Frost, G.I. and Stern, R. (2001) The six hyaluronidase-like genes in the human and mouse genomes. *Matrix Biology*, **20**, 499–508.

Csóka, A.B., Frost, G.I., Wong, T. and Stern, R. (1997) Purification and microsequencing of hyaluronidase isozymes from human urine. *FEBS Letters*, **417**, 307–310.

Csóka, A.B., Scherer, S.W. and Stern, R. (1999) Expression analysis of six paralogous human hyaluronidase genes clustered on chromosomes 3p21 and 7q31. *Genomics*, **60**, 356–361.

Danielli, J.F. (1940) Capillary permeability and oedema in the perfused frog. *Journal of Physiology*, 109–129.

David, G., Lodes, V., Decock, B., Marynen, P., Cassiman, J.J., Berghe, H. Van Den, et al. (1990) Molecular cloning of a phosphatidylinositol-anchored membrane heparan sulfate proteoglycan from human lung fibroblasts. *The Journal of Cell Biology*, **111**, 3165–3176.

Day, A.J. and Prestwich, G.D. (2002) Hyaluronan-binding Proteins: Tying Up the Giant. *Journal of Biological Chemistry*, **277**, 4585–4588.

DeAngelis, P.L. (1999) Hyaluronan synthases: Fascinating glycosyltransferases from vertebrates, bacterial pathogens, and algal viruses. *Cellular and Molecular Life Sciences*, **56**, 670–682.

DeAngelis, P.L. (2002) Evolution of glycosaminoglycans and their glycosyltransferases: Implications for the extracellular matrices of animals and the capsules of pathogenic bacteria. *The Anatomical Record*, **268**, 317–326.

Dicker, K.T., Gurski, L.A., Pradhan-Bhatt, S., Witt, R.L., Farach-Carson, M.C. and Jia, X. (2014) Hyaluronan: A simple polysaccharide with diverse biological functions. *Acta Biomaterialia*, **10**, 1558–1570.

Ding, H., Hashem, M., Wiehler, W.B., Lau, W., Martin, J., Reid, J., et al. (2005) Endothelial dysfunction in the streptozotocin-induced diabetic apoE-deficient mouse. *British Journal of Pharmacology*, **146**, 1110–1118.

Dora, K.A., Gallagher, N.T., Mcneish, A. and Garland, C.J. (2008) Modulation of endothelial cell K Ca 3 . 1-channels during EDHF signaling in mesenteric resistance arteries. *Circulation Research*,

102, 1247–1255.

Drake-Holland, J.A. and Noble, M.I.M. (2012) Update on the Important New Drug Target in Cardiovascular Medicine – the Vascular Glycocalyx. *Cardiovascular & Haematological Disorders - Drug Targets*, **12**, 76–81.

Duran-Reynals, F. (1933) Studies on a certain spreading factor existing in bacteria and its significance for bacterial invasiveness. *The Journal of Experimental Medicine*, **58**, 161–181.

Dusting, G.J., Moncada, S. and Vane, J.R. (1977) Prostacyclin (PGX) is the endogenous metabolite responsible for relaxation of coronary arteries induced by arachindonic acid. *Prostaglandins*, **13**, 3–15.

Edwards, G., Dora, K.A., Gardener, M.J., Garland, C.J. and Weston, A.H. (1998) K+ is an endothelium-derived hyperpolarizing factor in rat arteries. *Nature*, **396**, 269–272.

Eichler, I., Wibawa, J., Grgic, I., Knorr, A., Brakemeier, S., Pries, A.R., et al. (2003) Selective blockade of endothelial Ca^{2+} -activated small- and intermediate-conductance K^{+} -channels suppresses EDHF-mediated vasodilation. *British Journal of Pharmacology*, **138**, 594–601.

Elvevold, K., Simon-Santamaria, J., Hasvold, H., McCourt, P., Smedsrød, B. and Sørensen, K.K. (2008) Liver sinusoidal endothelial cells depend on mannose receptor-mediated recruitment of lysosomal enzymes for normal degradation capacity. *Hepatology*, **48**, 2007–2015.

Evanko, S.P. and Wight, T.N. (1999) Intracellular localization of hyaluronan in proliferating cells. *The Journal of Histochemistry and Cytochemistry*, **47**, 1331–1342.

Félétou, M. and Vanhoutte, P.M. (1988) Endothelium-dependent hyperpolarization of canine coronary smooth muscle. *British Journal of Pharmacology*, **93**, 515–524.

Félétou, M. and Vanhoutte, P.M. (2013) Endothelium-Dependent Hyperpolarization : No Longer an F-Word ! , **61**, 91–92.

Figtree, G.A., Mc Donald, D., Watkins, H. and Channon, K. (2003) Truncated Estrogen Receptor alpha 46-kDa Isoform in Human Endothelial Cells: Relationship to Acute Activation of Nitric Oxide Synthase. *Circulation*, **107**, 120–126.

Flouriot, G., Brand, H., Denger, S., Metivier, R., Kos, M., Reid, G., et al. (2000) Identification of a new isoform of the human estrogen receptor-alpha (hER-alpha) that is encoded by distinct transcripts and that is able to repress hER-alpha activation function 1. *The EMBO Journal*, **19**, 4688–4700.

Fraser, J.R., Appelgren, L.E. and Laurent, T.C. (1983) Tissue uptake of circulating hyaluronic acid. A whole body autoradiographic study. *Cell and Tissue Research*, **233**, 285–293.

Fraser, J.R., Laurent, T.C., Engström-Laurent, A. and Laurent, U.G.B. (1984) Elimination of hyyaluronic acid from the blod stream in the human. *Clinical and Experimental Pharmacology and Physiology*, **11**, 17–25.

Fraser, J.R., Laurent, T.C. and Laurent, U.B. (1997) Hyaluronan: its nature, distribution, functions and turnover. *Journal of Internal Medicine*, **242**, 27–33.

Frost, G.I., Csóka, A.B., Wong, T. and Stern, R. (1997) Purification, cloning, and expression of human plasma hyaluronidase. *Biochemical and Biophysical Research Communications*, **236**, 10–15.

Furchgott, R.F. and Zawadzki, J. V. (1980) The obligatory role of endothelial cells in the relaxation of arterial smooth muscle by acetylcholine. *Nature*, **288**, 373–6.

Furuno, K., Co, C. and Louis, S. (1982) Appearance of Autolysosomes in Rat Liver after Leupeptin Treatment. *The Biochemical Journal*, **91**, 1485–1494.

Galley, H.F. (2004) Physiology of the endothelium. *British Journal of Anaesthesia*, **93**, 105–113.

Gao, L. and Lipowsky, H.H. (2010) Composition of the endothelial glycocalyx and its relation to its thickness and diffusion of small solutes. *Microvascular research*, **80**, 394–401.

Garg, H.G. and Hales, C.A. (2004) *Chemistry and Biology of Hyaluronan.*

Garland, C.J., Hiley, C.R. and Dora, K.A. (2011) EDHF: Spreading the influence of the endothelium. *British Journal of Pharmacology*, **164**, 839–852.

Gasingirwa, M.-C., Thirion, J., Mertens-Strijthagen, J., Wattiaux-De Coninck, S., Flamion, B., Wattiaux, R., et al. (2010) Endocytosis of hyaluronidase-1 by the liver. *The Biochemical Journal*, **430**, 305–313.

Gerrity, R.G. (1981) The role of the monocyte in atherogenesis: II. Migration of foam cells from atherosclerotic lesions. *The American Journal of Pathology*, **103**, 191–200.

Girault, A., Haelters, J.-P., Potier-Cartereau, M., Chantome, A., Jaffres, P.-A., Bougnoux, P., et al. (2012) Targeting SKCa channels in cancer: potential new therapeutic approaches. *Current Medicinal Chemistry*, **11**, 4479–4487.

Green, M.R., Pastewka, J.V. and Peacock, A.C. (1973) Differential staining of phosphoproteins on polyacrylamide gels with a cationic carbocyanine dye. *Analytical Biochemistry*, **56**, 43–51.

Greyner, H.J., Wiraszka, T., Zhang, L.S., Petroll, W.M. and Mummert, M.E. (2010) Inducible macropinocytosis of hyaluronan in B16-F10 melanoma cells. *Matrix Biology*, **29**, 503–510.

Güemes, M., Rahman, S.A. and Hussain, K. (2015) What is a normal blood glucose? *Archives of disease in childhood.*

Le Guennec, J.-Y., Ouadid-Ahidouch, H., Soriani, O., Besson, P., Ahidouch, A. and Vandier, C. (2007) Voltage-gated ion channels, new targets in anti-cancer research. *Recent patents on anti-cancer drug discovery*, **2**, 189–202.

Guntenhöner, M.W., Pogrel, M.A. and Stern, R. (1992) A substrate-gel assay for hyaluronidase activity. *Matrix*, **12**, 388–396.

Gushulak, L., Hemming, R., Martin, D., Seyrantepe, V., Pshezhetsky, A. and Triggs-Raine, B. (2012) Hyaluronidase 1 and -hexosaminidase have redundant functions in hyaluronan and chondroitin sulfate degradation. *Journal of Biological Chemistry*, **287**, 16689–16697.

Harada, H. and Takahashi, M. (2007) CD44-dependent Intracellular and Extracellular Catabolism of Hyaluronic Acid by Hyaluronidase-1 and -2. *Journal of Biological Chemistry*, **282**, 5597–5607.

Harris, E.N., Kyosseva, S. V., Weigel, J.A. and Weigel, P.H. (2007) Expression, Processing, and Glycosaminoglycan Binding Activity of the Recombinant Human 315-kDa Hyaluronic Acid Receptor for Endocytosis (HARE). *Journal of Biological Chemistry*, **282**, 2785–2797.

Haxaire, K., Braccini, I., Milas, M., Rinaudo, M. and Pérez, S. (2000) Conformational behavior of hyaluronan in relation to its physical properties as probed by molecular modeling. *Glycobiology*, **10**, 587–594.

Hemming, R., Martin, D.C., Slominski, E., Nagy, J.I., Halayko, A.J., Pind, S., et al. (2008) Mouse Hyal3 encodes a 45- to 56-kDa glycoprotein whose overexpression increases hyaluronidase 1 activity in cultured cells. *Glycobiology*, **18**, 280–289.

Hovingh, P. and Linker, A. (1999) Hyaluronidase activity in leeches (Hirudinea). *Comparative Biochemistry and Physiology Part B: Biochemistry and Molecular Biology*, **124**, 319–326.

Ibrahim, N.M., Marinovic, A.C., Price, S.R., Young, L.G. and Fröhlich, O. (2000) Pitfall of an internal control plasmid: response of Renilla luciferase (pRL-TK) plasmid to dihydrotestosterone and dexamethasone. *BioTechniques*, **29**, 782–784.

Ihionkhan, C.E., Chambliss, K.L., Gibson, L.L., Hahner, L.D., Mendelsohn, M.E. and Shaul, P.W. (2002) Estrogen Causes Dynamic Alterations in Endothelial Estrogen Receptor Expression.

Circulation Research, **91**, 814–820.

Ihrcke, N.S., Wrenshall, L.E., Lindman, B.J. and Platt, J.L. (1993) Role of heparan sulfate in immune system-blood vessel interactions. *Immunology today*, **14**, 500–505.

Imundo, L., LeDuc, C.A., Guha, S., Brown, M., Perino, G., Gushulak, L., et al. (2011) A complete deficiency of Hyaluronoglucosaminidase 1 (HYAL1) presenting as familial juvenile idiopathic arthritis. *Journal of Inherited Metabolic Disease*, **34**, 1013–1022.

Itano, N. and Kimata, K. (2002) Mammalian Hyaluronan Synthases. *IUBMB life*, **1**, 195–199.

Itano, N., Sawai, T., Yoshida, M., Lenas, P., Yamada, Y., Imagawa, M., et al. (1999) Three isoforms of mammalian hyaluronan synthases have distinct enzymatic properties. *Journal of Biological Chemistry*, **274**, 25085–25092.

Jackson, D.G. (2009) Immunological functions of hyaluronan and its receptors in the lymphatics. *Immunological Reviews*, **230**, 216–231.

Jacobson, D., Pribnow, D., Herson, P.S., Maylie, J. and Adelman, J.P. (2003a) Determinants contributing to estrogen-regulated expression of SK3. *Biochemical and Biophysical Research Communications*, **303**, 660–668.

Kaneiwa, T., Miyazaki, A., Kogawa, R., Mizumoto, S., Sugahara, K. and Yamada, S. (2012) Identification of amino acid residues required for the substrate specificity of human and mouse chondroitin sulfate hydrolase (conventional hyaluronidase-4). *The Journal of Biological Chemistry*, **287**, 42119–42128.

Karlstam, B. and Ljunglöf, A. (1991) Purification and partial characterization of a novel hyaluronic acid-degrading enzyme from Antarctic krill (Euphausia superba). *Polar Biology*, **11**.

Kelly, R.F. and Snow, H.M. (2007) Characteristics of the response of the iliac artery to wall shear stress in the anaesthetized pig. *The Journal of Physiology*, **582**, 731–743.

Köhler, R., Degenhardt, C., Ku, M., Runkel, N., Paul, M. and Hoyer, J. (2000) Expression and function of endothelial CA2+-activated K+ channels in human mesenteric artery. *Circulation Research*, **87**, 496–503.

Kohler, M., Hirschberg, B., Bond, C.T., Kinzie, J.M., Marrion, N. V., Maylie, J., et al. (1996) Small-Conductance, Calcium-Activated Potassium Channels from Mammalian Brain. *Science*, **273**, 1709–1714.

Komori, K., Lorenz, R.R. and Vanhoutte, P.M. (1988) Nitric oxide, ACh, and electrical and mechanical properties of canine arterial smooth muscle. *American Journal of Physiology. Heart and Circulatory Physiology*, **255**, H207–H212.

Labat-Robert, J. and Robert, L. (2012) Fifty years of structural glycoproteins. *Pathologie Biologie*, **60**, 66–75.

Lancaster, B., Nicoll, R.A. and Perkel, D.J. (1991) Calcium activates two types of potassium channels in rat hippocampal neurons in culture. *The Journal of Neuroscience*, **11**, 23–30.

Laurent, T.C. and Fraser, J.R. (1992) Hyaluronan. *FASEB journal : official publication of the Federation of American Societies for Experimental Biology*, **6**, 2397–2404.

Laurent, T.C., Lilja, K., Brunnberg, L., Engström-Laurent, A., Laurent, U.B., Lindqvist, U., et al. (1987) Urinary excretion of hyaluronan in man. *Scandinavian Journal of Clinical and Laboratory Investigation*, **47**, 793–799.

Ledoux, J., Werner, M.E., Brayden, J.E. and Nelson, M.T. (2006) Calcium-activated potassium channels and the regulation of vascular tone. *Physiology (Bethesda)*, **21**, 69–78.

Lee, J.Y. and Spicer, A.P. (2000) Hyaluronan: A multifunctional, megaDalton, stealth molecule. *Current Opinion in Cell Biology*, **12**, 581–586.

Lennon, F.E. and Singleton, P.A. (2011) Hyaluronan regulation of vascular integrity. *American Journal of Cardiovascular Disease*, **1**, 200–213.

Li, L., Haynes, M.P. and Bender, J.R. (2003) Plasma membrane localization and function of the estrogen receptor alpha variant (ER46) in human endothelial cells. *PNAS*, **100**, 4807–4812.

Li, S., Kelly, S.J., Lamani, E., Ferraroni, M. and Jedrzejas, M.J. (2000) Structural basis of hyaluronan degradation by Streptococcus pneumoniae hyaluronate lyase. *The EMBO journal*, **19**, 1228–1240.

Liu, M.Y., Hattori, Y., Fukao, M., Sato, A., Sakuma, I. and Kanno, M. (2001) Alterations in EDHF-mediated hyperpolarization and relaxation in mesenteric arteries of female rats in long-term deficiency of oestrogen and during oestrus cycle. *British Journal of Pharmacology*, **132**, 1035–1046.

Luksha, L., Agewall, S. and Kublickiene, K. (2009) Endothelium-derived hyperpolarizing factor in vascular physiology and cardiovascular disease. *Atherosclerosis*, **202**, 330–344.

Mack, J.A., Feldman, R.J., Itano, N., Kimata, K., Lauer, M., Hascall, C., et al. (2012) Enhanced inflammation and accelerated wound closure following tetraphorbol ester application or full-thickness wounding in mice lacking hyaluronan synthases Has1 and Has3. *Journal of Investigative Dermatology*, **132**, 198–207.

Malek, A.M. and Izumo, S. (1996) Mechanism of endothelial cell shape change and cytoskeletal remodeling in response to fluid shear stress. *Journal of Cell Science*, **109**, 713–726.

Manea, S.A., Todirita, A. and Manea, A. (2013) High glucose-induced increased expression of endothelin-1 in human endothelial cells is mediated by activated CCAAT/enhancer-binding proteins. *PLoS ONE*, **8**.

Martin, D.C., Atmuri, V., Hemming, R.J., Farley, J., Mort, J.S., Byers, S., et al. (2008) A mouse model of human mucopolysaccharidosis IX exhibits osteoarthritis. *Human Molecular Genetics*, **17**, 1904–1915.

Mendelsohn, M.E. and Karas, R.H. (1999) The Protective Effects of Estrogen on the Cardiovascular System. *The New England Journal of Medicine*, **340**, 1801–1811.

Michiels, C. (2003) Endothelial cell functions. *Journal of Cellular Physiology*, **196**, 430–443.

Middleton, J., Patterson, A.M., Gardner, L., Schmutz, C. and Ashton, B.A. (2002) Leukocyte extravasation: Chemokine transport and presentation by the endothelium. *Blood*, **100**, 3853–3860.

Mikami, T. and Kitagawa, H. (2013) Biosynthesis and function of chondroitin sulfate. *Biochimica et Biophysica Acta*, **1830**, 4719–4733.

Mochizuki, S., Vink, H., Hiramatsu, O., Kajita, T., Shigeto, F., Spaan, J.A.E., et al. (2003) Role of hyaluronic acid glycosaminoglycans in shear-induced endothelium-derived nitric oxide release. *American Journal of Physiology. Heart and Circulatory Physiology*, **285**, H722–H726.

Nagaoka, A., Yoshida, H., Nakamura, S., Morikawa, T., Kawabata, K., Kobayashi, M., et al. (2015) Regulation of Hyaluronan (HA) Metabolism Mediated by HYBID (*HY* aluronan *B* inding Protein *I* nvolved in HA *D* epolymerization, KIAA1199) and HA Synthases in Growth Factor-stimulated Fibroblasts. *Journal of Biological Chemistry*, jbc.M115.673566.

Nagy, N., Kaber, G., Johnson, P.Y., Gebe, J.A., Preisinger, A., Falk, B.A., et al. (2015) Inhibition of hyaluronan synthesis restores immune tolerance during autoimmune insulitis. *The Journal of Clinical Investigation*, **125**, 1–14.

Natowicz, M.R., Short, M.P., Wang, Y., Dickersin, G.R., Gebhardt, M.C., Rosenthal, D.I., et al. (1996) Clinical and biochemical manifestations of hyaluronidase deficiency. *The New England Journal of Medicine*, **335**, 1029–1033.

Nawate, S., Fukao, M., Sakuma, I., Soma, T., Nagai, K., Takikawa, O., et al. (2005) Reciprocal changes in endothelium-derived hyperpolarizing factor- and nitric oxide-system in the mesenteric artery of adult female rats following ovariectomy. *British Journal of Pharmacology*, **144**, 178–189.

Nieuwdorp, M., Holleman, F., de Groot, E., Vink, H., Gort, J., Kontush, A., et al. (2007) Perturbation of hyaluronan metabolism predisposes patients with type 1 diabetes mellitus to atherosclerosis. *Diabetologia*, **50**, 1288–1293.

Oettl, M., Hoechstetter, J., Asen, I., Bernhardt, G. and Buschauer, A. (2003) Comparative characterization of bovine testicular hyaluronidase and a hyaluronate lyase from Streptococcus agalactiae in pharmaceutical preparations. *European Journal of Pharmaceutical Sciences*, **18**, 267–277.

Palmer, R.M., Ferrige, A.G. and Moncada, S. (1987) Nitric oxide release accounts for the biological activity of endothelium-derived relaxing factor. *Nature*, **327**, 524–526.

Palmer, W.J. and Meyer, K. (1934) Polysaccharide of Vitreous Humor. *Journal of Biological Chemistry*, **107**, 629–634.

Pearson, J.D. (1999) Endothelial cell function and thrombosis. *Best Practice & Research Clinical Haematology*, **12**, 329–341.

Perticone, F., Ceravolo, R., Pujia, A., Ventura, G., Iacopino, S., Scozzafava, A., et al. (2001) Prognostic significance of endothelial dysfunction in hypertensive patients. *Circulation*, **104**, 191–196.

Potier, M., Chantome, A., Joulin, V., Girault, A., Roger, S., Besson, P., et al. (2011) The SK3/K(Ca)2.3 potassium channel is a new cellular target for edelfosine. *British Journal of Pharmacology*, **162**, 464–479.

Potier, M., Joulin, V., Roger, S., Besson, P., Jourdan, M.-L., Leguennec, J.-Y., et al. (2006) Identification of SK3 channel as a new mediator of breast cancer cell migration. *Molecular Cancer Therapeutics*, **5**, 2946–2953.

Potter, D.R., Jiang, J. and Damiano, E.R. (2009) The recovery time course of endothelial-cell glycocalyx in vivo and its implications in vitro. *Circulation Research*, **104**, 1318–1325.

Pries, A.R., Secomb, T.W. and Gaehtgens, P. (2000) The endothelial surface layer. *Pflugers Archiv : European Journal of Physiology*, **440**, 653–666.

Puissant, E., Gilis, F., Dogné, S., Flamion, B., Jadot, M. and Boonen, M. (2014) Subcellular trafficking and activity of hyal-1 and its processed forms in murine macrophages. *Traffic*, **15**, 500–515.

Racine, R. and Mummert, M.E. (2012) *Hyaluronan Endocytosis: Mechanisms of Uptake and Biological Functions, Molecular Regulation of Endocytosis* (ed B Dr Ceresa).

Ranjan, V., Xiao, Z. and Diamond, S.L. (1995) Constitutive NOS expression in cultured endothelial cells is elevated by fluid shear stress. *The American Journal of Physiology*, **269**, H550–H555.

Rapraeger, A. (1989) Transforming growth factor (type beta) promotes the addition of chondroitin sulfate chains to the cell surface proteoglycan (syndecan) of mouse mammary epithelia. *Journal of Cell Biology*, **109**, 2509–2518.

Reitsma, S., Slaaf, D.W., Vink, H., van Zandvoort, M.A.M.J. and oude Egbrink, M.G.A. (2007) The endothelial glycocalyx: composition, functions, and visualization. *Pflügers Archiv : European Journal of Physiology*, **454**, 345–59.

Rigden, D.J. and Jedrzejas, M.J. (2003) Structures of Streptococcus pneumoniae Hyaluronate Lyase in Complex with Chondroitin and Chondroitin Sulfate Disaccharides: Insights into specificity and mechanism of action. *Journal of Biological Chemistry*, **278**, 50596–50606.

Ross, M.H. and Pawlina, W. (2006) *Histology: A Text and Atlas: With Correlated Cell and Molecular Biology*, 6th ed. Lippincott Williams&Wilkins, Baltimore, MD.

Russell, K.S., Haynes, M.P., Sinha, D., Clerisme, E. and Bender, J.R. (2000) Human vascular endothelial cells contain membrane binding sites for estradiol, which mediate rapid intracellular signaling. *PNAS*, **97**, 5930–5935.

Rye, C.S. and Withers, S.G. (2000) Glycosidase mechanisms. *Current Opinion in Chemical Biology*, **4**, 573–580.

Sabeur, K., Cherr, G., Yudin, A.I., Primakoff, P., Li, M.-W. and Overstreet, J.W. (1997) The PH-20 Protein in Human Spermatozoa. *Journal of Andrology*, **18**, 151–158.

Sabeur, K., Foristall, K. and Ball, B.A. (2002) Characterization of PH-20 in canine spermatozoa and testis. *Theriogenology*, **57**, 977–987.

Sandow, S.L., Neylon, C.B., Chen, M.X. and Garland, C.J. (2006) Spatial separation of endothelial small- and intermediate-conductance calcium-activated potassium channels (KCa) and connexins: Possible relationship to vasodilator function? *Journal of Anatomy*, **209**, 689–698.

Scott, J.E. (1989) Secondary structures in hyaluronan solutions: chemical and biological implications. *Ciba Foundation symposium*, **143**, 6–20.

Shuttleworth, T.L., Wilson, D.L., Wicklow, B.A., Wilkins, J.A. and Triggs-Raine, B.L. (2002) Characterization of the Murine Hyaluronidase Gene Region Reveals Complex Organization and Cotranscription of Hyal1 with Downstream Genes, Fus2 and Hyal3. *Journal of Biological Chemistry*, **277**, 23008–23018.

Singh, A., Fridén, V., Dasgupta, I., Foster, R.R., Welsh, G.I., Tooke, J.E., et al. (2011) High glucose causes dysfunction of the human glomerular endothelial glycocalyx. *American Journal of Physiology. Renal Physiology*, **300**, F40–F48.

Spicer, A.P., Seldin, M.F., Olsen, A.S., Brown, N., Wells, D.E., Doggett, N.A., et al. (1997) Chromosomal localization of the human and mouse hyaluronan synthase genes. *Genomics*, **41**, 493–497.

Stern, R. (2003) Devising a pathway for hyaluronan catabolism: Are we there yet? *Glycobiology*, **13**, 105–115.

Stern, R. (2004) Hyaluronan catabolism: a new metabolic pathway. *European Journal of Cell Biologyell*, **83**, 317–325.

Stern, R., Asari, A. a. and Sugahara, K.N. (2006) Hyaluronan fragments: An information-rich system. *European Journal of Cell Biology*, **85**, 699–715.

Stern, R. and Jedrzejas, M.J. (2006) Mechanisms of Action. *Chemical Reviews*, **106**, 818–839.

Stern, R., Kogan, G., Jedrzejas, M.J. and Šoltés, L. (2007) The many ways to cleave hyaluronan. *Biotechnology Advances*, **25**, 537–557.

Stridh, S., Palm, F. and Hansell, P. (2012) Renal interstitial hyaluronan: functional aspects during normal and pathological conditions. *American Journal of hysiology. Regulatory, integrative and comparative Physiology*, **302**, R1235–R1249.

Strunden, M.S., Bornscheuer, A., Schuster, A., Kiefmann, R., Goetz, A.E. and Heckel, K. (2012) Glycocalyx Degradation Causes Microvascular Perfusion Failure in the Ex Vivo Perfused Mouse Lung. *Shock*, **38**, 559–566.

Tamer, T.M. (2013) Hyaluronan and synovial joint: function, distribution and healing. *Interdisciplinary Toxicology*, **6**, 111–125.

Tang, Y.-R., Yang, W.-W., Wang, Y., Gong, Y.-Y., Jiang, L.-Q. and Lin, L. (2015) Estrogen regulates the expression of small-conductance Ca-activated K+ channels in colonic smooth muscle cells.

Digestion, **91**, 187–96.

Tarbell, J.M. and Pahakis, M.Y. (2006) Mechanotransduction and the glycocalyx. *Journal of Internal Medicine*, **259**, 339–350.

Tarbell, J.M., Simon, S.I. and Curry, F.-R.E. (2014) Mechanosensing at the vascular interface. *Annual Review of Biomedical Engineering*, **16**, 505–32.

Taylor, M.S., Bonev, A.D., Gross, T.P., Eckman, D.M., Brayden, J.E., Bond, C.T., et al. (2003) Altered expression of small-conductance Ca2+-activated K+ (SK3) channels modulates arterial tone and blood pressure. *Circulation Research*, **93**, 124–131.

Thankamony, S.P. and Knudson, W. (2006) Acyaltion of CD44 and Its Association with Lipid Rafts Are Required for Receptor and Hyaluronan Endocytosis. *Journal of Biological Chemistry*, **281**, 34601–34609.

Tomioka, H., Hattori, Y., Fukao, M., Sato, A., Liu, M., Sakuma, I., et al. (1999) Relaxation in different-sized rat blood vessels mediated by endothelium-derived hyperpolarizing factor: importance of processes mediating precontractions. *Journal of Vascular Research*, **36**, 311–320.

Törrönen, K., Nikunen, K., Kärnä, R., Tammi, M., Tammi, R. and Rilla, K. (2014) Tissue distribution and subcellular localization of hyaluronan synthase isoenzymes. *Histochemistry and Cell Biology*, **141**, 17–31.

Triggs-Raine, B. and Natowicz, M.R. (2015) Biology of hyaluronan: Insights from genetic disorders of hyaluronan metabolism. *World Journal of Biological Chemistry*, **6**, 110–120.

Triggs-Raine, B., Salo, T.J., Zhang, H., Wicklow, B. a and Natowicz, M.R. (1999) Mutations in HYAL1, a member of a tandemly distributed multigene family encoding disparate hyaluronidase activities, cause a newly described lysosomal disorder, mucopolysaccharidosis IX. *PNAS*, **96**, 6296–6300.

Trowbridge, J.M. and Gallo, R.L. (2002) Dermatan sulfate: new functions from an old glycosaminoglycan. *Glycobiology*, **12**, 117R–125R.

Urakami-Harasawa, L., Shimokawa, H., Nakashima, M., Egashira, K. and Takeshita, A. (1997) Importance of endothelium-derived hyperpolarizing factor in human arteries. *The Journal of Clinical Investigation*, **100**, 2793–2799.

Vigetti, D., Viola, M., Karousou, E., De Luca, G. and Passi, A. (2014) Metabolic control of hyaluronan synthases. *Matrix Biology*, **35**, 8–13.

Wakabayashi, I., Hatake, K., Kimura, N., Kakishita, E. and Nagai, K. (1987) Modulation of vascular tonus by the endothelium in experimental diabetes. *Life sciences*, **40**, 643–648.

Wang, A. and Hascall, V.C. (2004) Hyaluronan Structures Synthesized by Rat Mesangial Cells in Response to Hyperglycemia Induce Monocyte Adhesion. *Journal of Biological Chemistry*, **279**, 10279–10285.

Watanabe, H., Cheung, S.C., Itano, N., Kimata, K. and Yamada, Y. (1997) Identification of hyaluronan-binding domains of aggrecan. *Journal of Biological Chemistry*, **272**, 28057–28065.

Weigel, P.H. and DeAngelis, P.L. (2007) Hyaluronan Synthases: A Decade-plus of Novel Glycosyltransferases. *Journal of Biological Chemistry*, **282**, 36777–36781.

Weissmann, B. and Meyer, K. (1954) The Structure of Hyalobiuronic Acid and of Hyaluronic Acid from Umbilical Cord. *Journal of the American Chemical Society*, **76**, 1753–1757.

Wittekindt, O., Jauch, A., Burgert, E., Schärer, L., Holtgreve-Grez, H., Yvert, G., et al. (1998) The human small conductance calcium-regulated potassium channel gene (hSKCa3) contains two CAG repeats in exon 1, is on chromosome 1q21.3, and shows a possible association with schizophrenia. *Neurogenetics*, **1**, 259–265.

Xia, X.M., Fakler, B., Rivard, A., Wayman, G., Johnson-Pais, T., Keen, J.E., et al. (1998) Mechanism of calcium gating in small-conductance calcium-activated potassium channels. *Nature*, **395**, 503–507.

Xiao, Z., Zhang, Z., Ranjan, V. and Diamond, S.L. (1997) Shear stress induction of the endothelial nitric oxide synthase gene is calcium-dependent but not calcium-activated. *Journal of Cellular Physiology*, **171**, 205–211.

Yap, F.C., Taylor, M.S. and Lin, M.T. (2014) Ovariectomy-Induced Reductions in Endothelial SK3 Channel Activity and Endothelium-Dependent Vasorelaxation in Murine Mesenteric Arteries. *PLoS ONE*, **9**, e104686.

Yoshida, H., Nagaoka, A., Kusaka-Kikushima, A., Tobiishi, M., Kawabata, K., Sayo, T., et al. (2013) KIAA1199, a deafness gene of unknown function, is a new hyaluronan binding protein involved in hyaluronan depolymerization. *PNAS*, **110**, 5612–5617.

Zechel, D.L. and Withers, S.G. (2000) Glycosidase mechanisms: Anatomy of a finely tuned catalyst. *Accounts of Chemical Research*, **33**, 11–18.

Zhang, L., Bharadwaj, A.G., Casper, A., Barkley, J., Barycki, J.J. and Simpson, M.A. (2009) Hyaluronidase activity of human Hyal1 requires active site acidic and tyrosine residues. *The Journal of biological chemistry*, **284**, 9433–9442.

Zuurbier, C.J., Demirci, C., Koeman, A., Vink, H. and Ince, C. (2005) Short-term hyperglycemia increases endothelial glycocalyx permeability and acutely decreases lineal density of capillaries with flowing red blood cells. *Journal of Applied physiology*, **99**, 1471–1476.

Zygmunt, P.M., Edwards, G., Weston, A.H., Larsson, B. and Högestätt, E.D. (1997) Involvement of voltage-dependent potassium channels in the EDHF-mediated relaxation of rat hepatic artery. *British Journal of Pharmacology*, **121**, 141–149.